INFORMATION TO USERS

This manuscript has been reproduced from the microfilm master. UMI films the text directly from the original or copy submitted. Thus, some thesis and dissertation copies are in typewriter face, while others may be from any type of computer printer.

The quality of this reproduction is dependent upon the quality of the copy submitted. Broken or indistinct print, colored or poor quality illustrations and photographs, print bleedthrough, substandard margins, and improper alignment can adversely affect reproduction.

In the unlikely event that the author did not send UMI a complete manuscript and there are missing pages, these will be noted. Also, if unauthorized copyright material had to be removed, a note will indicate the deletion.

Oversize materials (e.g., maps, drawings, charts) are reproduced by sectioning the original, beginning at the upper left-hand corner and continuing from left to right in equal sections with small overlaps. Each original is also photographed in one exposure and is included in reduced form at the back of the book.

Photographs included in the original manuscript have been reproduced xerographically in this copy. Higher quality 6" x 9" black and white photographic prints are available for any photographs or illustrations appearing in this copy for an additional charge. Contact UMI directly to order.

UMI®

Bell & Howell Information and Learning
300 North Zeeb Road, Ann Arbor, MI 48106-1346 USA
800-521-0600

Possibilistic Sonar Modeling and Localization for Mobile Robots

Mohammad Molhim

A Thesis

in

The Department

of

Mechanical Engineering

Presented in Partial Fulfillment of the Requirements

for the Degree of Master of Applied Science at

Concordia University

Montréal, Québec, Canada

August 1997

ABSTRACT

Possibilistic Sonar Modeling and Localization for Mobile Robots

Mohammad Molhim

Sonar sensors are widely used in mobile robots applications such as navigation, map building, and localization. The performance of these sensors is affected by the environmental phenomena, sensor design, and target characteristics. Therefore, the readings obtained from these sensors are uncertain. This uncertainty is often modeled by using *Probability Theory*. However, the probabilistic approach is valid when the available knowledge is precise which is not the case in sonar readings. In this thesis a new model of uncertainty in sonar readings is proposed by using *Possibility Theory*. The possibilistic approach is valid when the available knowledge is imprecise and coherent as in sonar readings. It is verified experimentally that the behavior of the sonar readings obtained from a corner is the same as the behavior of these obtained from a wall only when the sensor is at distances less than 75cm. Based on this finding, a new approach for corner detection is implemented on the mobile robot, Pioneer 1. Unlike signal and image processing approaches, our approach is not time consuming because it depends on direct interpretation of readings obtained from different sensors in the same time (TOF). Stationary and dynamic localization methods are presented and applied on Pioneer1. These methods can be generalized for different robots configurations, especially the ones with a ring configuration.

ACKNOWLEDGEMENTS

I would like to thank Dr. K. Demirli for his professional supervision, guidance, and patience, throughout this study. It was pleasure working with him especially in the last few months when the real action took place. I would also like to thank Dr. A. Bulgak for his supervision, understanding, and valuable advice regarding the thesis.

The financial support of the Canadian International Development Agency (CIDA) and Natural Science and Engineering Research Council of Canada (NSERC) are gratefully acknowledged.

TABLE OF CONTENTS

LIST OF FIGURES vii

LIST OF TABLES xiv

1 Introduction **1**

1.1 Mobile Robots 1

1.2 Literature survey 3

1.3 Outline of the Thesis 11

2 Ultrasonic Transducers **12**

2.1 Time of Flight Measurement (TOF) 12

2.2 Factors affecting ultrasonic sensors behavior 14

3 Uncertainty Modeling and Possibility Theory **23**

3.1 Introduction 23

3.2 Types of available information 28

3.3 Modeling of Uncertainty 29

3.4 Fuzzy Measures 31

3.5 Evidence Theory 32

3.6 Possibility Theory 36

3.7 Possibilistic approach for modeling uncertainty in physical measurements 37

3.8 Possibilistic measurement 37

3.9 Possibilistic Histograms 38

4 Modeling Uncertainty in Sonar Sensors **45**

4.1 Experimental Setup 46
4.2 Modeling angular uncertainty and radial imprecision for sonar readings reflected from a wall 47
4.3 Reduction of angular uncertainty and radial imprecision in the wall case 55
4.4 Modeling angular uncertainty and radial imprecision for sonar readings reflected from a corner 64

5 Application to Mobile Robots **74**
5.1 Sensor based localization 75
5.2 Pioneer 1 Configuration 76
5.3 Localization for Pioneer 1 76

6 Discussion and Conclusions **92**
6.1 Discussion 92
6.2 Summary and Conclusions 96
6.3 Future Work 98

A Appendix A **105**

LIST OF FIGURES

2.1 Typical echo produced by exciting the ultrasonic transducer with a short-duration voltage pulse. 13

2.2 A possible beam pattern. 17

2.3 The effect of beam width on the sonar readings. 18

2.4 Beam spread can cause object surfaces to be blurred. 19

2.5 Scattering of the echo in different directions when the beam incidence angle is more than the critical angle of the surface. 21

2.6 Sonar sensor gives a false reading after bouncing off other objects in the environment 22

3.1 A simple Possibilistic histogram with its candidate points (top). Three examples of piecewise linear continuous approximations (top). 44

4.1 Experimental setup. 46

4.2 Experiments for studying the behavior of the sonar sensor when it is in front of a wall (top) and a corner (bottom). 48

4.3 Possibility distribution for the field of view of a sonar sensor. 52

4.4 Error calculation for sonar reading coming from a wall at a certain distance and angle. 53

4.5 Radial imprecision represented by possibility distributions when the sensor is at a distance from 50cm to 175cm (top), when the distance is from 200cm to 275cm (middle), and when the distance is from 300cm to 370cm (bottom). 54

4.6 Three possible cases for the readings obtained from two sensors. . . . 57

4.7 Two sonar sensors detecting the same wall. 58
4.8 Reduced angular uncertainty for readings coming from a wall, $ds1 < ds2$ (top), $ds2 > ds1$ (middle), and $ds1 = ds2$ (bottom). 58
4.9 Shortest distance estimating from radial imprecision and angular uncertainty. 60
4.10 Reduced radial imprecision when the sensor incidence angle is 1^o and the distance from a wall is from 50cm to 175cm (top), from 200cm to 275cm (middle), and from 300cm to 370cm (bottom). 62
4.11 Reduced radial imprecision when the sensor incidence angle is 7.5^o and the distance from a wall is from 50cm to 175cm (top), from 200cm to 275cm (middle), and from 300cm to 370cm (bottom). . . . 63
4.12 Error calculations when the senor detects a corner at distance L from the sensor. 65
4.13 Possibility distribution for field of view of a sonar sensor facing a corner. 67
4.14 (Possibility distribution for radial imprecision when the distance between the sensor and the corner is from 50cm to 175cm (top). Possibility distribution for radial imprecision when the sensor is at distance from 200cm to 275cm (middle). Possibility distribution for radial imprecision when the sensor is at distance from 300cm to 370cm (bottom). 68
4.15 Reduced angular uncertainty for readings come from a corner, when $ds1 < ds2$ (top), when $ds2 < ds1$ (middle), and when $ds1 = ds2$ (bottom). 70

4.16 Reduced radial imprecision for readings coming from a corner when the incidence angle is 3^o. The distance between the sensor and the corner is from 50cm to 175cm (top), when the distance is from 200cm to 275cm (middle), and when the distance is from 200cm to 275cm (bottom). 71

4.17 Reduced radial imprecision for readings coming from a corner when the incidence angle is 7.5^o. The distance between the sensor and the corner is from 50cm to 175cm (top), when the distance is from 200cm to 275cm (middle), and when the distance is from 200cm to 275cm (bottom). 72

4.18 Reduced radial imprecision for readings coming from a corner when the incidence angle is 5^o. The distance between the sensor and the corner is from 50cm to 175cm (top), when the distance is from 200cm to 275cm (middle), and when the distance is from 200cm to 275cm (bottom). 73

5.1 Pioneer 1 Configuration. 77

5.2 The map of the environment. 78

5.3 The robot trying to follow a wall. 79

5.4 Possibility distribution of the value of X in the sensor's coordinates when $\theta = 3^o$ (top - left). Possibility distribution of the value of X in the robot's coordinates for $\theta = 3^o$ (top - right). Possibility distribution of the value of X in the sensor's coordinates when $\theta = 7.5^o$ (middle - left). Possibility distribution of the value of X in the sensor's coordinates when $\theta = 7.5^o$ (middle - right). Combined possibility distribution of (top - right) and (middle - right) that represents the value of X in the robot's coordinates (bottom). 82

5.5 The possibility distribution of the normal distance in the robot's coordinates when $\theta = 1^o$ (left), when $\theta = 7.5^o$ (right), the possibility distribution that represents the combination between the left and the right (bottom). 83

5.6 The four possible initial stationary location of the robot in our test environment. 85

5.7 The detection of a front wall may reduce the initial possible locations. 87

5.8 Matching between the initial location and the new one after an increase in the readings obtained from $S0$ occurs. 91

6.1 Two-transducer system at zero incidence angle from wall and corner. θ_s is the angle for echo amplitude for the corner. 93

6.2 Amplitude versus incidence angle for wall reflector (top). Amplitude versus incidence angle for corner reflector (bottom). 94

A.1 Incidence angle versus radial imprecision for readings obtained from a wall at distance 25cm. 119

A.2 Incidence angle versus radial imprecision for readings obtained from a wall at distance 50cm. 119
A.3 Incidence angle versus radial imprecision for readings obtained from a wall at distance 75cm. 120
A.4 Incidence angle versus radial imprecision for readings obtained from a wall at distance 100cm. 120
A.5 Incidence angle versus radial imprecision for readings obtained from a wall at distance 125cm. 121
A.6 Incidence angle versus radial imprecision for readings obtained from a wall at distance 150cm. 121
A.7 Incidence angle versus radial imprecision for readings obtained from a wall at distance 175cm. 122
A.8 Incidence angle versus radial imprecision for readings obtained from a wall at distance 200cm. 122
A.9 Incidence angle versus radial imprecision for readings obtained from a wall at distance 225cm. 123
A.10 Incidence angle versus radial imprecision for readings obtained from a wall at distance 250cm. 123
A.11 Incidence angle versus radial imprecision for readings obtained from a wall at distance 275cm. 124
A.12 Incidence angle versus radial imprecision for readings obtained from a wall at distance 300cm. 124
A.13 Incidence angle versus radial imprecision for readings obtained from a wall at distance 325cm. 125

A.14 Incidence angle versus radial imprecision for readings obtained from a wall at distance 350cm. 125
A.15 Incidence angle versus radial imprecision for readings obtained from a wall at distance 370cm. 126
A.16 Incidence angle versus radial imprecision for readings obtained from a corner at 25cm. 127
A.17 Incidence angle versus radial imprecision for readings obtained from a corner at 50cm. 127
A.18 Incidence angle versus radial imprecision for readings obtained from a corner at 75cm. 128
A.19 Incidence angle versus radial imprecision for readings obtained from a corner at 100cm. 128
A.20 Incidence angle versus radial imprecision for readings obtained from a corner at 125cm. 129
A.21 Incidence angle versus radial imprecision for readings obtained from a corner at 150cm. 129
A.22 Incidence angle versus radial imprecision for readings obtained from a corner at 175cm. 130
A.23 Incidence angle versus radial imprecision for readings obtained from a corner at 200cm. 130
A.24 Incidence angle versus radial imprecision for readings obtained from a corner at 225cm. 131
A.25 Incidence angle versus radial imprecision for readings obtained from a corner at 250cm. 131

A.26 Incidence angle versus radial imprecision for readings obtained from a corner at 275cm. 132
A.27 Incidence angle versus radial imprecision for readings obtained from a corner at 300cm. 132

LIST OF TABLES

4.1 The field of view of the sonar sensor at different distances from a wall. 49

4.2 Radial imprecision intervals when the sensor in front of a wall at different distances. 55

4.3 The reduced radial imprecision intervals when $ds1 < ds2$ and the incidence angle is 1^o. 61

4.4 The reduced radial imprecision intervals when $ds1 < ds2$ and the incidence angle is 7.5^o. 61

4.5 The field of view of the sonar sensor at different distances from a corner. 66

4.6 The radial imprecision of sonar readings reflected from a corner at different distances. 67

5.1 Error accumulation in dead reckoning over the distance at a velocity of 90mm/sec. 76

5.2 Error accumulation in dead reckoning over the distance at a velocity of 180mm/sec. 76

5.3 Summary of all possible cases for $ds1$, $ds2$, $ds3$, and $ds4$. 86

A.1 Sonar readings from a wall 25cm away from the sensor. 106

A.2 Sonar readings from a wall 50cm away from the sensor. 107

A.3 Sonar readings from a wall 75cm away from the sensor. 107

A.4 Sonar readings from a wall 100cm away from the sensor. 108

A.5 Sonar readings from a wall 125cm away from the sensor. 108

A.6 Sonar readings from a wall 150cm away from the sensor. 109
A.7 Sonar readings from a wall 175cm away from the sensor. 109
A.8 Sonar readings from a wall 200cm away from the sensor. 110
A.9 Sonar readings from a wall 225cm away from the sensor. 110
A.10 Sonar readings from a wall 250cm away from the sensor. 111
A.11 Sonar readings from a wall 275cm away from the sensor. 111
A.12 Sonar readings from a wall 300cm away from the sensor. 112
A.13 Sonar readings from a wall 325cm away from the sensor. 112
A.14 Sonar readings from a wall 350cm away from the sensor. 113
A.15 Sonar readings from a wall 370cm away from the sensor. 113
A.16 Sonar readings from a 90 corner at 25cm from the sensor and x=y=17.67cm from the near walls. 114
A.17 Sonar readings from a 90 corner at 50cm from the sensor and x=y=35.35cm from the near walls. 114
A.18 Sonar readings from a 90 corner at 75cm from the sensor and x=y=53.0cm from the near walls. 114
A.19 Sonar readings from a 90 corner at 100cm from the sensor and x=y=70.7cm from the near two walls. 115
A.20 Sonar readings from a 90 corner at 125cm from the sensor and x=y=88.4 from the near two walls. 115
A.21 Sonar readings from a 90 corner 150cm from the sensor and x=y=106.0cm from the near two walls. 115
A.22 Sonar readings from a 90 corner 175cm from the sensor and x=y=123.7cm from the near two walls. 116

A.23 Sonar readings from a 90 corner 200cm from the sensor and x=y=141.4cm from the near two walls. 116
A.24 Sonar readings from a 90 corner 225cm from the sensor and x=y=152.0cm from the near two walls. 116
A.25 Sonar readings from a 90 corner 250cm from the sensor and x=y=176.8 from the near two walls. 117
A.26 Sonar readings from a 90 corner 275cm from the sensor and x=y=194.5cm from the near two walls. 117
A.27 Sonar readings from a 90 corner 300cm from the sensor and x=y=212.13cm from the near two walls. 117
A.28 Sonar readings from a 90 corner 325cm from the sensor and x=y=229.8cm from the near two walls. 118
A.29 Sonar readings from a 90 corner 350cm from the sensor and x=y=247.5cm from the near two walls. 118
A.30 Sonar readings from a 90 corner 370cm from the sensor and x=y=261.6cm from the near two walls. 118

Chapter 1

Introduction

1.1 Mobile Robots

A robot is a mechanical device equipped with different types of sensors working under a certain architecture. The data obtained by the sensors are send to the processor. A new stream of data is created by the processor then send to the controller which gives certain commands to the actuators to do some functions suitable for the robot's task. There are various types of robots such as: a manipulator arm, multiple arm, a multi joint multi-fingered hand, wheeled or legged vehicle, free-flying platform, or a combination of these and each has its own tasks [1]. Mobile robots depend on their movements, either translation or rotation or both of them, to perform different tasks such as: patrolling warehouses and storage areas, transporting materials, and fighting fires. Mobile robots should perform their tasks without the interface of the humans. Our study is concerned only with mobile robots.

Sensors are one of the most important components of the robots. Their importance for robots is the same as the eyes, ears, etc, for the humans. With these

sensors, robots have the ability to work in unknown environments and replace humans when the workplace is not safe. Moreover, they give the robots more flexibility; without them the robot can work in a limited fashion. For example it can perform repetitive task in a well controlled workplace. However, robots should automatically decide what motions to execute in order to achieve a specific task.

There are various researchers who are trying to build robots and furnish them with different sensors to reach fully autonomous capabilities. The resulting robots countered some problems due to limited computational resources, communication, and sensors' uncertainties. To work on a reliable mobile robot becomes an elusive dream for most researchers. The problems facing mobile robots developers come from the fact that the robot must interact with the objects that make up the environment. They must be able to move from a known location to a goal location without any contact with stationary or moving objects. To do this, the robots must be equipped with certain types of sensors that sense the robots' surroundings. Furthermore, they must be equipped with techniques to represent this information in short time by using the limited storage and computational resources of mobile robots. These kinds of sensors are called proximity sensors or time-of-flight (TOF) range finders. There are many types for these sensors such as ultrasonic or sonar sensors, infrared sensors, and laser range finders. TOF ranging systems measure the traveling time needed for a pulse of emitted energy to detect a reflecting surface, then return back to a receiver. Then the distance is obtained from the measured traveling time (round-trip time) and the velocity of the energy wave. Nowadays many researchers are using sonar sensors on their mobile robots. This is generally due to the low cost of these sensors, and the ease with which the sonar data can be processed directly to provide range information. Moreover, the range of sonar

sensors is better when compared to infrared sensors and they are inexpensive when compared to laser range finders. All TOF systems are useful only over a finite range interval, in other words, they are suitable for indoor environments. The operation of mobile robots in an outdoor environment adds more challenges to their tasks. For example, the robots need more sophisticated systems such as GPS for location information and some types of large scale range finders that can detect far obstacles. In addition, these new capabilities may add more expenses [2].

Unfortunately, sonar sensors have many drawbacks such as beam width, which causes uncertainty in the direction of the detected objects. In addition, some environmental factors and the angular uncertainty in the sonar readings cause an error in the measured distance itself. There is also the phenomenon known as *false reflections* that result from detecting mirror like reflectors that cause the energy beam to detect near objects and then go to the receiver, which means big error in the round-trip time [3]. A more detailed discussion about drawbacks of sonar sensors will be presented in Chapter 2. The uncertainty in sonar readings are often modeled by probability theory [4]. In this study we present a novel approach for modeling the uncertainty in sonar sensors by using possibility theory. In the next section, a literature survey of using sonar sensors on mobile robots is presented.

1.2 Literature survey

There are always three questions facing a mobile robot going to navigate in a certain environment:

- What is my current location?
- What is my goal location?

- How can I go there?

The first question is concerned with the location of the robot at any time while it is moving or stationary. The second one deals with planning and tasking, and the third one is about local and global path control [5].

A mobile robot requires a navigation system to determine a reasonable path to its goal based on the information gathered about the crossed environment.

G.Honderd et al. [6] introduce a method for generating a path for a mobile robot between two known points in the robot's environment, the starting point and the goal point. The method depends on a combination between two image processing steps, skeleton extraction and distance transformation. It was a assumed that the robot has a map of the working environment. The map is discretized, that is the operation area is divided into grids of standard size, to which the robot is either allowed entrance (bit value 0) or is not (bit value 1). Their robot was equipped with two types of sensors: collision sensors (tactile sensors) and ultrasonic sensors. The collision system consists of 8 tactile sensors placed on the radius at equal angular distances, and the ultrasonic system consists of four sensors, two are lined in the front and the others are lined in the back. If an obstacle is detected by these tactile sensors the robot starts to rely on sonar sensor to avoid the obstacles and go through a new generated path. The new path is generated between the goal point and the most close reference point near the detected obstacle.

Cho and Lim [7] suggest a path planning method for a mobile robot inside an unknown environment based on certainty grid method. Certainty grids method is a probabilistic, finite-element representation of the robot's spatial knowledge, often called the "Occupancy Grids". The authors introduced a new sensor updating model based on Bayesian formula. By using this model they were able to identify occupied

cells and empty cells while the robot is moving. The cells in the sensor footprint can be numbered and arranged according to their distance from the sensor. The cells at the sensor wedge front fall into the occupied region, and those inside the wedge into the empty region. The probability that a certain cell is occupied or empty can be estimated and updated based on the position of the cell from the sensor location, and the angle from the centerline of the sensor wedge. The proposed method depends on a large number of sonar readings in one scan. The authors used a simulated model for mobile robot equipped with 24 sonar sensors each is 15 degree apart.

Beaufrere and Zeghloul [8] analyze the robot's environment by using a limited number of distance information. The analysis was used for navigation algorithm that uses fuzzy logic approach. In the beginning the robot has no information about its surroundings. It starts to collect distance information by using 12 sonar sensors placed on the horizontal front of the rectangular base of the mobile robot. The available information from the sensors is not enough to describe the environment in detailed fashion. More knowledge about the environment can be obtained by analyzing the available information. This can be done by comparing the distance information provided by three successive sensors. It was shown that there are three types of configurations; edge, vertex, and channel. Based on this information Beaufrere and Zeghloul introduced a path planning algorithm that use fuzzy logic.

Demirli [9], and Demirli and Türksen [10] use GMP with multi antecedent decomposition to make navigation decisions. This navigation method starts by identifying the closest obstacle in the environment, approaching this obstacle, then follows the boundaries of the obstacle without collision. The distance and the direction of the obstacle (antecedents) are identified by using fuzzy sets such as *too-far*, *to the right*, etc. The robot's actions also are described by fuzzy sets such as *turn*

left, *turn right*, etc.

Freedman and Liu [11] use sonar readings to make perceptual hypotheses about the environment. The authors propose modeling the uncertainty in sonar readings by using fuzzy sets. The readings obtained by the sonar can be label as *short*, *medium*, or *long*, where these labels were presented using three non-overlapping intervals between 0 and 1. They consider that these readings are coming from an object as if the acoustic beam was very narrow. This uncertainty model was used with fuzzy inference mechanism to decide the location of an obstacle to the left or to the right of the robot.

The other use of sonar sensors in mobile robot applications is map building. A conventional sonar map can be built from a set of points representing the distances from the sensors to the boundaries of the environment's objects. Building a world model from sonar data is a complex task [12]. A single sonar reading provides information about a larger area with a wide beam spread, but the uncertainty in the directions of the reflected points are correspondingly high. The uncertain data introduce uncertainty into the environment map, and increase the difficulty of navigation tasks. To use sonar data the environment is assumed planner.

Flyn [13] use two types of range finders, infrared sensors, and sonar sensors on a mobile robot for map building. The two sensors were coupled to produce data that are better for building the map than if the sensors were used individually. The sonar sensors measure the distance to an object, but has poor angular resolution due to its beam width. In contrast, the infrared sensors, have good angular resolution in detecting the absence or the presence of objects. By using both sensors to scan the environment, as shown in this study, the robot is able to build a good map of its environment.

Bozma and Kuc [14] propose a method for building a map depending on the characteristics of the echo signals reflected from the environment's boundaries. The proposed method depends on differentiating between smooth, moderately rough, and rough surfaces based on the echo energy and echo duration of the detected signal. The echo energy and echo duration maps of a certain environment were built from different places and then integrated to build the global map. In another study Kuc et al. [15] introduce a method for mapping a certain environment based on the characteristics of the echo returned from planes, corners, and edges.

A sonar sensor made of one transmitter and two receivers was used for mapping an environment by Nagashima and Yuta [16]. By computing the difference in the time of flight (TOF) between left and right rercivers, the inclination angles and the surface normals of the walls inside the environment were determined. While the robot was moving, local maps were built which consists of the normal directions of the walls detected from the current locations of the robot. A global map was constructed from different local maps. The starting location of the robot was known in the environment.

Fuzzy sets are used by Poloni and Vendittelli [17] for map building. The environment can be represented by grids with certain dimensions. Fuzzy sets were used to characterize these grids as occupied or free. The grid state can be determined by projecting the sonar model iteratively on the grids given that the position and the orientation of the grids is known from the sensor location. Several measures are taken from different known points in the environment, then the global map is reconstructed.

Sonar sensors are widely used for mobile robots localization in the literature. Localization is an important issue for mobile robots. Before doing any task, the robot

must be able to determine its initial location inside its environment. A dynamic localization method is introduced by Crowley [18] for a mobile robot navigating a known environment. That is, the initial position in the environment is known. The method depends on extracted line segments from sonar data and then match them with the given global map. The line segments were extracted from sonar readings by using Kalman filter. The model used for modeling the uncertainty in sonar readings considered that the echo detected by the sensor is coming from an arc shaped region. The arc radius represents the uncertainty in the measured distance and the arc length represents the uncertainty in the angle of the detected point.

A method for robot localization based on 360^o scan of the environment while the robot is stationary was introduced by Drumheller [19]. In this method the possible matches between the environment model and the sonar contour obtained from the scan were determined, then possibilities that are inconsistent with the fact that beam can not penetrate solid objects, this is referred to as (sonar barrier test), were excluded. This method is capable of dealing with clutter and moving objects while the robot was scanning the environment.

Demirli and Turksen [20] [21] use fuzzy triangulation technique to determine the location of a mobile robot based on only sonar readings. The method consists of two parts; the first one is called initial localization. In this part the main issue is to determine an approximate location of the robot in the environment after matching the sonar readings with a real map of the environment given to the robot. This part is necessary when the user doesn't have any information about the initial location of the robot, and also it is important when the robot is lost. The second part is called detailed localization, in which the robot location uncertainty can be reduced to a fuzzy region. This fuzzy region identifies different locations of the robot each

with a degree of certainty or confidence. This region is determined based on the combination of two fuzzy sets each representing the location of the robot from a wall in the environment. This method is the only one which considers the problem of angular uncertainty in sonar readings.

Saffiotti and Wesley [22] introduce a perceptual based localization using fuzzy sets. The perceptual-based localization techniques depends on the matching between fuzzy perceptual clues built by the robot while navigating and current clues extracted by the robot. The results of the match are represented by fuzzy sets, and an approximate location of the robot is determined. This method was applied in long scale environments such as corridors. A similar approach was presented in [23]. In this approach the robot describes an object in the environment based on four sonar readings obtained from this object. The uncertainty in the measured distances is represented by using trapezoidal fuzzy sets which are constructed based on confidence intervals. In this study the angular uncertainty in sonar readings is not considered.

Different types of sensors; sonar sensors, infrared, and wheel encoders, are used by Curran and Kyriakopoulos [24] for localization. Extended Kalman filter was used to combine the sensors readings and the information from the known map of the environment. The uncertainty in wheel encoders and sonar sensors is represented by Gaussian distribution.

Beom and Cho [25] include two cylinders having different diameters in the environment to determine the location of the mobile robot by triangulation. The sonar readings obtained from scanning the environment were used to detect the presence of the cylinders, then from the position of the cylinders in the environment, the robot can determine its location. For this method to work, the presence of the

two cylinders within the scan is a must.

Malik and Polkowski [26] estimate the location of a mobile robot based on corner detection by using a vision system. However, vision systems are not practical because they need time to process the collected information. An image consists of huge amount of information that describes the objects inside the robot environment. Moreover, there are huge numbers of relations between these objects to be calculated. For the issue of localization this huge amount of information is not necessary.

In the literature, the uncertainty in sonar readings is often modeled by using *Probability Theory*. However, the probabilistic approach is valid when precise knowledge is available which is not the case of the sonar sensors. Different approaches were used for corner detection such as: vision systems [26] and signal processing methods [27]. These approaches require more time for processing the data to detect the corner. Moreover, localization for mobile robot based on corner detection is not often used because of the large errors in the sonar readings obtained from a corner. In this thesis, the behavior of sonar readings reflected from walls and corners are studied, then new models of angular uncertainty and radial imprecision for sonar readings obtained from corners and walls are proposed. These models are represented by using *possibility theory*, mainly *possibility distributions*. These possibility distributions are used for estimating the initial location of a mobile robot, Pioneer 1, inside a known environment. Pioneer 1 has seven sonar sensors; five in the front, one on the left side, and one on the right side. By combining the information obtained from these sensors, the initial location is estimated based on a corner and wall detection. This is referred to as stationary localization. Since any environment consists of more than one corner, this initial location has more than one possibility. The robot must move in its environment to collect new pieces of evidence that reduce

these possibilities and estimate the current location of the robot. This is referred to as dynamic localization.

1.3 Outline of the Thesis

In Chapter 2, the physical principle of sonar sensors is reviewed. In addition, the factors that affect the sensors' performance are discussed. In Chapter 3, uncertainty modeling theories, including possibility theory, are reviewed. This is followed, in Chapter 4, by using possibility distributions in modeling the angular uncertainty and the radial imprecision in sonar readings reflected from walls and corners. In Chapter 5 these possibility distributions are used in stationary and dynamic localization for Pioneer 1. The discussion and conclusions are presented in Chapter 6.

Chapter 2

Ultrasonic Transducers

2.1 Time of Flight Measurement (TOF)

Most conventional sonar ranging systems employ a single transducer that acts as both a transmitter and receiver. Acoustic signals are scattered whenever a change in the acoustic impedence is encountered by propagating pulse. The acoustic impedence is a product of the density and the speed of sound of the medium. The propagation medium for mobile robots is the air, which has a very small acoustic impedence, and all solid objects exhibit much greater impedence values. Hence whenever any obstacle is encountered, acoustic scattering occurs. After the transmitted pulse encounters an object, an echo may be detected by the same transducer acting as a receiver. The waveform of a typical echo observed at the output of the detection circuit is shown in Figure 2.1. A *threshold* level, denoted τ, is included to suppress erroneous readings generated by electronic or acoustic noise. A TOF system produces a range value computed from the time the echo waveform first exceeds the threshold. This is shown to occur at time t_o in Figure 2.1. A range

measurement R_o is obtained from round-trip time-of-flight by [28]:

$$R_o = \frac{ct_o}{2} \tag{2.1}$$

where c is the speed of sound in air, equal to 343 m/s at room temperature. The minimum range of the transducer is determined by the time required for the transducer to switch from being a transmitter to a receiver and allowing the large transmit voltage transients to decay below the threshold value. On the other hand, the maximum range is usually determined by the range after which no echo is detected by the receiver.

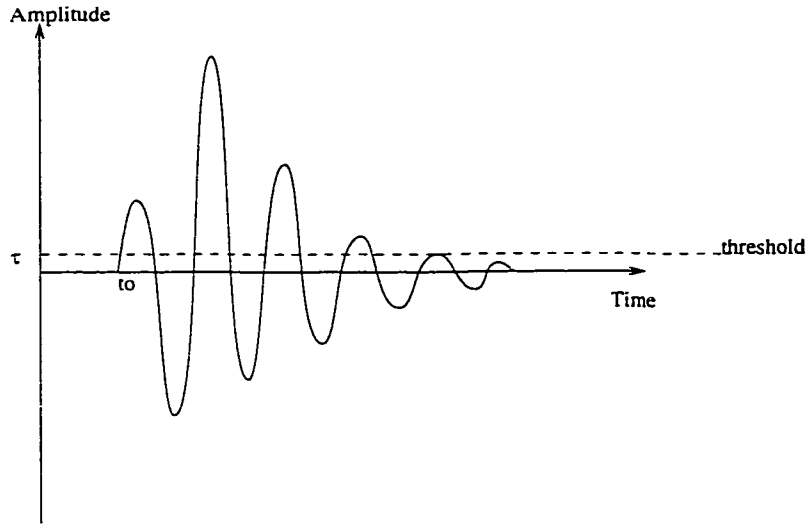

Figure 2.1: Typical echo produced by exciting the ultrasonic transducer with a short-duration voltage pulse.

Sound results from a vibratory mechanical perturbation that travels through an elastic medium as longitudinal wave. Each medium has its effect on the propagation speed of the sound waves. For example the speed of sound in the water is more than its in the air. The wave length of acoustical energy is directly proportional to the speed of propagation as shown below [29]:

$$\lambda = \frac{s}{f} \tag{2.2}$$

where:

λ = wavelength

s = speed of sound

f = operating frequency.

2.2 Factors affecting ultrasonic sensors behavior

The performance of ultrasonic ranging systems is significantly affected by environmental phenomena, transducer design, and target characteristics, as are discussed below.

2.2.1 Environmental Phenomena

1. **Atmospheric Attenuation:**

   The power of the acoustical wave decreases as the traveled distance increases. The following equation represents the relation between the traveled distance and the acoustic power [2]:

$$I = \frac{I_o}{4\pi R^2} \tag{2.3}$$

   where:

   I = intensity (power per unit area) at distance R

   I_o = maximum (initial) intensity

R = range

The medium has an effect on the power of the acoustical wave. This effect can be represented by [2]:

$$I = I_o e^{-2\alpha R} \tag{2.4}$$

where α is the attenuation coefficient for medium. The humidity and dust content of the air affect the value of α as well as the operating frequency does. The maximum range that can be detected by the ultrasonic transducer is dependent on both emitted power and the frequency of operation. By combining the above two equations, the governing equation for intensity can be described by [2]:

$$I = \frac{I_o e^{-2\alpha R}}{4\pi R^2} \tag{2.5}$$

This equation shows how the intensity changes as a function of square of the distance R. This means that the error in the sonar readings is distance dependent. The farther the distance the larger the error. This is one of the many factors that affects the radial imprecision of sonar sensors.

2. **Air Turbulence:**

The variation of wind in the direction and speed, especially in outdoor environment, can affect the speed and the direction of propagation of the acoustical wave. The velocity of propagation of the acoustic wave increases if the wind is in the direction of propagation and decrease if the wind is against the direction of propagation. Cross wind component must be taken into consideration in addition to the component parallel to the path of the wave or against it. Cross wind component forces the acoustic wave off its path causing longer traveling distances, the error in the measured distance. This error is considered when the robot is working outside environments when this effect takes

place. Therefore, sonar sensors are hardly used in outdoor environments.

3. **Temperature:**

   The speed of sound in air is temperature dependent. Temperatures variations occur in indoor environments. These variations produce error in the measured distance. For example, there is an error of 1 foot if there is a change in the temperature over a span of 60^o to 90^oF. This error can be encountered by using a correction factor based on the ambient temperature, which can be measured by an external sensor mounted on the robot.

   The correction of range is based on the ambient temperature in the proximity of the sensor. However, there is a possibility of temperature gradient between the sensor and the target which means that there is existence of the error in the readings still exist. In most industrial environment, where mobile robots are working, this factor has a main effect on sonar readings. However, in office environment, like our environment, this factor doesn't have a great effect on the sonar readings.

2.2.2 Transducer Design

When the radius of the transmitting aperture a is much larger than the acoustic wavelength λ, the radiation forms a beam as shown in Figure 2.2, in which the acoustic energy is a directed beam. This type of transmitter is commonly modeled by flat piston of radius a, enclosed in an infinitely large baffle that is vibrating at frequency f. The beam pattern that is produced has two distinct regions: the *near zone* and the *far zone*. The former extends from the face of the transmitter to a range approximately equal to $\frac{a^2}{\lambda}$. In the far zone, the angular distribution of the energy in the beam is described by Bessel function, and the propagating pulse is

considered to be a series of plane waves sweep across the aperture of the receiver. In addition, in this region the beam diverges with *half-angle* θ_o which represents the first off-axis zero of the Bessel function. *Half-angle* θ_o can be obtained from [30]:

$$\theta_o = sin^{-1}\frac{0.61\lambda}{a} \tag{2.6}$$

where λ = wavelength of the acoustic signal, and a is the transducer diameter. Since the wavelength is frequency dependent, then the beam width so is. The higher the frequency of the emitted energy, the narrower and more directional the beam, and hence greater the angular resolution.

The presence of the beam width has a noticeable effect on the certainty of the data obtained by sonar sensor. Firstly, the beam width adds *radial imprecision* in the measured distances, which results from the fact that the beam is reflected from the portion of the target closest to the sensor. Secondly, when there is an object detected by the sensor, there is uncertainty in the direction of the detected object from the sensor line of sight. Therefore, we can define two types of uncertainty related to sonar sensors; *radial imprecision* , and *angular uncertainty.* In addition to temperature changes, air attenuation, and air turbulence, the beam width has a contribution in the the radial imprecision in the measured distances.

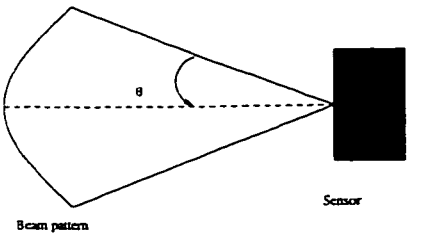

Figure 2.2: A possible beam pattern.

- **Radial Imprecision:**

When a sonar sensor is directed perpendicular to a wall, the error in the reading obtained by the sensor is mainly due to temperature variations, and air attenuation. However, when the sensor directed in a certain angle from the surface normal of the wall, the beam width starts to contribute in the error in the sonar readings. In Figure 2.3 the beam is directed in an angle θ from the surface normal of the wall, this angle is called the *incidence angle*. The expected reading is $|OB|$, but due to the fact that the beam is reflected from the portion of the target closet to the sensor, the reading obtained by the sensor is $|OA|$. The difference between the expected reading and the sensor's one is the radial imprecision. This error is affected by the value of the incidence angle θ.

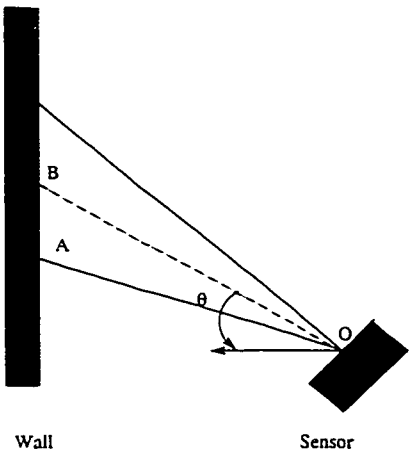

Figure 2.3: The effect of beam width on the sonar readings.

- **Angular Uncertainty:**

  Due to beam width, there is uncertainty in the direction of the object detected by the sensor [21]. It is impossible to determine the direction of the object from the centerline of the sonar beam. But we can say that this object is within

the beam width if it is detected by the sensor. Beam width causes problems in navigation; it can cause small obstacles to appear wider, and openings to appear closed as demonstrated in Figure 2.4.

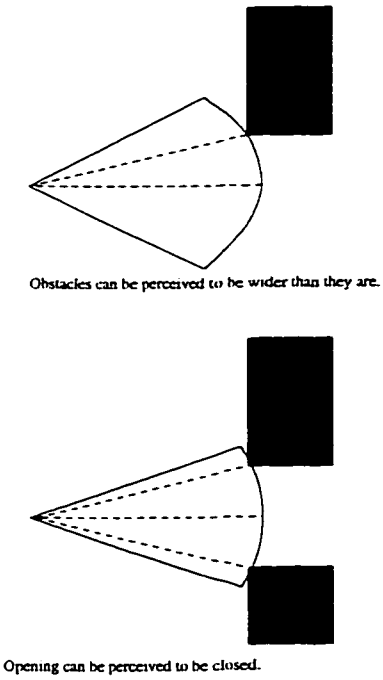

Figure 2.4: Beam spread can cause object surfaces to be blurred.

2.2.3 Target reflectivity

Surfaces can be classified as smooth, moderately rough, and rough surfaces [15]. This classification is based on the Gaussian distribution of the surface irregularities, with zero mean and standard deviation σ_s, and the acoustic wavelength λ. For instance, if $\sigma_s << \lambda$, this surface can be described as smooth. Moderately rough surfaces have $\sigma_s \approx \lambda$, and rough surfaces have $\sigma_s >> \lambda$. In case of smooth surfaces, the angle of reflection is equal to the angle of incidence. The detection of the reflected beam occurs when it falls on the receiver element and produce a signal with an amplitude

greater than the threshold τ. The detected part of the reflected beam is the one that reflects from the portion of the probing beam that is perpendicular to the surface. This kind of reflection is called specular reflection or mirror-like reflection. In rough and moderately rough surfaces, part of the echo energy is scattered in various directions because of surface irregularities. Therefore, the energy of the echo reflected from smooth surfaces is more than the energy of the echo reflected from rough surfaces. The reflection from rough surfaces is called *diffuse reflection.* The surfaces in our environment are flat and smooth. Therefore, the acoustic waves reflect in an angle that is equal to the incidence angle θ.

Each surface has a certain angle after which the sonar beam is not reflected to the transducer. The reason for this effect is that the surface normal of the object becomes out of the beam boundaries as the incidence angle of the sonar beam becomes shallow as shown in Figure 2.5. This angle is called the critical angle and it is a function of the operating frequency and the surface roughness. If a sonar reading returns while the incidence angle is more than the critical angle of the surface, this means that the reflected pulse may not be detected or it will be detected after being bounced off some objects in the environment. This phenomenon is called *false reflections.* In other words, false reflections occur when an object is detected to be very far from its real location (see Figure 2.6). One method of eliminating the possibility of a reading to be false reflection is to combine readings from two consecutive sensors [19] [21]. If the two readings are close none of them is false reflection.

In the next chapter, different causes of uncertainty are reviewed. Moreover, traditional and new theories for tackling uncertain information are discussed. A new procedure for modeling uncertainty in physical measurements by using possibility

distributions is explained.

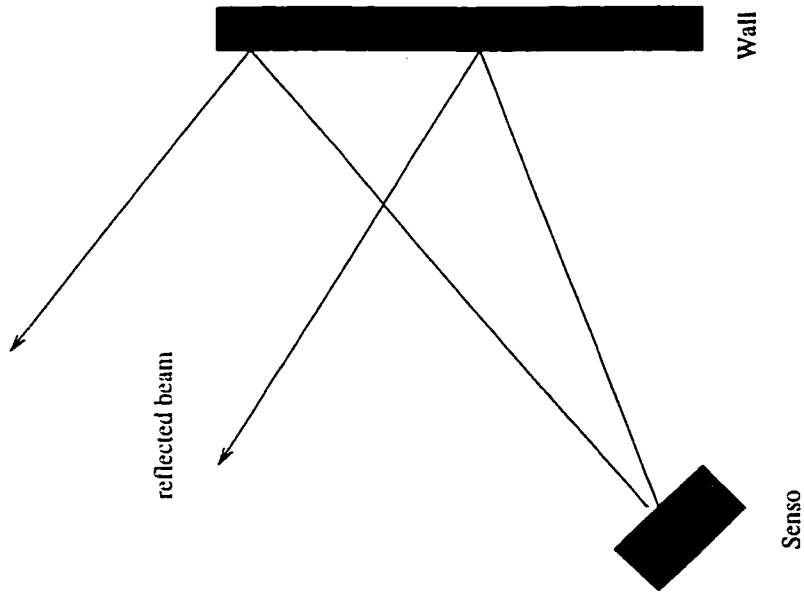

Figure 2.5: Scattering of the echo in different directions when the beam incidence angle is more than the critical angle of the surface.

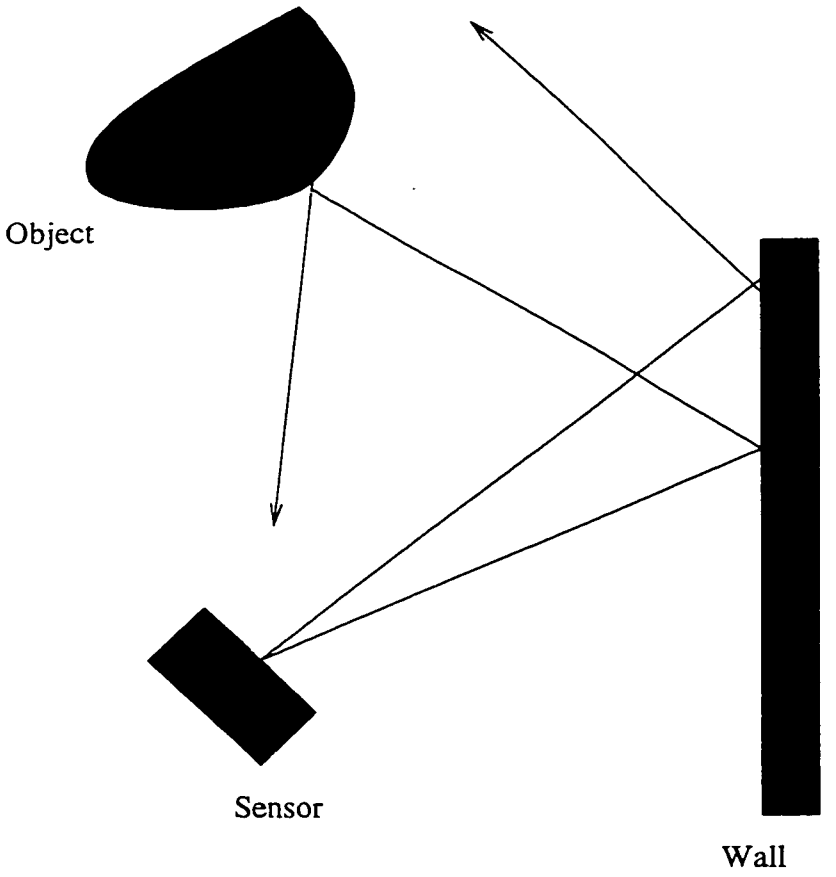

Figure 2.6: Sonar sensor gives a false reading after bouncing off other objects in the environment

Chapter 3

Uncertainty Modeling and Possibility Theory

3.1 Introduction

Through the literature Zimmerman [31], Klir [32], and Dubois and Prade [33] discussed the "Uncertainty"and its causes in different ways. Zimmerman defines the "Uncertainty" as "*the case when one has quantitatively and qualitatively the appropriate information to describe, prescribe or predict deterministically and numerically a system, its behavior or other phenomena*". Anything is not described by this definition shall be called"Uncertain". Furthermore, Zimmerman introduces a classification of uncertainty causes based on the quality and quantity of the available information. He classifies the causes of uncertainty as follows:

1. **Lack of Information:** This cause of uncertainty may be considered as the most frequent one. For example, in decision logic, one calls "Decision Under Uncertainty" the case in which a decision making process lacks information about the possible states of nature that will occur. This kind of information

which is not available can be considered as quantitative lack of information. The counterpart of this kind of information lack is the qualitative one. In this case, the decision making process has information about the probabilities for the occurance of various states but it is not sure which state will occur, this is called "Decision Making Under Risk". "Approximation" is another situation that can be described by lack of information. This depends on the presented situation, for instance, one can consider that the available information is sufficient for his/her situation and he/she does not have or does not want to gather more information to make an exact description. Transition from a situation of "Uncertainty" caused by a lack of information to a situation of "Certainty" can be achieved by increasing the available information or collecting information with better quality which depends on the situation. In our study, there is a lack of information a bout the initial location of the robot in the global map. Because our method depends on detecting a corner and a wall, it is difficult to decide which corner in the global map is detected. Therefore, the robot must collect more information by navigating in its environment to reduce the uncertainty in the initial location.

2. **Abundance of Information (Complexity):**

This is due to the capability of a system to process large amount of data in the same time. To reduce the complexity, people tend to classify the available data into understandable form by using coarser grid or rougher "granularity" or by concentrating on the most important features and neglecting the not useful information for that situation. To do so, especially in scientific activities, some kind of "Scaling"is used. This scaling method is used in obstacle avoidance behaviors. The readings obtained from the sonar sensors are classified in

different ranges, then the robot rotation action is proportional to these ranges. For example, if the obstacle is detected from a close region the robot rotation must be very sharp.

3. **Conflicting Evidence:** This situation occurs when the available information describing two different behaviors of a system are conflicting. The reason for this conflict may be the erroneous available information, it may also be information of irrelevant features of the system is being used, or the model which the observer has of the system is wrong. In this situation, correcting the available information can make transition from "Uncertain" to state of "Certain". False reflection phenomenon is a good example of conflicting pieces of evidence. When the readings of two sonar sensors detecting the same object are very far, this means that the information provided by one sensor is not right.

4. **Ambiguity:** Ambiguity is a situation in which certain information has different meaning based on the situation. From mathematical point of view, it is the situation in which we have one to many mapping. This type of uncertainty can be classified under lack of information because adding more information about the situation may put us in a situation closer to certainty.

5. **Measurement:** Measurement means describing the physical properties of a system or objects such as; weigh, temperature, length, etc. The precision of the measured quantity depends on the accuracy of the used tools. The quality of measuring technology has increased with time but it hasn't reached the perfection. In this situation we have uncertainty about the real measure and the only available information is the indicated measure. This type of

uncertainty may be classified as lack of information.

6. **Belief:** This cause of uncertainty appear when subjective information is available as a kind of belief in a certain situation. This belief is built by an observer from past subjective information about the system (expert) or by statistical data about the system.

Klir [32] found that there are six definitions of "Uncertain" in the dictionary:

- not certainly known, questionable, problematical;
- vague, not definite or determined;
- doubtful, not having certain knowledge, not sure;
- ambiguous;
- not steady or constant, varying;
- liable to change or vary, not dependable or reliable.

When a more detailed investigation about these meanings was done, Klir found that uncertainty can be captured by two classes; vagueness, and ambiguity. The former is related to the difficulty of making sharp or precise distinction in the world. The latter is associated with one-to-many relations, which means situations with two or more alternatives in which the choice between them is left unspecified. In addition, Klir introduced a recent definition of uncertainty based on its connection with the information theory. The most fundamental aspect of this connection is that uncertainty included in any situation is a result of some information deficiency. Information may be incomplete, imprecise, fragmentary, not fully reliable, vague, contradictory, or deficient in some other way.

Dubois and Prade [33] state that imprecision and uncertainty can be considered as two complementary aspects of a single reality, that of imperfect information. It has been observed that much of this information often cannot be obtained as precise and definite numbers for various reasons; imperfect measuring instruments, the fact that the sole source of information is a human being, and the information is imprecise, incoherent, and in any case incomplete. Dubios and Prade could clearly distinguish the concepts of imprecision and uncertainty: imprecision is associated with the content of a piece of information, while uncertainty is associated with its truth. Uncertainty can be judged by means of different qualifiers such as *probable*, *possible*, or *necessary*. *Probable* has two different meanings, one is related to statistical experiments, and the other is related to a subjective judgment. Like probable, *possible* has two interpretations: physical (as a measure of material difficulty of performing an action), and subjective judgment. On the other hand, *necessary* has much stronger notion, in either the physical or the subjective sense. A piece of information will be called *precise* when the subset associated with its value or component cannot be subdivided. There are different qualifiers associated with imprecision, for example, *vague*, *fuzzy*, or *ambiguous*. *Ambiguity* is allied to language. But vagueness or fuzziness in a piece of information resides in the absence of clear boundary to the set of values attached to this piece of information.

From the above overview about uncertainty and it causes it is our opinion that Dubois and Prade's definition of uncertainty is more comprehensive and practical than the others. The readings obtained from sonar sensors contain imprecision in their values and uncertainty in their directions. The imprecision results from the factors that are affecting the behavior of the sound waves in the environment. Thus, the information provided by the sensor is not precise. The direction from which the

sonar readings are obtained, belongs to the field of view of the sensor, but with a degree of truth. Therefore, there is uncertainty in the direction of the reflected beam.

3.2 Types of available information

There are four types of information; numerical, linguistic, interval-valued, and symbolic.

1. **Numerical Information:** Some systems can be described by numbers, but since there are different sources of information, it is not enough to accept only the numbers, but they must be related to a certain scale. There are five types of scale levels; nominal, ordinal, ratio, interval, and absolute scale level. For our scope of research it is enough to distinguish nominal, ordinal, and cardinal scale levels. On the nominal scale level, the number provided only has the function of a name (label). For example, when a distance is defined as *far* or *too far*. On the ordinal scale level, the provided numbers are in an ordering type. Finally, on the cardinal scale level the numbers indicate the differences between the ordered quantities. In our study we are using the ordinal scale to represent the imprecision in the sonar readings, and the uncertainty in the incidence angle. The information about the incidence angle is available in the form of interval information. These intervals represent the range of the incidence angles of the sonar beam that guarantee the reflection of the beam.

2. **Interval-Information:** In this case the available information is described over a certain range. In other words, this information is valid over a certain interval on the ordinal scale.

3. **Linguistic Information:** This means that the available information take the form of the natural language and is not in the formal language.

4. **Symbolic Information:** Sometimes information is introduced by symbols. There are different ways to introduce these symbols, either by numbers, letters, and pictures, or by words. The words is not obvious as the other three types because it is known that words have natural meanings while the others do not have.

The types of available information in our study, obtained from sonar sensors, are numerical information and interval information.

3.3 Modeling of Uncertainty

3.3.1 Traditional Models for Uncertainty

Traditionally, two methods of representing imperfect information are available: probability theory and what is known as interval analysis. Probability theory is a tested mathematical theory: it has a clear set of axioms and it has has been developed extensively. The basic axiom in probability is that the probability of disjoint events can be added. There are three schools that interpreted probability theory in different ways. The first school interpretation is based on "Calculus of Chances" in games of chance, where the probability of an event is defined as proportion between the number of favorable cases to the total number of possible cases. The second interpretation belongs to what is known as "Frequentist School" in which the probability of an event is defined as limit of the frequency of appearance of this event. The third school is called "Subjective School", by whom the probability is defined as

proportional to sum an individual would like to pay if a proposition that he asserts prove false.

Interval analysis, used extensively by the physicist, tends to represent the inaccuracy in a measuring instrument, in the form of interval, through the measured quantity. Mathematically, one evaluates the image of a function whose arguments are subsets. Interval analysis has no gradation: while one does not know the exact value of a parameter, one does know the exact limits of its domain of variation.

It commonly occurs that imprecision of the error-of-measurement kind is present at the heart of a series of trials intended to exhibit a random phenomenon. In such a case it can be observed that one can hardly represent the information in a purely probabilistic form without introducing further hypothesis. In fact, a hypothesis fundamental to the applicability of probability to statistics is that there should be relation between the sample space and the event space: to every event there is an associated the set of sample points that realize it(which is nonempty if the event is not impossible), and for every point of distinct events there is at least one sample point that realizes one but not the other. This hypothesis therefore allows the sure event to be partitioned into elementary events, each corresponding to a specific sample point. In the case of collection of statistical data, this amounts to supposing that there is a nontrivial partition of the set of realizations such that the result of each experiment can be associated with one and only one element of this partition.

A probabilistic model is suitable for the expression of precise but dispersed information. Once the precision is lacking, one tends to question the validity of the model. Because sonar readings are imprecise, probability model is not suitable to represent this imprecision.

3.3.2 New Methods for Modeling Uncertainty

Nowadays, non-probabilistic mathematical methods for the representation of uncertainty are developed. Klir [34] calls these methods " General Information Theory (GIT)". GIT consists of fuzzy sets, systems, and logic; fuzzy measures; random set and Dempester-Shafer evidence theory; possibility theory; imprecise probabilities; probability bounds; rough set theory; and others. The importance of such theories become evident when used in engineering applications. Fuzzy systems theory is the most prevalent component of GIT, and until recently possibility theory has been tightly linked to fuzzy systems [35]. Traditional fuzzy semantics is based on the interpretation of fuzzy sets as representations of human, cognitive categories. The other components of GIT are measurement methods other than cognitive modeling. Semantics of possibility theory beyond the traditional fuzzy semantic has been extended to include the modeling of complex systems without regard to the presence of human, cognitive agent.

3.4 Fuzzy Measures

Definition 1 (Fuzzy Measure) *Given a universal set Ω and the set of all its crisp subsets (power set) $\mathcal{P}(\Omega)$, a function*

$$g : \mathcal{P}(\Omega) \rightarrow [0, 1]$$

is defined such that $g(A)$ indicates the degree of certainty that an element of Ω belongs to a certain crisp set A. In order to achieve this purpose, function g must meet the following requirements:

- $g(\phi) = 0$ *and* $g(\Omega) = 1$

- *for all* A, $B \in \mathcal{P}(\Omega)$, *if* $A \subseteq B$, *then* $g(A) \leq g(B)$.

The first requirement is called boundary requirement and it says that, the empty set does not contain any element, therefore, it cannot contain the element of our interest, either. On the contrary, the universal set, contains all elements, therefore, the presence of our element in the universal set is sure. The second requirement is called the monotonicity requirement, which states that the evidence of the membership of an element in a subset of another set must be smaller or equal to the evidence that the element belongs to the big set itself. Since both $A \cap B \subseteq A$ and $A \cap B \subseteq B$ for any two sets A and B, it follows from the monotonicity requirement of fuzzy measures that the inequality:

$$g(A \cap B) \leq \min[g(A), g(B)] \tag{3.1}$$

is satisfied for any three sets A, B, $A \cap B \in \mathcal{P}(\Omega)$. Similarly, since both $A \subseteq A \cup B$ and $B \subseteq A \cup B$ and $B \subseteq A \cup B$ for any two sets, the monotonicity of fuzzy measures implies that the inequality

$$g(A \cup B) \geq \max[g(A), g(B)] \tag{3.2}$$

is satisfied for any three sets A, B, $A \cup B \in \mathcal{P}(\Omega)$.

3.5 Evidence Theory

Evidence theory is based on two dual non additive measures: *belief* measures and *plausibility* measures. Given a universal set Ω, assumed here to be finite, a belief measure is a function:

$Bel : \mathcal{P}(\Omega) \rightarrow [0, 1]$

such that $Bel(\phi)$=0, $Bel(\Omega)$=1, and

$Bel(A_1 \cup A_2 \cup \ldots \cup A_n) \geq \sum_j Bel(A_j)$

$$- \sum_{j<k} Bel(A_j \cap A_k) + \ldots + (-1)^{n+1} Bel(A_1 \cap A_2 \cap \ldots \cap A_n) \tag{3.3}$$

For each $A \in \mathcal{P}(\Omega)$, $Bel(A)$ is interpreted as the degree of belief that a given element of Ω belongs to the set A.

When the sets $A_1, A_2, \ldots, A_n$, in equation (3.3) are pair-wise disjoint, the inequality requires that the degree of belief related to singleton sets. In this case the belief measure becomes a probability measure. This means that probability measures are special cases of belief measures for which the equality in (3.3) is always satisfied.

Equation (3.3) implies the monotonicity requirement of fuzzy measure, then the following fundamental property of belief measures can be defined [34]:

$$Bel(A) + Bel(\overline{A}) \leq 1 \tag{3.4}$$

Another measure called the plausibility measure PI is coupled with the belief measure, and it can be defined by the equation

$$PI(A) = 1 - Bel(\overline{A}) \tag{3.5}$$

for all $A \in \mathcal{P}(\Omega)$. Similarly,

$$Bel(A) = 1 - PI(\overline{A}) \tag{3.6}$$

From the above equations it is shown that *Belief* measures and *Plausibility* measures are mutually dual. But *Plausibility* measures can be defined separately from *Belief* measures. Therefore, a *Plausibility* measure is a function

$$PI : \mathcal{P}(\Omega) \rightarrow [0, 1] \tag{3.7}$$

such that $PI(\phi) = 0$, $PI(\Omega) = 1$. and

$PI(A_1 \cap A_2 \cap \ldots \cap A_n) \leq \sum_j PI(A_j)$

$$- \sum_{j \leq k} PI(A_j \cup A_k) + \ldots + (-1)^{n+1} PI(A_1 \cup A_2 \cup \ldots \cup A_n) \tag{3.8}$$

then, similar to (3.4)

$$PI(A) + PI(\overline{A}) \geq 1 \tag{3.9}$$

Belief and *Plausibility* measures can conveniently be defined by a function

$$m : \mathcal{P}(\Omega) \rightarrow [0, 1] \tag{3.10}$$

such that $m(\phi)$=0 and

$$\sum_{A \in \mathcal{P}(\Omega)} m(A) = 1 \tag{3.11}$$

This function is called a basic probability assignment. For each set $A \in \mathcal{P}(\Omega)$, the value $m(A)$ express the degree to which all available and relevant evidence emphasizes the claim that a certain element of Ω belongs to set A. This value $m(A)$ associated with only one set A does not represent any additional claim regarding subsets of A. If there is some additional information strengthening the claim that the element belongs to a subset of A, say $B \subseteq A$, it must be expressed by another value $m(B)$.

Even though there is a similarity between equation (3.11) and the equation for probability distribution function, there is a fundamental difference between them. The latter is defined on Ω, while the former is defined on $\mathcal{P}(\Omega)$.

Basic probability assignment has the following properties:

- it is not required that $m(\Omega) = 1$;
- it is not required that $m(A) \leq m(B)$ when $A \subseteq B$; and

- no relationship between $m(A)$ and $m(\overline{A})$ is required.

It follows from these properties that the basic assignments are not fuzzy measures. However, given a basic assignment m, a belief measure and a plausibility measure are uniquely determined for all set $A \in \mathcal{P}(\Omega)$ by the formulas

$$Bel(A) = \sum_{B|B \subseteq A} m(B) \tag{3.12}$$

$$PI(A) = \sum_{B|A \cap B \neq \phi} m(B) \tag{3.13}$$

From equation (3.12), $m(A)$ and $Bel(A)$ has the following meaning: $m(A)$ represents the degree of evidence or belief that an element belongs to the set A alone, and $Bel(A)$ represents the total evidence or belief that the element belongs to A as well as to the various special subsets of A. The plausibility measure $PI(A)$, as defined in (3.13), has a different meaning: it represents not only the total evidence or belief that an element belongs to set A or to any of its subsets, but also the additional evidence associated with sets that overlap with A. Hence,

$$PI(A) \geq Bel(A) \tag{3.14}$$

for all $A \in \mathcal{P}(\Omega)$.

Every set $A \in \mathcal{P}(\Omega)$ for which $m(A) \geq 0$ is usually called a focal element of m. Focal elements are subsets of Ω on which the available evidence focuses. When Ω is finite, m can be fully characterized by a list of its focal elements A with the corresponding values $m(A)$. The pair $\langle \mathcal{F}, m \rangle$, where $\mathcal{F}$ and m denote a set of focal elements and associated basic assignment, respectively, is often called a body of evidence.

Total ignorance is expressed in terms of the basic assignment by $m(\Omega) = 1$ and $m(A) = 0$ for all $A \neq \Omega$. That is, we know that the element is in the universal

set, but we have no evidence about its location in any subset of Ω. It follows from (3.12) that the expression of total ignorance in terms of the corresponding belief measure is exactly the same: $Bel(\Omega) = 1$ and $Bel(A) = 0$ for all $A \neq \Omega$. However, the expression of total ignorance in terms of the associated plausibility measure is quite different: $PI(\phi) = 0$ and $PI(A) = 1$ for all $A \neq \phi$. This expression follows directly from 3.13.

3.6 Possibility Theory

Possibility theory is a special branch of evidence theory that deals only with bodies of evidence whose focal elements are nested. Special counterparts of *Belief* measures and *Plausibility* measures in possibility theory are called *Necessity* and *Possibility* measures, respectively. Let a given finite body of evidence $\langle \mathcal{F}, m \rangle$ be nested. Then, the associated belief and plausibility measures have the following properties for all $A, B \in \mathcal{P}(\Omega)$:

$$Bel(A \cap B) = \min[Bel(A), Bel(B)] \tag{3.15}$$

$$PI(A \cup B) = \max[Bel(A), Bel(B)] \tag{3.16}$$

Since necessity measures are special *Belief* measures and *Possibility* measures are special plausibility measures, they satisfy equations (3.4) - (3.6) and (3.9). Hence,

$$Nec(A) + Nec(\overline{A}) \leq 1 \tag{3.17}$$

$$Pos(A) + Pos(\overline{A}) \geq 1 \tag{3.18}$$

$$Nec(A) = 1 - Pos(\overline{A}) \tag{3.19}$$

Furthermore, it follows immediately from (3.15) and (3.16) that

$$\min[Nec(A), Nec(\overline{A})] = 0 \tag{3.20}$$

$$\max[Pos(A), Pos(\overline{A})] = 1 \tag{3.21}$$

3.7 Possibilistic approach for modeling uncertainty in physical measurements

When we need Possibilistic data, it is almost always preferable to collect them in a form similar to their Possibilistic representation. Thus objective empirical measurement procedures are required that yield data in accordance with semantic aspects of possibility theory. The additivity of frequency data results from the specifity of observations of singletons. Therefore, we need non-specific data which are possibly non-disjoint, and thus not yielding traditional frequency distributions. This is the concept of set statistics. Joslyn Cliff [36] used interval valued set statistics, obtained from studying a certain physical phenomenon, and then their empirical random sets, to develop a method for constructing possibility distributions in the form of Possibilistic histograms [37] [38] [39] [40] [36] [41].

3.8 Possibilistic measurement

To derive a possibility distribution from an empirical source, it is necessary to observe subsets $B_s \subseteq \Omega$. These subsets are called *general measuring record* as defined below:

Definition 2 (Measuring Record) *A general measuring record is a vector*

$$\vec{B} := \langle B_s \rangle = \langle B_1, B_2, \ldots, B_M \rangle$$

where $1 \leq s \leq M$, *and* B_i*'s are subsets of* Ω.

Definition 3 (Empirical Focal Set) *Given a general measuring record* $\vec{B}$, *let*

$$\mathcal{F}^E := \{B_s\} = \{B_1, B_2, \ldots, B_N\}$$

be an empirical focal set derived by eliminating the duplicates from $\vec{B}$, *where:* $1 \leq j \leq N$, $N \leq M$, $\forall B_j \in \mathcal{F}^E, \exists B_s \in \vec{B}, B_s = B_j$.

Definition 4 (Set-Frequency Distribution) *Given a general measurement record* $\vec{B}$ *and empirical focal set* $\mathcal{F}^E$, $C_j := C(B_j)$ *is the number of occurrences of* B_j *in* $\vec{B}$ $\forall B_j \in \mathcal{F}^E$. *Then a set-frequency distribution is a function* $m^E : \mathcal{F}^E \rightarrow [0, 1]$ *where:* $m^E(B_j) := \frac{C_j}{\sum_{B_j \in \mathcal{F}^E} C_j}$, $\quad m_j^E := m^E(B_j)$.

Definition 5 (Random Set) *Given an evidence function* m, $\mathcal{S} := \{\langle B_j, m_j \rangle : m_j > 0\}$ *is a finite random set where* $B_j \subseteq \Omega$ *and* $m_j := m(B_j)$

The mathematics of the random sets is complicated, but for our purposes, and especially in the finite case, they can be seen simply as random variables taking values on subsets of Ω.

3.9 Possibilistic Histograms

Possibility distributions derived from consistent empirical random sets can be properly described as Possibilistic histograms, similar to ordinary (stochastic) histograms, but resulting from overlapping interval observations, and thus governed by the mathematics of random sets.

Definition 6 (Possibilistic Histograms) *Assume $\mathcal{S}^E$ is consistent, or is a consistent approximation. Then a Possibilistic histogram is the possibility distribution π determined from the plausibility assignment formula (3.13).*

The Possibilistic histogram can be obtained as follows:

$$\pi(\omega) = \sum_{B_j \ni \omega} m_j^E = \frac{\sum_{B_j \ni \omega} C_j}{M} \tag{3.22}$$

Definition 7 (Empirical Focal Set Components) *Let $\Omega = \Re$, and assume a random set $\mathcal{S}^E$.*

- Let each observed subset $B_j \in \mathcal{F}^E$ be closed interval denoted by its endpoints $B_j := [l_j, r_j]$
- Let $l_{(j)}$ and $r_{(j)}$ be the order and "reverse order" statistics of the left and right end points, so that

$$l_{(1)} \leq l_{(2)} \leq \ldots \leq l_{(N)}, \qquad r_{(N)} \leq r_{(N-1)} \leq \ldots \leq r_{(1)} \tag{3.23}$$

  are permutation of the l_j, r_j.
- Denote the vectors of endpoints and ordered endpoints as

  $\vec{E}^l := \langle l_1, l_2, \ldots, l_N \rangle$,

  $\vec{E}^r := \langle r_1, r_2, \ldots, r_N \rangle$,

  $\vec{E} := \langle l_1, l_2, \ldots, l_N, r_1, r_2, \ldots, r_N \rangle$,

  $\hat{E} := \langle l_{(1)}, l_{(2)}, \ldots, l_{(N)}, r_{(N)}, r_{(N-1)}, \ldots, r_{(1)} \rangle$.
- If $\mathcal{F}^E$ is consistent then

  1. $\max_j l_j = l_{(N)} \leq r_{(N)} = \min_j r_j$,

     so that $C(\pi) = [l_{(N)}, r_{(N)}]$.

2. the joint linear order on $\hat{E}$ is

$$l_{(1)} \leq l_{(2)} \leq \ldots \leq l_{(N)} \leq r_{(N)} \leq r_{(N-1)} \leq \ldots \leq r_{(1)} \tag{3.24}$$

Definition 8 (Possibilistic Histogram Components)

- Let

  $E := \{e_k\}, \quad E^l := \{e^l_{k^l}\}, \quad E^r := \{e^r_{k^r}\}$

  be the sets of endpoints with duplicates omitted from $\vec{E}$, $\vec{E}^l$ and $\vec{E}^r$ respectively, and ordered as in (3.24), where

  $\forall e_k \in \vec{E}, \quad \forall e^r_{k^r} \in \vec{E}^r, \quad \forall e^l_{k^l} \in \vec{E}^l,$

  $1 \leq k \leq Q := |E|, \quad 1 \leq k^l \leq Q^l := |E^l|, \quad Q^r := |E^r| \geq k^r \geq 1,$

  so that $E = E^l \cup E^r$ and $Q^l + Q^r = Q$.

- Let

$$G_k := \begin{cases} [e_k,\, e_{k+1}) & e_k,\, e_{k+1} \in E^l \\ [e_k,\, e_{k+1}] & e_k \in E^l,\, e_{k+1} \in E^r \\ (e_k,\, e_{k+1}] & e_k,\, e_{k+1} \in E^r. \end{cases}$$

  for $1 \leq k \leq Q - 1$.

- Let

$$T_k := \{\langle x, y\rangle \in \Re \times [0,1] : x \in G_k, y = \pi(x)\}.$$

  for $1 \leq k \leq Q - 1$

- For an interval $I \in \Re$ and $y \in [0,1]$, let $\pi(I) = y$ denote that $\forall x \in I$, $\pi(x) = y$. For more explanation see the example in section 3.9.3.

Definition 9 (Possibilistic Histogram Form) *If π is a Possibilistic histogram, then*

1. $\mathbf{C}(\pi)=[e^l_{Q^l}, e^r_{q^r}]$, is the core of the possibility distribution π.
2. $\mathbf{U}(\pi)=[e^l_1,e^r_1]=\cup_{k=1}^{Q-1}G_k$, is the support of the possibility distribution π.
3. $\pi([\ -\infty, e^l_1))=\pi((e^r_1, \infty\ ])=0$.

3.9.1 Continuous Approximation

Definition 10 (Continuous Approximation) *Let $\overline{\pi}$ be a continuous possibility distribution which approximates a Possibilistic histogram π.*

One of the most significant differences between Possibilistic and stochastic histograms is that the former are collections of the intervals T_k, not discrete points. Therefore, normal interpolation or approximation methods(such as curve-fitting or maximum-likelihood estimation) are not appropriate. Instead, a representative set of points from the intervals T_k should be selected from π, and then a continuous curve $\overline{\pi}$ is fitted to them.

3.9.2 Candidate Points

Definition 11 (Possibilistic Histogram Candidate points) *Assume a Possibilistic histogram considered as a locus of points*

$$\pi := \{\langle e_k, \pi(e_k)\rangle\} \subseteq \Re \times [0,1]$$

Then denote:

- The left and right endpoints of each of the T_k, $1 \leq k \leq Q-1$:

$$t_k^l := \begin{cases} \langle\, e_k,\, \pi(e_k)\,\rangle, & e_k \in E^l \\ \langle\, e_k,\, \pi(e_{k+1})\rangle, & e_k \in E^r. \end{cases}$$

$$t_k^r := \begin{cases} \langle\, e_{k+1},\, \pi(e_k)\,\rangle, & e_k \in E^l \\ \langle\, e_{k+1},\, \pi(e_{k+1})\rangle, & e_k \in E^r. \end{cases}$$

- The midpoints of each of the T_k, $1 \leq k \leq Q-1$:

$$h_k := \left\langle \frac{e_k + e_{k+1}}{2}, \pi(e_k) \right\rangle$$

- The midpoint of the core:

$$c := h_{Q^l} = \left\langle \frac{l_{(N)} + r_{(N)}}{2}, 1 \right\rangle$$

- The endpoints of the support on the axis:

$$l := t_1^l = \left\langle l_{(1)}, 0 \right\rangle, \qquad r := t_{Q-1}^r = \left\langle r_{(1)}, 0 \right\rangle.$$

- The set of all the interval mid- and end-points to which a continuous curve may be fit:

$$K' := \{t_k^l, t_k^r, h_k\}.$$

- The set of all the interval mid- and end-points to which a continuous curve actually will be fit: $K \subseteq K'$.

- Finally, the set of all the points to which the curve will be fit:

$$D := \{c, l, r\} \cup K \subseteq \pi$$

where K may be any subset of K'. Note that $K = \phi$ is allowed.

3.9.3 Example

Consider the example in Figure 3.1. The top shows two intervals in dashed lines below the axis, each of which is observed once. The components of the T_k with $N = M = 2$, $Q = 3$, and $c = h_2$ are also shown. t_1^l and t_3^r are excluded from K due conflicts with l and r, leaving a candidate set:

$$K' = \{h_1, t_1^r, t_2^l, t_3^l, h_3, t_3^r\}$$

Any subset $K \subseteq K'$ (including the empty set) can be chosen as long as it does not contain either set of conflicts $\{t_1^r, t_2^l\}$ or $\{t_2^r, t_3^l\}$.

3.9.4 Piecewise Linear Approximations

Once a set of points is selected, a variety of curve-fitting methods are available to determine $\overline{\pi}$. The simplest and most direct is to connect them with line segments, producing a piecewise linear, continuous distribution. Three of these are shown in Fig 3.1 for the sets $K = \{h_1, t_2^l, t_2^r, h_3\}$, ϕ, $\{t_1^r, t_3^l\}$. An advantage of the line-segment method is that the approximated $\overline{\pi}$ has the same form as the fuzzy intervals and numbers typically used in fuzzy systems applications.

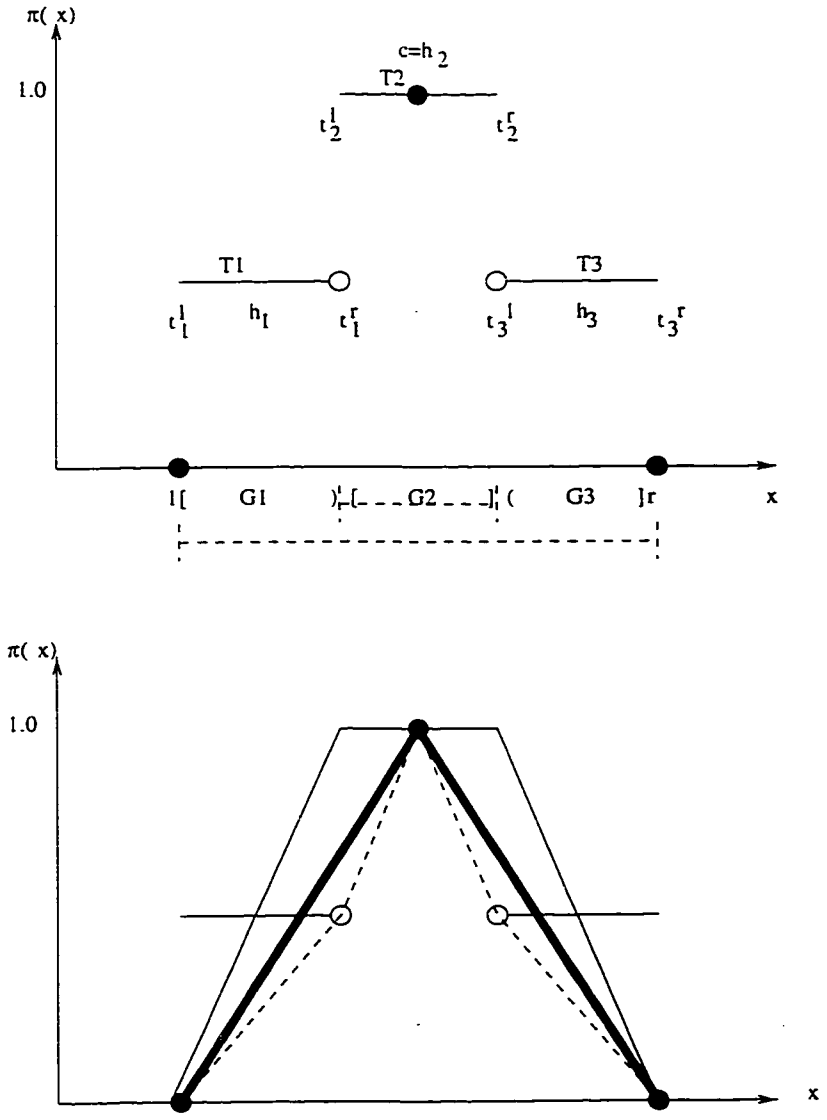

Figure 3.1: A simple Possibilistic histogram with its candidate points (top). Three examples of piecewise linear continuous approximations (top).

Chapter 4

Modeling Uncertainty in Sonar Sensors

In this chapter models of angular uncertainty and radial imprecision for sonar readings reflected from a wall and a 90° corner are represented by using possibility distributions discussed in Chapter 3. These models are used in estimating the initial stationary location of a mobile robot when its sensors detect a wall and a corner at the same time. To build these possibility distributions, it is important to study the behavior of sonar readings when they are reflected from a wall and a 90° corner, two common components of any indoor environment. The experimental setup described in Section 1 is used for this purpose. In Section 2 the angular uncertainty and radial imprecision models for one sonar sensor is presented. Then the angular uncertainty and the radial imprecision are reduced by combining the readings from another sensors that are reflected from the same wall. In Section 3 similar models are presented if the reflecting object is a corner. Finally, in Section 4 these models, for the corner and the wall, are used for localization of mobile robot, Pioneer 1, inside a known environment.

4.1 Experimental Setup

Our experimental setup consists of a sonar sensor, a rotary table, a computer, and a mobile robot. The sonar sensor is mounted on a rotary table and it is wired directly to Pioneer 1. The robot receives the sonar firing commands from the computer through a special software called Saphira. Both the robot and the computer have radio modems for communication Figure 4.1. The rotary table is controlled by the computer through a serial link. The rotary table is adjusted to rotate in steps of two degrees.

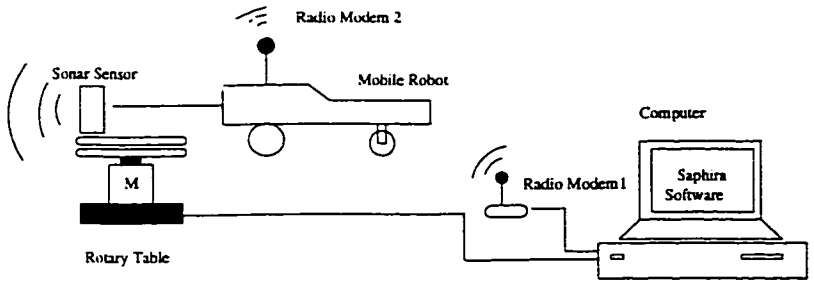

Figure 4.1: Experimental setup.

The sonar sensor is placed in front of a wall at distance d and an initial direction perpendicular to the wall, i.e., $\theta = 0$. A command is issued from the computer to the robot to fire the sonar sensor. After the sensor detects the echo received from the wall the reading that represents the distance to the wall is sent directly to the computer. This reading represents the measured distance to the wall. The error is calculated as the difference between the actual distance and the measured one. The direction of the sonar sensor (the incidence angle θ) is increased in a step of 2^o by commanding the rotary table to rotate to the left one step Figure 4.2, then the sensor is fired and the measured distance is registered as well as the direction θ.

This procedure was continued until no readings were received from the wall. The direction θ is then decreased in steps of two degrees by rotating the table to the right and the measured distances as well as the direction were registered until no echo is received. This experiment is then repeated for different distances: 25, 50, 75, 100, 125, 150, 175, 200, 225, 250, 275, 300, 325, 350, and 370cm. This last distance represents the maximum range of the sonar sensor, i.e., after 370cm there is no reading coming from the wall. The second set of experiments is done while the sensor is facing a 90° degree corner. The same steps in the case of the wall are repeated and the results were tabulated in Tables A.1 to A.30 in appendix A.

The most significant issue for representing the angular uncertainty in sonar sensors is the *field of view* of these sensors when the sensor's readings are reflected from walls and corners. The *field of view* can be defined as the interval of angles which contains the sensor direction when an object is detected. Table 4.1 summarizes the field of view of a sonar sensor at different distances from a wall. Following the procedure discussed in Chapter 3, a possibility distribution that represents the angular uncertainty in sonar readings can be formed.

4.2 Modeling angular uncertainty and radial imprecision for sonar readings reflected from a wall

In this section, angular uncertainty for a sonar sensor is represented by possibility distributions. Based on the assumption that the field of view is not a function of the distance d as the Table 4.1 shows, the intervals of the field of view of the sensor can be considered as random sets obtained from an empirical source. Then possibility

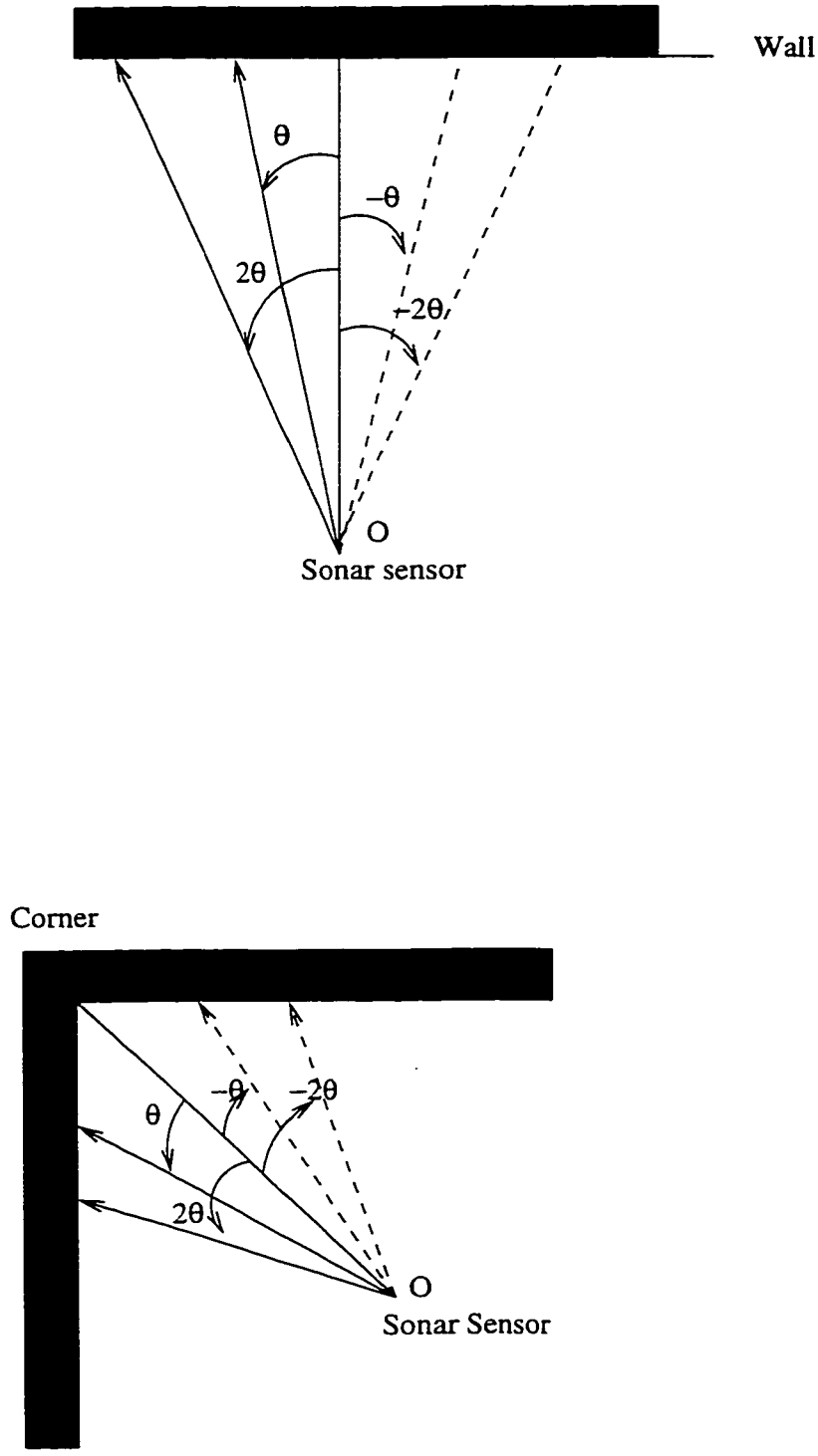

Figure 4.2: Experiments for studying the behavior of the sonar sensor when it is in front of a wall (top) and a corner (bottom).

Distance from a wall(cm)	Field of view of the sensor
50	[-14, 14]
75	[-10, 12]
100	[-12, 14]
125	[-10, 12]
150	[-12, 12]
175	[-10, 16]
200	[-10, 14]
225	[-10, 12]
250	[-10, 14]
275	[-10, 14]
300	[-10, 14]
325	[-10, 14]
350	[-10, 12]
370	[-10, 12]

Table 4.1: The field of view of the sonar sensor at different distances from a wall.

distributions can be constructed as follows:

- the general record is represented by the vector

  $\vec{B} := \Big\langle [-14, 14], [-10, 12], [-12, 14], [-10, 12],$
  $[-12, 12], [-10, 16], [-10, 14], [-10, 12], [-10, 14],$
  $[-10, 14], [-10, 14], [-10, 14], [-10, 12], [-10, 12] \Big\rangle$

- the empirical focal set is given by:

  $$\mathcal{F} := \{[-10, 12], [-10, 14], [-14, 14], [-12, 12], [-10, 16], [-12, 14]\}$$

  Where N=6, and M=14.

- the set frequency distribution is given by: $m(B_1 = [-10, 12]) = 5/14$, $m(B_2 = [-10, 14]) = 5/14$, $m(B_3 = [-14, 14]) = 1/14$, $m(B_4 = [-12, 12]) = 1/14$, $m(B_5 = [-10, 16]) = 1/14$, $m(B_6 = [-12, 14]) = 1/14$.

- the order and reverse order statistics of the left and right endpoints is

  $-14 \leq -12 \leq -12 \leq -10 \leq -10,\ 12 \leq 12 \leq 12 \leq 14 \leq 14 \leq 14 \leq 16$

- The vectors of endpoints and ordered endpoints are:

  $\vec{E}^r := \langle -10, -10, -14, -12, -10, -12 \rangle$, $\vec{E}^l := \langle 12, 14, 14, 14, 12, 16, 14 \rangle$, $\hat{E} := \langle -14, -12, -12, -10, -10, 12, 12, 12, 14, 14, 14, 16 \rangle$

- the sets of endpoints with duplicates omitted from $\vec{E}$, $\vec{E}^l$, $\vec{E}^r$ are: $E := \{-14, -12, -10, 12, 14, 16\}$, $E^l = \{-14, -12, -10\}$, $E^r = \{12, 14, 16\}$ note that $1 \leq k \leq Q = 6$, and $1 \leq k^l \leq Q^l = 3$, $1 \leq k^r \leq Q^r = 3$.

- consistency requirement:

  $\max_j l_j = l_{(N)} \leq r_{(N)} = min_j r_j$ $-10 \leq 12$. So that the core of the possibility distribution is [-10, 12]. The core represents the case of high confidence that the sonar beam can be reflected from this field of view.

- G_k can be defined as follows:

  $G_1 := [-14, -12)$, $G_2 := [-12, -10)$, $G_3 := [-10, 12]$, $G_5 := (12, 14]$, $G_5 := (14, 16]$.

- T_k can be obtained as follows:

  $T_1 := \{\langle x_1, \pi([-14, -12)) = \pi(-14) = 1/14 \rangle : x_1 \in G_1\}$

  $T_2 := \{\langle x_2, \pi([-12, -10)) = \pi(-12) = 1/14 + 2/14 = 3/12 \rangle : x_2 \in G_2\}$

  $T_3 := \{\langle x_3, \pi([-10, 12]) = 1 \rangle : x_3 \in G_3\}$

  $T_4 := \{\langle x_4, \pi((12, 14]) = \pi(14) = 8/14 \rangle : x_4 \in G_4\}$

  $T_5 := \{\langle x_5, \pi((14, 16]) = \pi(16) = 1/14 \rangle : x_5 \in G_5\}$

- The core of this possibility distribution is [-10, 12] which represents the case of high confidence that the sonar beam can be reflected from this field of view, i.e., from [-10, 12]. The support of the possibility distribution is [-14, 16] which represents a random set which has less specifity, i.e., it is not as specific as the core.

- the left and right endpoints of each of the T_k are:

  $t_k^l := \{\langle -14, 1/14\rangle, \langle -12, 3/14\rangle, \langle -10, 1\rangle, \langle 12, 8/14\rangle, \langle 14, 1/14\rangle\}$

  $t_k^r := \{\langle -12, 1/14\rangle, \langle -10, 3/14\rangle, \langle 12, 1\rangle, \langle 14, 8/14\rangle, \langle 16, 1/14\rangle\}$

- the midpoints of each of the T_k are:

  $h_k : \{\langle -13, 1/14\rangle, \langle -11, 3/14\rangle, \langle 1, 1\rangle, \langle 13, 8/14\rangle, \langle 15, 1/14\rangle\}$

- the midpoint of the core:

  $c := \langle 1, 1\rangle$

- the endpoints of the support:

  $l := \langle -14, 0\rangle, \langle 16, 0\rangle$

- the set of all the interval mid- and end-points to which a continuous curve may be fit:

  $K' := \{t_k^l, t_k^r, h_k\}$

- the set of all the interval mid- and end-points to which a continuous curve actually will be fit:

  $K \subseteq K'.\ K = \{-10, 12\}$

- the set of all the points to which the curve will be fit:

  $D := \{1, -14, 16\} \cup \{-10, 12\}$

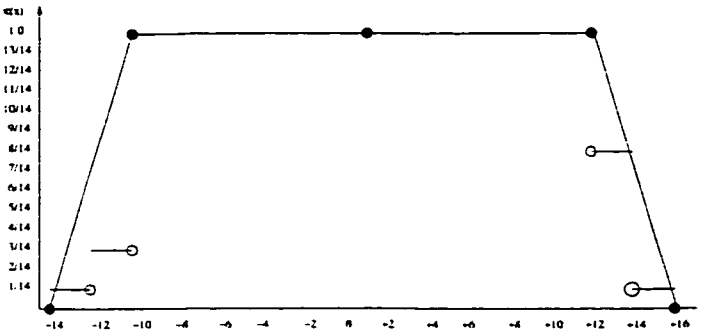

Figure 4.3: Possibility distribution for the field of view of a sonar sensor.

In Figure 4.3 the possibility distribution of the field of view of the sonar sensor facing a wall is presented. The information that can be taken from this distribution is that there is a possibility 1 for getting a sonar reading from the wall if the incidence angle of the sensor is in the interval $[-10^o, 12^o]$ and there is less possibility to get readings if the incidence angle is less than -10^o and greater than 12^o. Since we have the possibility distribution ready, this can be utilized in finding new nested pieces of evidence. The most important new piece of evidence is the support and the core. They are nested because $[-10^o, 12^o] \subseteq [-14^o, 16^o]$. It is clear that the angular uncertainty of the sonar sensor is very high when it is facing a wall. The next step is to find the possibility distributions that represent the radial imprecision in sonar readings. Radial imprecision can be defined as the actual distance minus the measured one (the reading from the sensor). The radial imprecision can be calculated from

$$e = \frac{OA}{\cos\theta} - OC \tag{4.1}$$

where, OA is the vertical distant between the sensor and the wall and OC is the distance detected by the sensor as shown in Figure 4.4.

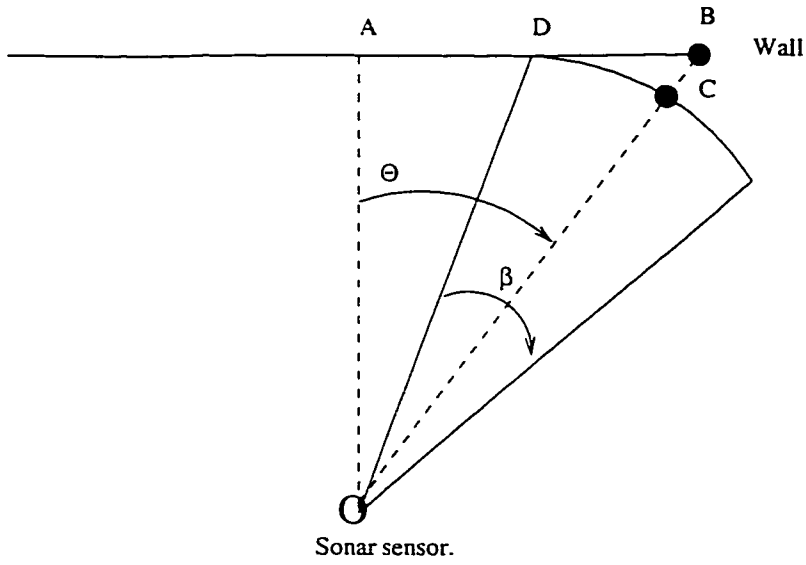

Figure 4.4: Error calculation for sonar reading coming from a wall at a certain distance and angle.

Following the same procedure for angular uncertainty three possibility distributions for radial imprecision for readings approximately from 50cm to 175cm, from 200cm to 275cm, and from 300cm to 370cm are constructed. This partitioning of the range is done because the radial imprecision is a function of the distance d as shown in Table 4.2. These possibility distributions are shown in Figure 4.5. In the next section the angular uncertainty and the radial imprecision in sonar readings obtained from a wall are reduced based on new information.

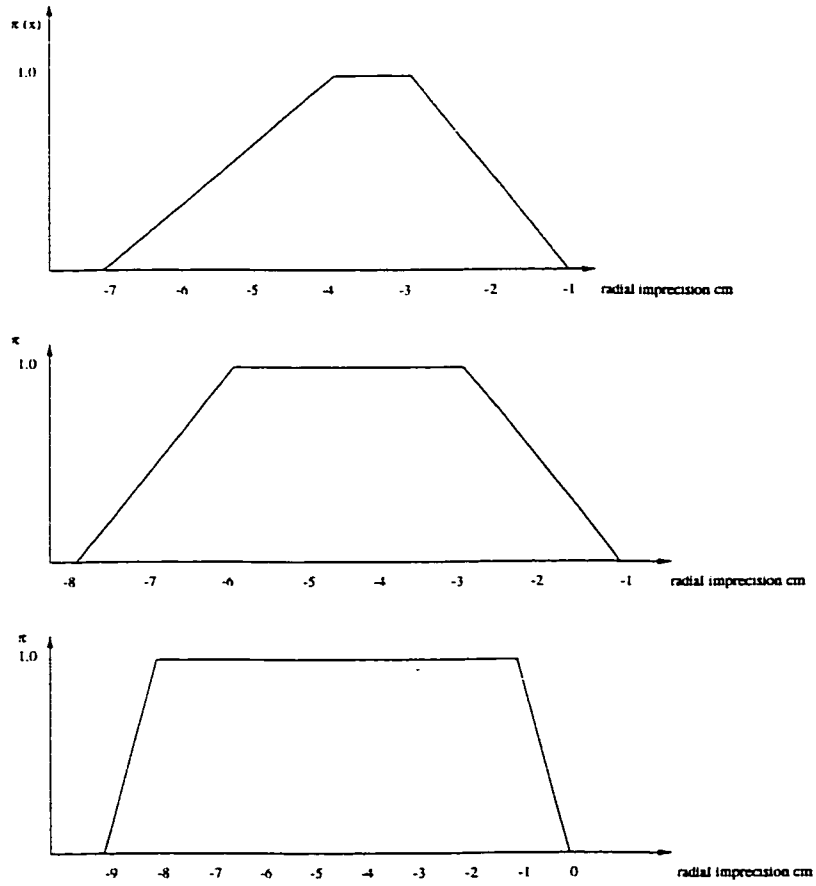

Figure 4.5: Radial imprecision represented by possibility distributions when the sensor is at a distance from 50cm to 175cm (top), when the distance is from 200cm to 275cm (middle), and when the distance is from 300cm to 370cm (bottom).

Distance from a wall(cm)	Radial imprecision (cm)
50	[-7, -3]
75	[-4, -3]
100	[-6, -2]
125	[-5, -2]
150	[-5, -2]
175	[-6, -2]
200	[-6, 0]
225	[-7, -2]
250	[-7, -1]
275	[-8, -1]
300	[-8, 0]
325	[-9, 0]
350	[-9, 0]
370	[-9, -1]

Table 4.2: Radial imprecision intervals when the sensor in front of a wall at different distances.

4.3 Reduction of angular uncertainty and radial imprecision in the wall case

To reduced the angular uncertainty and the radial imprecision, additional information is needed. This information may come from another source of information such as another sensor facing the same wall and placed in a known angle from the first sensor. If two sonar sensors are detecting the same wall, the readings coming from the two sensors may vary in their values according to the direction of each sensor. The shortest reading is the one that is coming from the sensor with the smallest incidence angle from the wall as shown in Figure 4.7 [20]. Actually this is a new information that can be used to reduce the angular uncertainty in sonar sensors. This new information can be used for constructing less uncertain possibility distribution for negative surface normal to the wall. Based on the principle of minimum specificity [42], a natural approach is to select the least specific body of evidence

that contains as many elements as possible. We have a less specific field of view of an interval [-14, 16], then based on the shortest distance information, three significant cases are obtained as shown by Demirli and Turksen [20]:

1. $\theta_1 = 16^o$ and $\theta_2 = 1^o$

   In this case θ_1 is on the left boundary of the field of view and it is shown in Figure 4.6 (top). Due to the fact that the angle between the two sensors is 15^o, then $\theta_2 = 1^o$. Since, θ_2 has the minimum incidence angle, $ds2$ is expected to be the minimum distance reading between the two, i.e., $ds2 < ds1$, i.e., the shortest distance is $ds2$, where $ds1$ is the reading obtained from $S1$ and $ds2$ is the reading obtained from $S2$. In this case the surface normal is $\theta = \theta_2 + 1$

2. $\theta_1 = 7.5^o$ and $\theta_2 = -7.5^o$

   In this case $ds1 = ds2$ and the surface normal is $\theta = \theta_1 - 7.5^o$ or $\theta = \theta_2 + 7.5^o$. This is shown in Figure 4.6 (middle).

3. $\theta_2 = -14^o$ and $\theta_1 = 1^o$

   This case is shown in Figure 4.6 (bottom). The shortest distance is $ds1$ and the surface normal is $\theta = \theta_1 - 1$

Based on this analysis, we have the following possibilities of the surface normal:

- from cases 2 and 3, if $ds1 < ds2$ then:

  $\pi([\theta_1, \theta_1 - 1)) = 0.0$, and $\pi([\theta_1 - 1, \theta_1 - 7.5]) = 1.0$, and $\pi((\theta_1 - 7.5, \theta_1 - 15]) = 0.0$

- from cases 1 and 2, if $ds2 < ds1$ then:

  $\pi([\theta_2 + 1, \theta_2 + 7.5]) = 1.0$, and $\pi((\theta_2 + 7.5, \theta_2 + 14]) = 0.0$.

- from cases 2 and 3, if $ds1 = ds2$ then:

  $\pi([\theta_1, \theta_1 - 7.5)) = 0.0$, $\pi([\theta_1 - 7.5]) = 1.0$, and $\pi((\theta_1 - 7.5, \theta_1 - 15]) = 0.0$, or

  $\pi((\theta_2, \theta_2 + 7.5]) = 0.0$, $\pi([\theta_2 + 7.5]) = 1.0$, and $\pi((\theta_2 + 7.5, \theta_2]) = 0.0$.

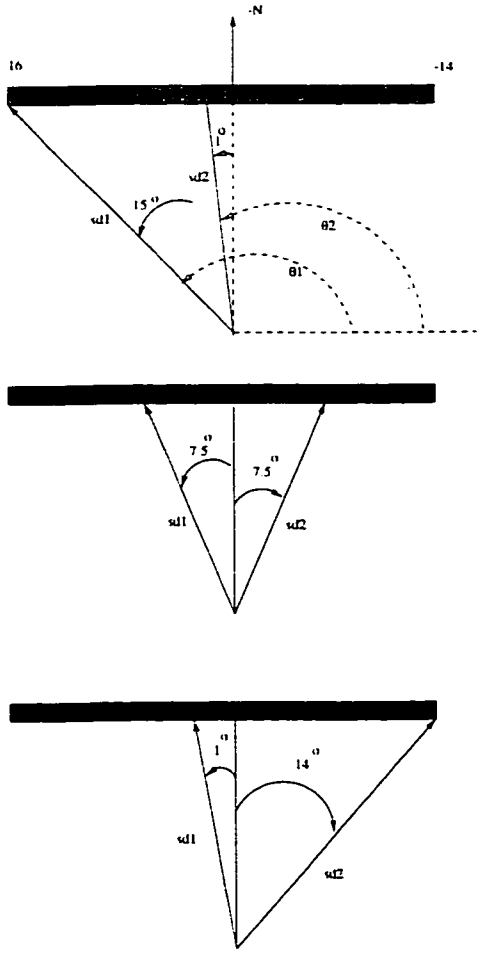

Figure 4.6: Three possible cases for the readings obtained from two sensors.

From these possibilities value of the surface normal three possibility distributions are obtained and shown in Figure 4.8. These possibility distributions are considered the reduced model for angular uncertainty in sonar readings coming from a wall. Because the angular uncertainty is reduced, this will be projected on the

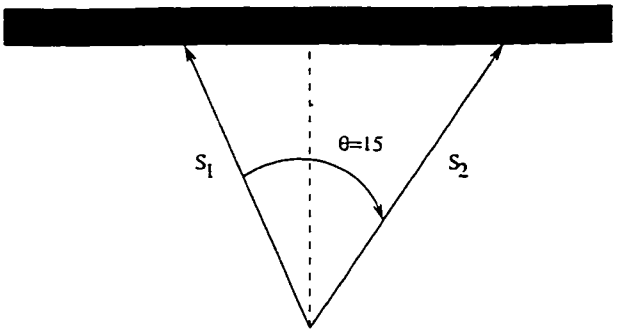

Figure 4.7: Two sonar sensors detecting the same wall.

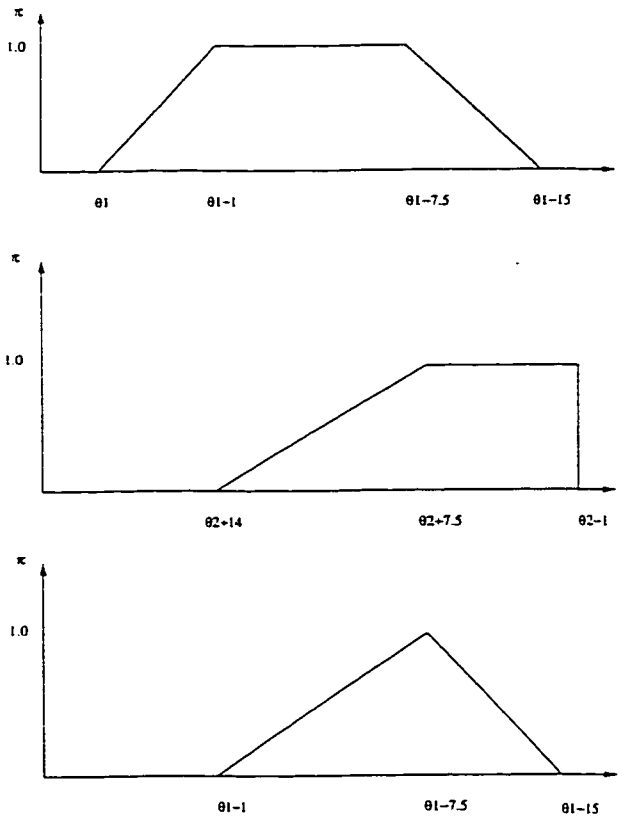

Figure 4.8: Reduced angular uncertainty for readings coming from a wall, $ds1 < ds2$ (top), $ds2 > ds1$ (middle), and $ds1 = ds2$ (bottom).

radial imprecision. For the above three cases, it is shown below how the reduced angular uncertainty affect the radial imprecision, and how the shortest distance to the wall is estimated from the sensors readings, reduced angular uncertainty, and the reduced radial imprecision.

- if $ds1 < ds2$, the sensor direction belongs to the intervals $[1^o, 7.5^o]$ with possibility one. Moreover, the incidence angle belongs to the intervals $]0^o, 1^o[$ and $]7.5^o, 15^o[$ with a certain possibility as shown in Figure 4.8. Any angle belongs to these intervals is considered as a source of information with reliability equals to the possibility value of this incidence angle. Therefore, the radial imprecision has different possibility distributions associated with this incidence angle. By considering the reliability of the source, i.e., the possibility of the incidence angle, the radial imprecision associated with each incidence angle is changed as follows [43]:

$$\pi\prime = min(\pi, w) \tag{4.2}$$

where, π the possibility distribution of the radial imprecision at a certain incidence angle before taking into account the reliability of this incidence angle, w is the reliability of the incidence angle, and $\pi\prime$ is the possibility distribution after taking into account the reliability of the incidence angle. For example, if the reliability of the incidence angle is one, as the case for 1^o and 7.5^o, the possibility distribution for their radial imprecision is the same after taking into account their reliability. On the other hand, if the incidence angle has a reliability less than one, i.e., the incidence angle belongs to the interval $]7.5^o, 15^o[$, the possibility distribution of the radial imprecision of this incidence angle has a maximum value less than one. Therefore, this possibility distribution has to be renormalized but this is out of the scope of this study. Consequently,

only the incidence angles that belong to the interval [1°, 7.5°] are considered. From $ds1$ and the possibility distributions for radial imprecision at 1° and 7.5° obtained from Tables 4.3 and 4.4, the shortest distance between the sensor and the wall is estimated by rotating the distance ds1 from the incidence angle to direction of the negative surface normal of the wall. This rotation is achieved after considering the radial imprecision associated with the incidence angle. In this situation two possibility distributions representing the shortest distance to the wall are obtained. These possibility distributions are combined disjunctively (union) [43] to obtain a new possibility distribution for the shortest distance to the wall [20]. This is shown in Figure 4.9.

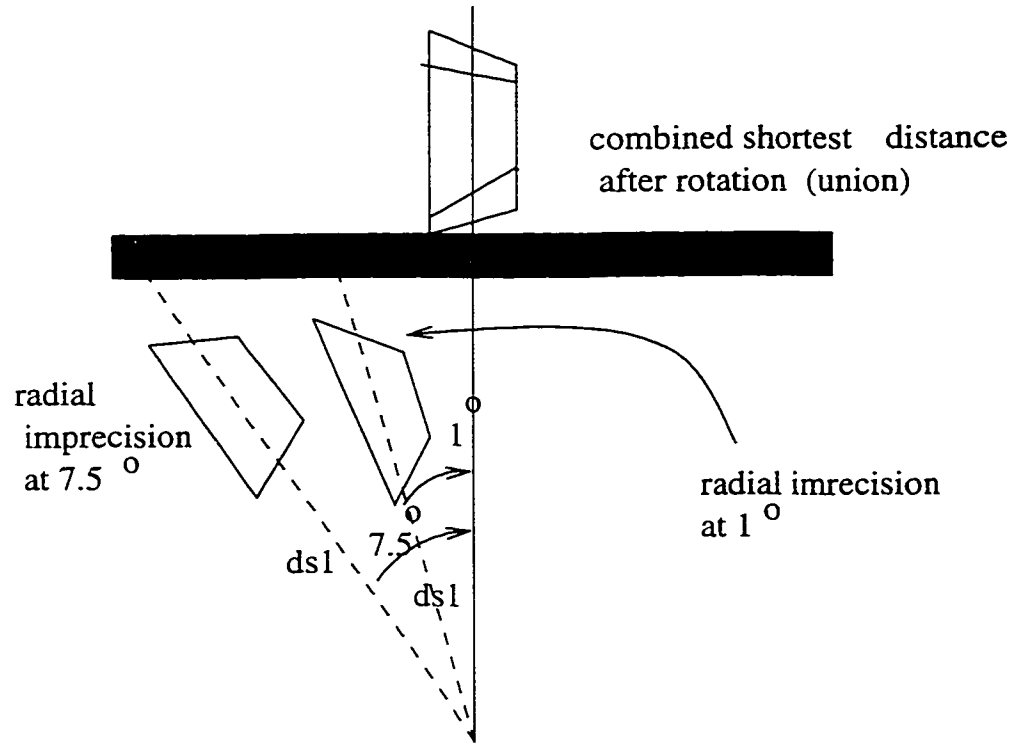

Figure 4.9: Shortest distance estimating from radial imprecision and angular uncertainty.

Distance from a wall(cm)	Reduced radial imprecision(cm)
50	[-4, -3]
75	[-4, -3]
100	[-4, -3]
125	[-5, -3]
150	[-5, -3]
175	[-6, -3]
200	[-7, -5]
225	[-7, -6]
250	[-7, -6]
275	[-8, -6]
300	[-8, -7]
325	[-9, -7]
350	[-9, -7]
370	[-9, -7]

Table 4.3: The reduced radial imprecision intervals when $ds1 < ds2$ and the incidence angle is 1^o.

Distance from a wall(cm)	Reduced radial imprecision(cm)
50	[-4, -3]
75	[-4, -3]
100	[-4, -3]
125	[-5, -3]
150	[-5, -3]
175	[-6, -3]
200	[-6, -3]
225	[-7, -4]
250	[-7, -4]
275	[-8, -4]
300	[-8, -5]
325	[-9, -5]
350	[-9, -5]
370	[-9, -4]

Table 4.4: The reduced radial imprecision intervals when $ds1 < ds2$ and the incidence angle is 7.5^o.

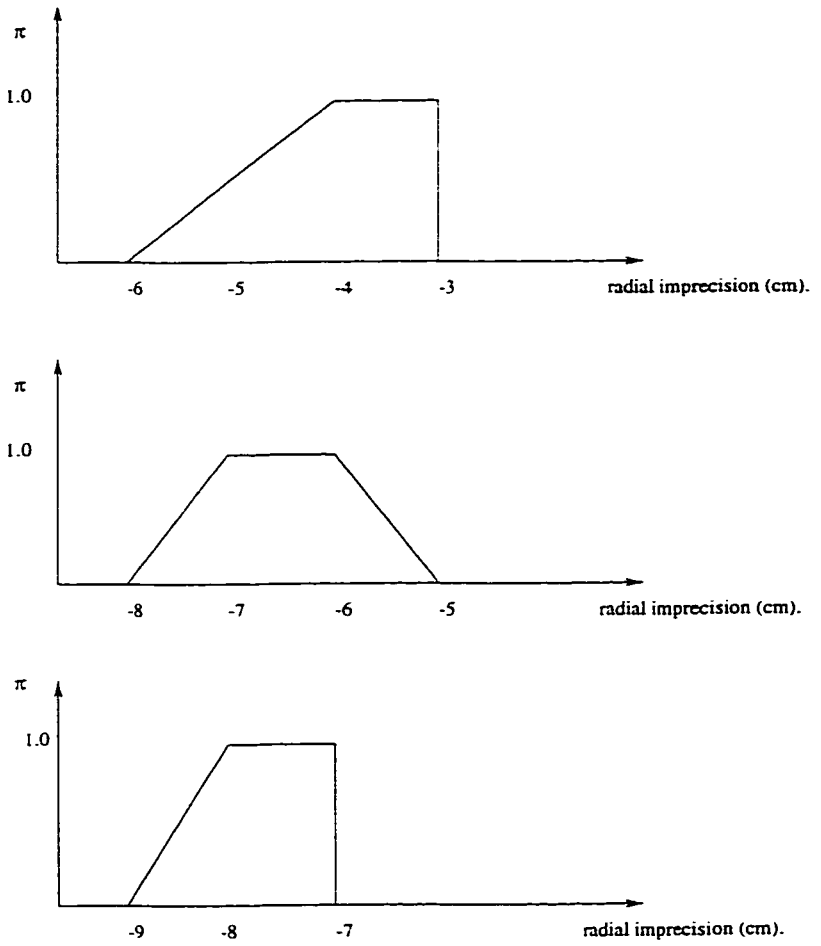

Figure 4.10: Reduced radial imprecision when the sensor incidence angle is 1^o and the distance from a wall is from 50cm to 175cm (top), from 200cm to 275cm (middle), and from 300cm to 370cm (bottom).

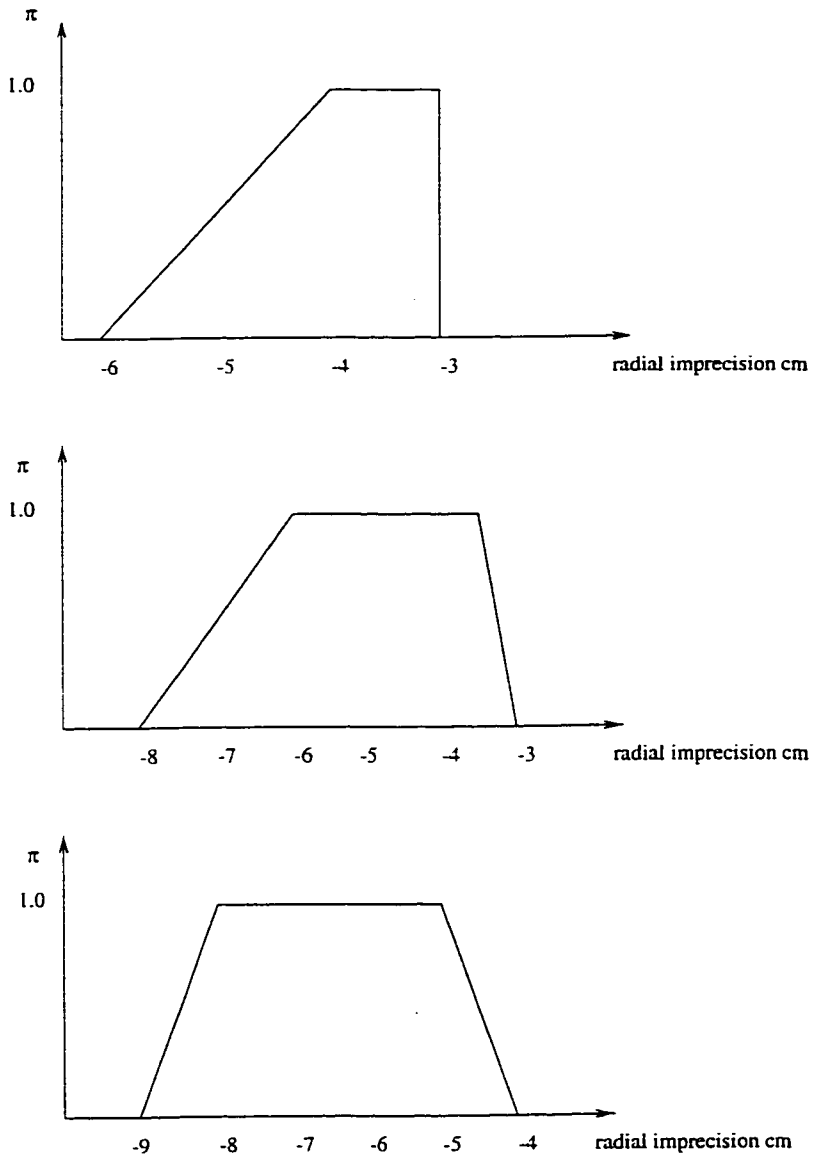

Figure 4.11: Reduced radial imprecision when the sensor incidence angle is 7.5^o and the distance from a wall is from 50cm to 175cm (top), from 200cm to 275cm (middle), and from 300cm to 370cm (bottom).

- if $ds2 < ds1$, the incidence angle belongs to the interval $[1^o, -7.5^o]$ with possibility one. The same possibility distributions in the previous case for the radial imprecision can be used. However, these possibility distribution are rotated counter clockwise to be projected on the negative surface normal of the wall.

- if $ds1 = ds2$, in this case the incidence angle of each sensor has a possibility one to be 7.5^o but on opposite directions from the surface normal of the wall.

4.4 Modeling angular uncertainty and radial imprecision for sonar readings reflected from a corner

A model for the angular uncertainty and radial imprecision of sonar readings reflecting from a corner can be constructed by following the same procedure for building the model for readings reflected from a wall. From Figure 4.12 the radial imprecision for readings coming from a corner can be obtained as:

$$e = \frac{2 * X}{\cos(45 - \theta)} + \frac{2 * X}{\cos(45 - \theta)} * \cos(90 - \theta) - 2 * r. \tag{4.3}$$

where, e is the error in the obtained reading from the sensor reading r, and X as defined in Figure 4.12. The radial imprecision values, labeled method 1 in Tables A.16 to A.30, are calculated based on the assumption that the field of view of sonar readings reflected from a wall is the same as the field of view of the readings reflected from a corner [28]. This assumption is discussed in Chapter 5. On the other hand, the radial imprecision values, labeled method 1 in Tables A.16 to A.30, are obtained from equation (4.3).

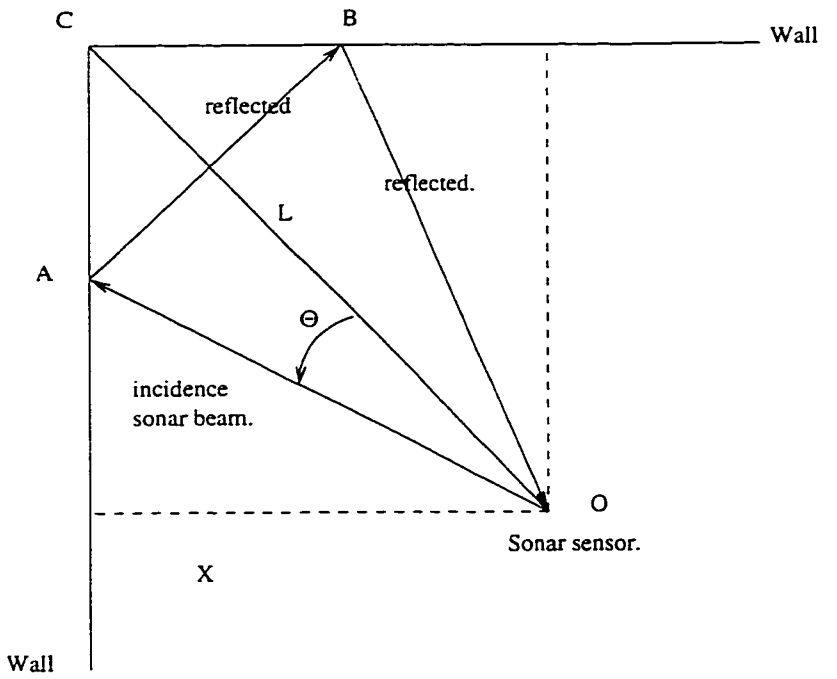

Figure 4.12: Error calculations when the senor detects a corner at distance L from the sensor.

Tables 4.5 and 4.6 summarize the field of view of the sonar sensor and the radial imprecision, respectively, when the sensor is facing a 90^o corner at different distances.

Distance from a corner(mm)	Field of view of the sensor
250	[-6, 10]
500	[-10, 8]
750	[-6, 10]
1000	[-8, 10]
1250	[-6, 10]
1500	[-10, 8]
1750	[-8, 8]
2000	[-12, 6]
2250	[-10, 6]
2500	[-12, 6]
2750	[-12, 6]
3000	[-12, 6]
3250	[-10, 6]
3500	[-6, 8]
3700	[-8, 6]

Table 4.5: The field of view of the sonar sensor at different distances from a corner.

From Table 4.5, the possibility distribution of angular uncertainty of sonar readings can be seen in Figure 4.13. The possibility distributions that represent the radial imprecision is also shown in Figure 4.14, and it is obtained from Table 4.6.

The angular uncertainty for readings coming from two sensors can be shown in Figure 4.15 . The reduction in angular uncertainty in Figure 4.15 is made based on the fact that the angle between the two sensors is 15^o. The reduction of angular uncertainty can lead to a reduction in radial imprecision, like the case of the wall, based on the shortest distance information. Therefore we have the following three cases:

- $ds1 < ds2$

Distance from a corner(mm)	Radial imprecision (cm)
500	[-13, -3]
750	[-13, -4]
1000	[-13, -4]
1250	[-12, -4]
1500	[-14, -4]
1750	[-9, -3]
2000	[-9, 0]
2250	[-10, -4]
2500	[-8, 0]
2750	[-10, -3]
3000	[-10, 0]
3250	[-10, -3]
3500	[-8, -3]
3700	[-9, -3]

Table 4.6: The radial imprecision of sonar readings reflected from a corner at different distances.

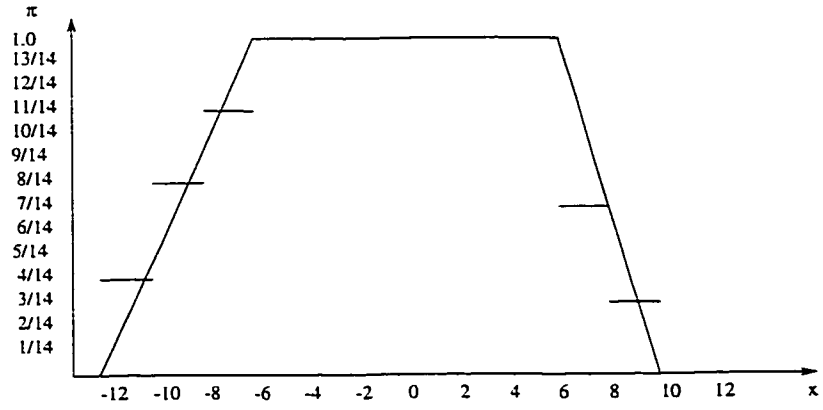

Figure 4.13: Possibility distribution for field of view of a sonar sensor facing a corner.

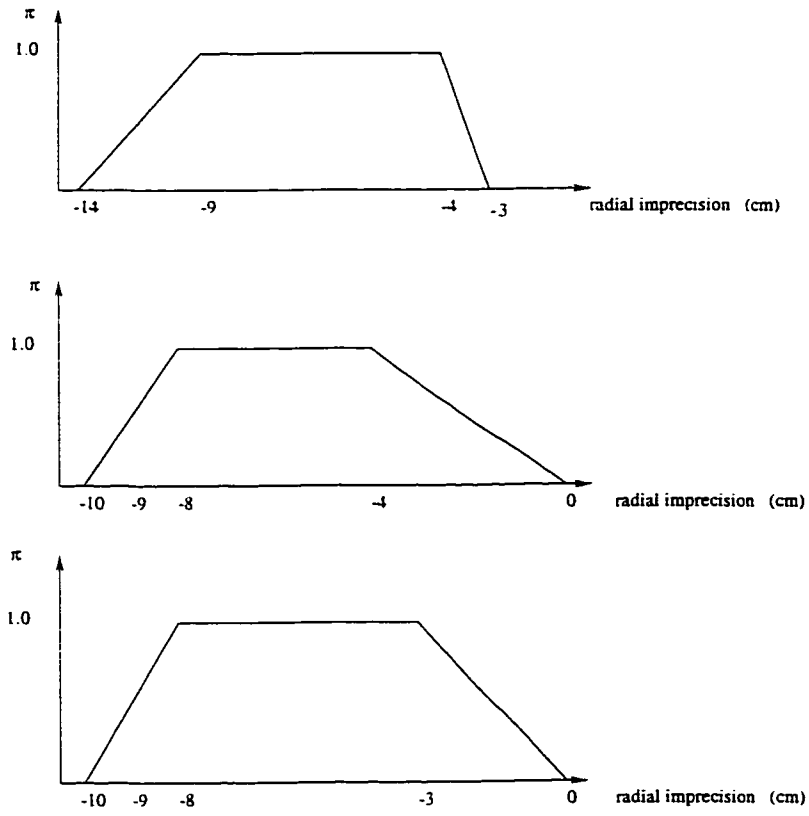

Figure 4.14: (Possibility distribution for radial imprecision when the distance between the sensor and the corner is from 50cm to 175cm (top). Possibility distribution for radial imprecision when the sensor is at distance from 200cm to 275cm (middle). Possibility distribution for radial imprecision when the sensor is at distance from 300cm to 370cm (bottom).

As shown in Figure 4.15 (top), to estimate the distance X in Figure 4.12 based on the value of $ds1$, two possibility distributions for the radial imprecision when the incidence angle is 3^o and 7.5^o are used. These possibility distributions are shown in Figures 4.16 and 4.17. From equation (4.3), the value of X is represented by two possibility distributions. These possibility distributions are aggregated disjunctively as in the case of the wall.

- $ds2 < ds1$

  As shown in Figure 4.15 (middle), the possibility distribution when the incidence angle is 5^o is necessary to estimate the value of X in Figure 4.12 from equation (4.3). This possibility distribution is shown in Figure 4.18.

- $ds1 = ds2$

  In this case X can be estimated from the possibility distribution of the radial imprecision when the incidence angle is either -7.5^o or 7.5^o.

In the next chapter the reduced models of angular uncertainty and radial imprecision for readings obtained from a corner and a wall are used in estimating the stationary and dynamic location of the mobile robot, Pioneer 1.

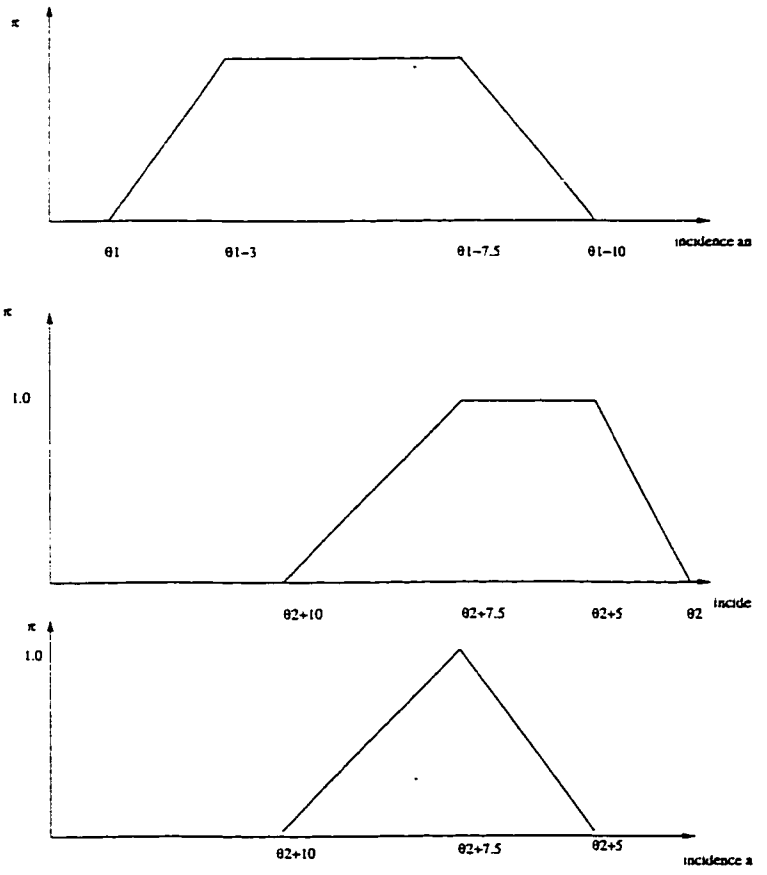

Figure 4.15: Reduced angular uncertainty for readings come from a corner, when $ds1 < ds2$ (top), when $ds2 < ds1$ (middle), and when $ds1 = ds2$ (bottom).

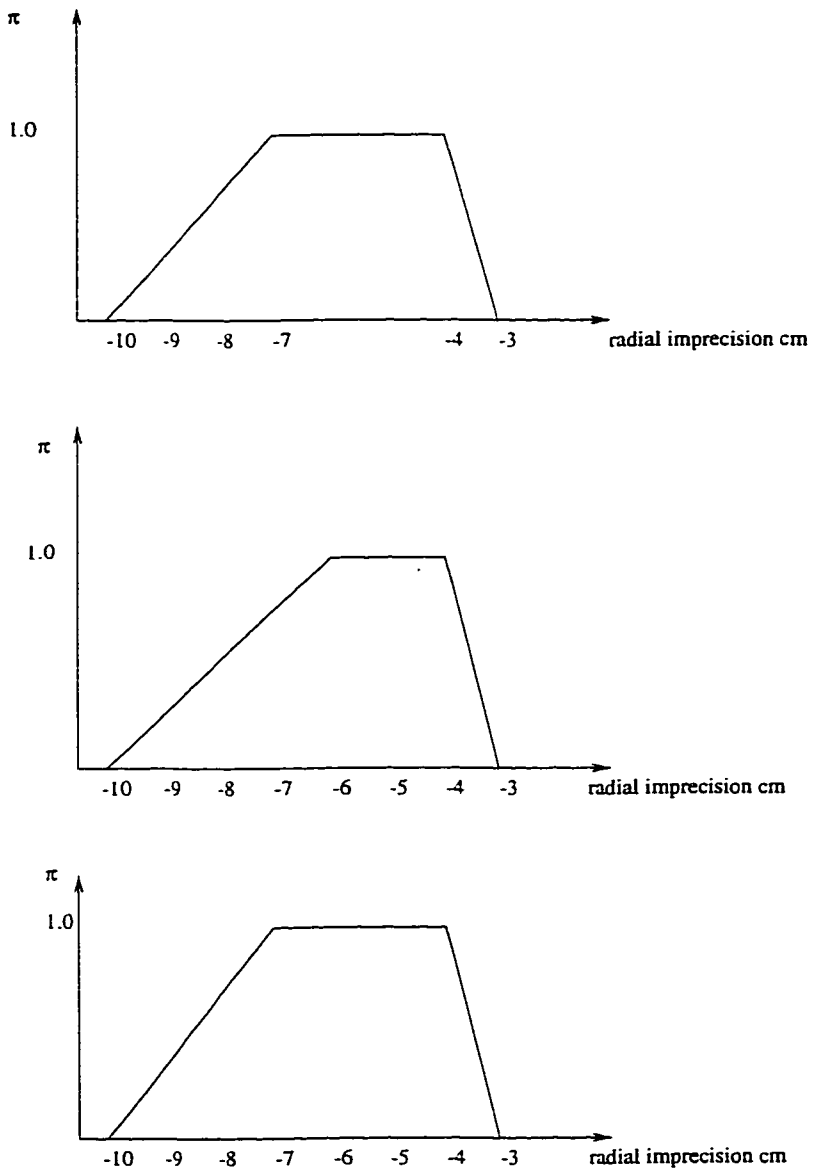

Figure 4.16: Reduced radial imprecision for readings coming from a corner when the incidence angle is 3°. The distance between the sensor and the corner is from 50cm to 175cm (top), when the distance is from 200cm to 275cm (middle), and when the distance is from 200cm to 275cm (bottom).

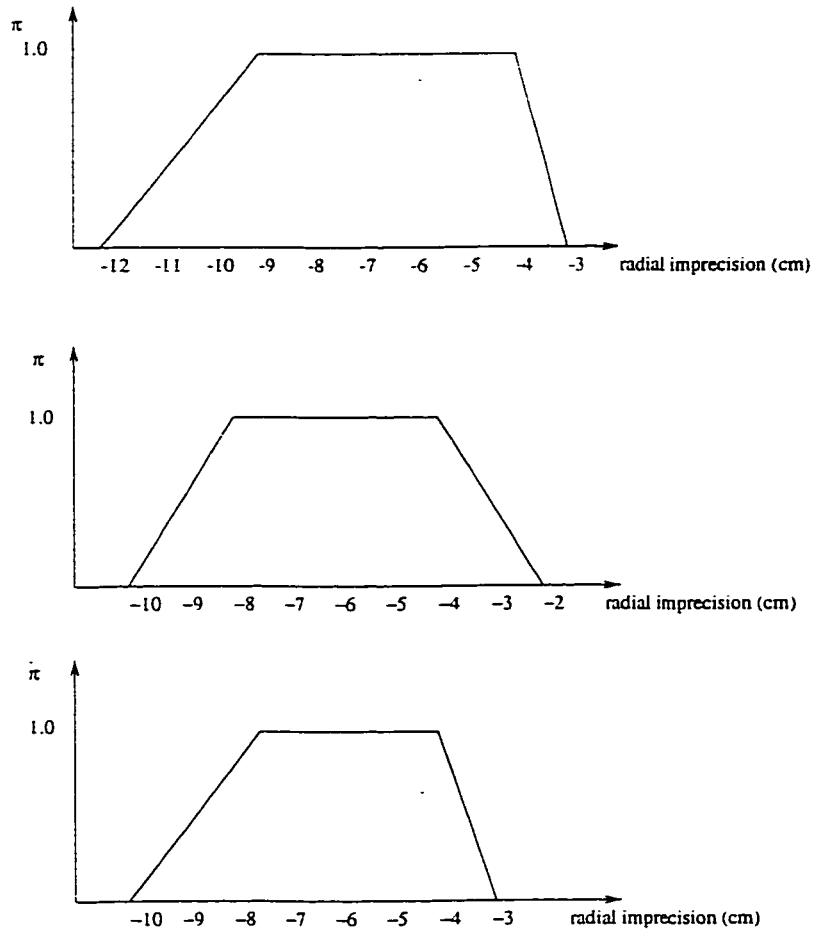

Figure 4.17: Reduced radial imprecision for readings coming from a corner when the incidence angle is 7.5°. The distance between the sensor and the corner is from 50cm to 175cm (top), when the distance is from 200cm to 275cm (middle), and when the distance is from 200cm to 275cm (bottom).

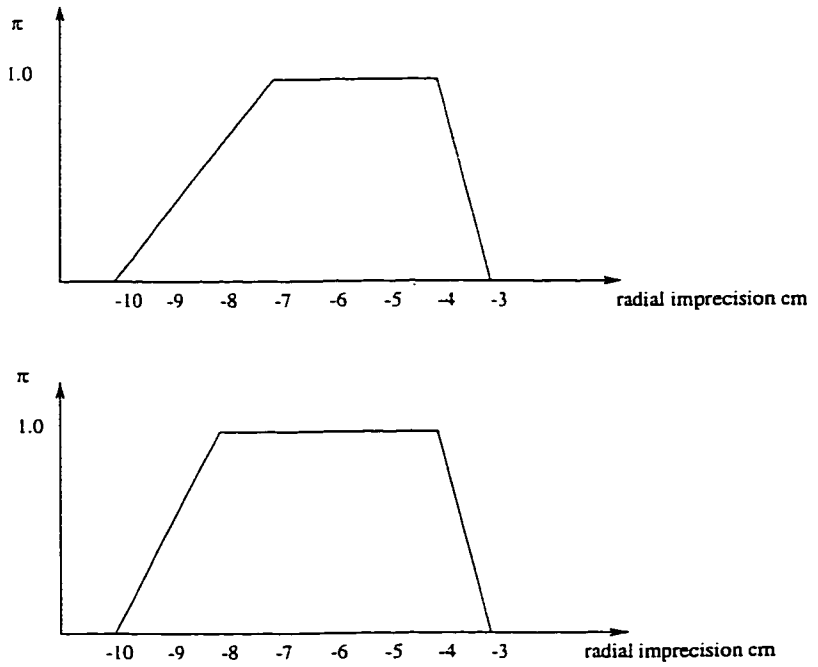

Figure 4.18: Reduced radial imprecision for readings coming from a corner when the incidence angle is 5°. The distance between the sensor and the corner is from 50cm to 175cm (top), when the distance is from 200cm to 275cm (middle), and when the distance is from 200cm to 275cm (bottom).

Chapter 5

Application to Mobile Robots

So far we consider the case of two sensors detecting the same object, and from the readings obtained from these sensors the direction of the sensors and the distance from the object can be determined in the local map, i.e., in the sensor's or the robot's coordinates. However, in mobile robots applications, especially in localization, two sensors are not sufficient. For example, if the two sensors are facing a corner, it is difficult for the robot to realize that this is a corner, and the same is valid in the case of a wall. In order to overcome this problem, usually more than two sensors are mounted on these robots. The number of sensors varies from one robot to another based on the robot's architecture and the tasks it performs. Because sonar sensors are inexpensive, most mobile robots manufacturers tend to mount a ring of sonar sensors around the robot. This helps the robot to recognize objects by combining information from different sensors. The number of sensors on a ring also varies, but in general manufacturers design the ring for 24 sensors with 15^o between any two consecutive sensors. Since the configuration of Pioneer 1 consists of five sonar sensors, it can only detect a corner and a wall in the same scan in the environment. This information is considered as the core for our localization method.

5.1 Sensor based localization

Localization based on the robot's sensors can be divided into three parts; localization based on dead reckoning method, localization based on solely information from proximity sensors information, and a combination of both. Dead reckoning is a simple mathematical method for estimating the current location of a robot. The current location is calculated from the knowledge of the robot's velocity and the time needed to reach the new location. This simple method is problematic because of the large estimated errors and their accumulation effect. The major errors are generated due to following reasons:

- slipping of the wheels
- road conditions
- resolution of the encoders.

However, dead reckoning is reliable over short distances. To show the effect of the problems associated with dead reckoning, our test robot, Pioneer 1, is moved for a certain period of time at a constant velocity and on a linear path. The initial position of the robot is marked. Then when it is stopped, the traveled distance was measured by a metric tape and compared with the registered one from the dead reckoning. Tables 5.1 and 5.2 show the magnitude of the accumulated error over the distance. Although the magnitude of the accumulated error varies from one robot to another, this is a general problem in all mobile robots.

Localization based on the information provided by proximity sensors, like sonar sensors, is limited by the maximum range of the sensors and the environmental constrains. This method can be used when the robot has the map of its environment. The current location of the robot is estimated based on a matching between the new

Dead reckoning reading(mm)	Actual traveled distance(mm)	Error(mm)
718	600	-118
1766	1270	-496
2700	1830	-870

Table 5.1: Error accumulation in dead reckoning over the distance at a velocity of 90mm/sec.

Dead reckoning reading(mm)	Actual traveled distance(mm)	Error(mm)
1150	1000	-150
2930	2135	-795
4930	3170	-1760

Table 5.2: Error accumulation in dead reckoning over the distance at a velocity of 180mm/sec.

and the past information provided by sonar sensors. This is the adopted approach in our localization algorithm which will be shown in the next section.

5.2 Pioneer 1 Configuration

Pioneer 1 is a mobile robot manufactured by RWI, Real World Interface. It consists of two driving wheels and one driven wheel. The driving wheels are controlled separately by different motors. It also has two encoders one for each wheel for dead reckoning estimation. The seven sonar sensors are mounted on the robot as shown in Figure 5.1.

5.3 Localization for Pioneer 1

This section describes a method for determining the location of Pioneer 1 inside a known environment given to the robot. Our localization method is based on the readings obtained from five adjacent sensors with total angle of 60^o, i.e., the angle between any two adjacent sensors is 15^o. From these readings a corner and a wall can

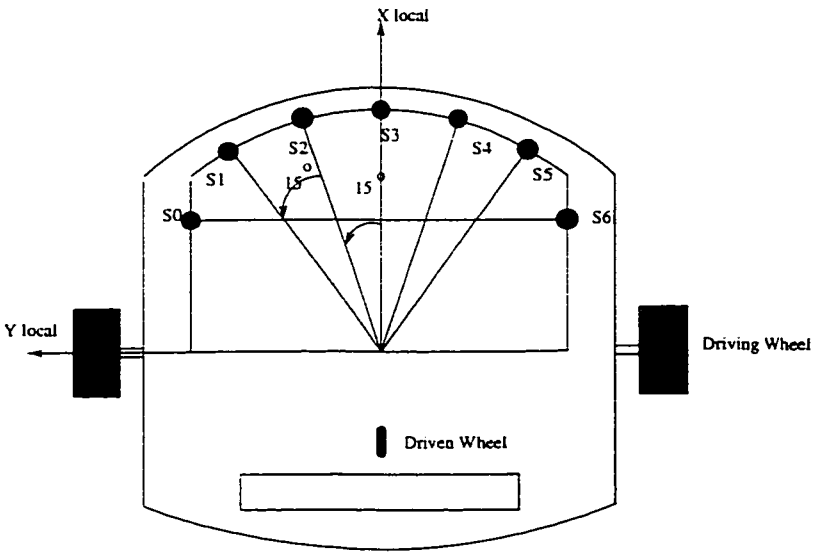

Figure 5.1: Pioneer 1 Configuration.

be recognized at the same time or in the same scan. By this configuration of Pioneer 1, it is impossible to detect the two walls separated by 90°. Our method consists of two parts; stationary and dynamic localization. The stationary location of the robot is estimated when the robot is not in motion and facing recognized features such as walls and corners. This can be done by using the sonar readings obtained from the detected wall and the corner after considering the radial imprecision and the angular uncertainty in these readings. Because any environments contains more than one corner, the initial stationary location of the robot has different alternatives. Therefore, the robot starts navigating in its environment to collect more information to reduce these alternatives. The dynamic location of the robot is estimated while the robot is navigating in its environment. When the robot extracts new local features based on the the sonar readings, it matches them with relevant features in the global map. The feature with maximum degree of match is considered the candidate feature detected by the robot. Then, the location of the robot in the global

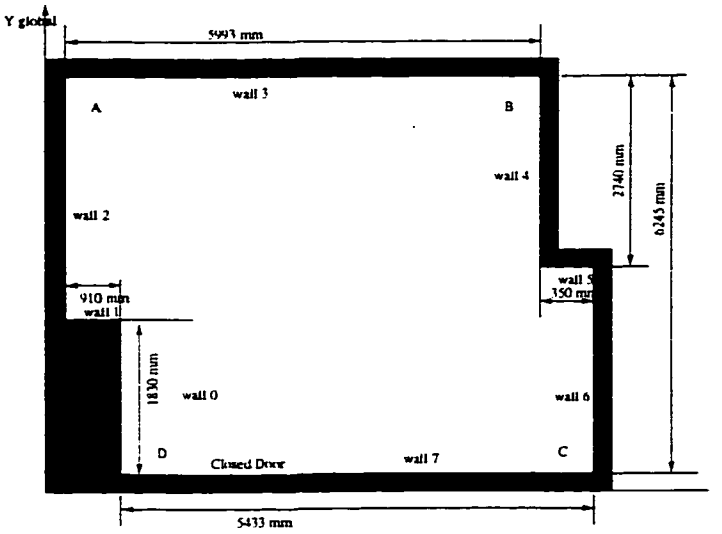

Figure 5.2: The map of the environment.

map is estimated from the sonar readings and the global location of this features. If two features are found to be candidates, then the robot has two possible global locations until further evidence is collected and a unique location is identified. The following steps are used for stationary and dynamic localization.

1. In the beginning, the robot has no information about its location in its environment (Please see Figure 5.2 for our test environment). The robot scans its environment until its *Y local* (see Figure 5.1) becomes parallel to any wall in the environment. This situation can be detected if $S3$, $S4$ or $S2$, $S3$ can give close readings. If the reading obtained from $S3$ is greater than 100cm the robot moves forward until it gets closer to the wall. On the other hand if the reading is less than 100cm, the robot moves back until it goes farther. This value is considered as a safety displacement between the robot and the walls.

2. The information from the side sensors $S0$ and $S6$ is used to check if there is another wall close to the robot from the left or the right. If there is one wall

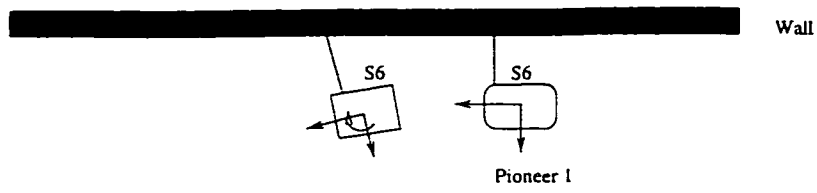

Figure 5.3: The robot trying to follow a wall.

detected to the right or to the left, the robot rotates 90^o in the direction of the wall. For example if $S0$ gives reading then the robot rotates 90^o counter clockwise keeping the detected wall in Step 1 on its right side. If both $S0$ and $S6$ give readings the robot rotates in the direction of the smallest one.

3. The robot starts moving parallel to the side wall. One of the limitations of Pioneer 1 is that it cannot move in a straight path. Therefore, to keep the robot following the wall, the robot rotates 3^o counter clockwise if there is decrease more than 10mm in the readings obtained from the side sensor facing the wall. And it rotates the same degree clockwise if there is an increase more than 10mm in the readings obtained from the same sensor Figure 5.3.

4. When the readings obtained from the side sensor facing the wall and the reading obtained from $S3$ and $S2$ or $S3$ and $S4$ are approximately close or close to each other, the robot stops and starts rotating in the direction of the side sensor (which gives the smaller readings) searching for a corner. The corner is detected if there are readings obtained from sensors $S1$, $S2$, $S4$, and $S5$, given that the reading from $S1$ is very close to the reading obtained from S2, and the reading obtained from $S4$ is close to that obtained from $S5$. If a corner is detected, it will be either in front of $S1$ and $S2$ or in front of $S4$ and $S5$. Sensors $S1$ and $S2$ are in front of the corner if $\min(S1, S2) > \max(S4, S3)$

and in this case $S4$ and $S5$ are in front of the wall. The opposite situation is valid when the corner is detected by $S4$ and $S5$. On the other hand, if the robot couldn't detect the presence of the corner, it will keep rotating until the wall which was in front of the side sensor before scanning the corner is detected. Then the robot repeats the steps as if it was the first detected wall.

5. If a corner is detected, the robot determines its stationary location from the smallest reading obtained from the two sensors which are in front of the corner, and from the smallest readings of the two sensors which are in front of the wall. However, there is no unique initial stationary global location of the robot because any environment contains more than one corner. If the corner is detected $S1$ and $S2$, the robot rotates approximately θ_{rotate} angle in the clockwise direction, and starts navigating in its environment to collect more pieces of evidence about its initial location. If the corner is detected by $S4$ and $S5$, the robot rotates approximately θ_{rotate} angle in counter clockwise direction. The following example shows how our algorithm estimates the initial stationary location of the robot. This example is valid for any environment. The stationary localization uses the angular uncertainty and radial imprecision models for readings coming from a corner and a wall.

   Example:

   Pioneer 1 detects a corner and a wall when the readings obtained from sensors $S1$, $S2$, $S3$, and $S4$, are 1358mm, 1366mm, 907mm, and 910mm, respectively. The corner was detected by $S4$ and $S5$ because $\min(1358, 1366) > \max(907, 910)$. The reduced angular uncertainty model for readings coming from corner can be used to determine the angle of $S4$ from the corner. Then

the reduced radial imprecision is used for estimating the value of X in equation (4.3) which represents one of the components of the initial local stationary location of the robot. The other component is obtained from the reduced angular uncertainty and radial imprecision models for readings coming from a wall. In this example $ds1 < ds2$, then the incidence angle belongs to the interval [3^o, 7.5^o]. By substituting these two angles in equation (4.3), X can be obtained from the following equations:

$$X = \frac{e + 2r}{2.83} \tag{5.1}$$

$$X = \frac{e + 2r}{2.86} \tag{5.2}$$

where equation (5.1) is valid for $\theta = 3$ and equation (5.2) is valid for $\theta = 7.5$. Then the value of e has four possible values for each incidence angle which are the possibility distribution parameters of the radial imprecision for readings obtained from a corner at 3^o in equation (5.1) and at 7.5^o in equation (5.2). Therefore, two new possibility distribution are obtained that represent the possible values of X in the sensor's coordinates. Then these distributions are transformed to the robot's coordinates by considering the position of the sensor with respect to the robot's coordinates, i.e., X becomes $X + ls4 * \cos(45 - \theta)$, where $ls4$ is the distance from the center of the robot to the sensor position. Then these possibility distributions are aggregated disjunctively [43] to get the possibility distribution that represents one of the initial stationary local components of the robot. This procedure is shown in Figure 5.4.

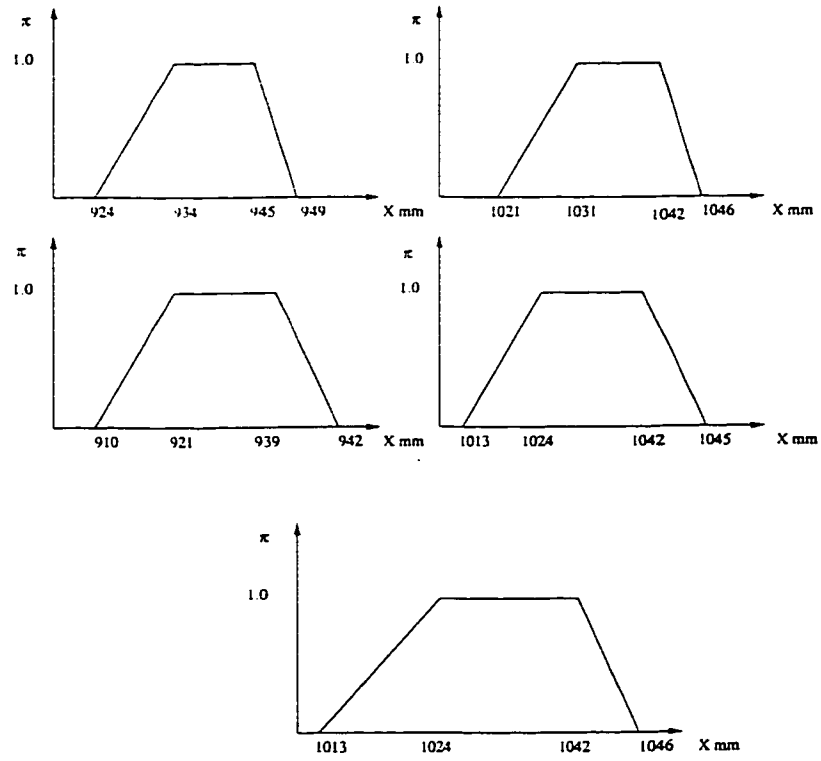

Figure 5.4: Possibility distribution of the value of X in the sensor's coordinates when $\theta = 3^o$ (top - left). Possibility distribution of the value of X in the robot's coordinates for $\theta = 3^o$ (top - right). Possibility distribution of the value of X in the sensor's coordinates when $\theta = 7.5^o$ (middle - left). Possibility distribution of the value of X in the sensor's coordinates when $\theta = 7.5^o$ (middle - right). Combined possibility distribution of (top - right) and (middle - right) that represents the value of X in the robot's coordinates (bottom).

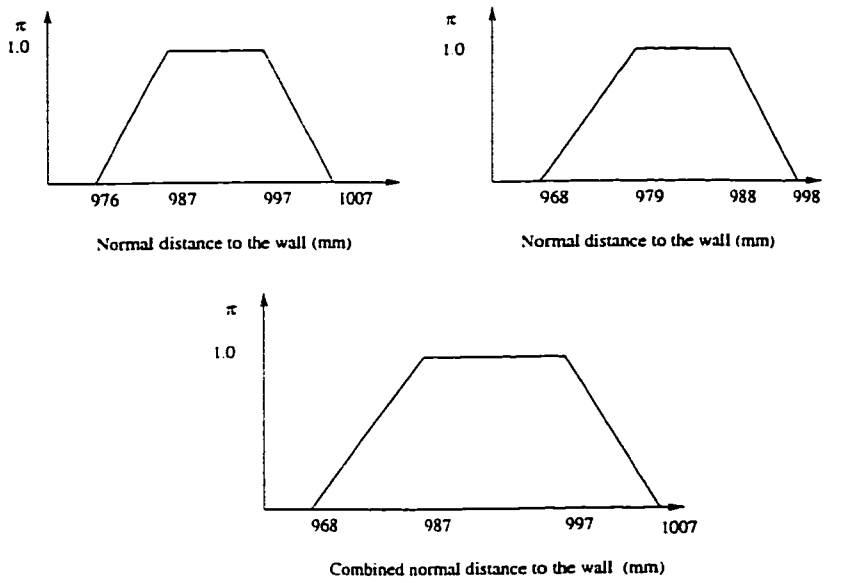

Figure 5.5: The possibility distribution of the normal distance in the robot's coordinates when $\theta = 1^o$ (left), when $\theta = 7.5^o$ (right), the possibility distribution that represents the combination between the left and the right (bottom).

The other component of the initial stationary location of the robot can be estimated from the reading obtained from $S4$. This can be achieved by rotating the possibility distribution that represents the distance $ds1$, i.e., along the direction of the candidates incidence angle after the consideration of the radial imprecision, to be in the direction of the negative surface normal of the wall. In this situation (when $ds4 < ds5$) there are two possibility distributions represent this case; one in the direction of $\theta = 1^o$, and the other is in the direction of $\theta = 7.5^o$. This resultant possibility distributions after the rotation represent the normal distance between the sensor and the wall. Then, these two possibility distributions are transformed to the robot's coordinates and aggregated disjunctively to obtain the possibility distribution that represents the normal distance between the robot and the wall (see Figure 5.5).

The heading angle of the robot can be taken as a crisp value calculated from the interval [3°, 7.5°]. The heading angle of the robot is the angle of $S3$. If we consider the average of the direction of $S1$, then the direction of $S3$ can be calculated because the angle between $S3$ and $S4$ is 15°. Therefore the local heading angle of the robot is approximately 25°. The robot must rotate in angle $\theta_{rotate} = 120^o$ clockwise to become parallel to the detected wall. From these two components, the initial stationary global location of the robot can be estimated based on the global coordinates of the environment. Figure 5.6 shows the four possible initial locations of the robot in our test environment shown in Figure 5.2.

In our approach for corner detection, we make use of TOF information only. The fact that the angle between two consecutive sensors is 15° enables us to detect the corner for the all possible cases of $ds1$, $ds2$, $ds4$, and $ds5$. i.e., $ds1 < ds2$ and $ds4 < ds5$ or any possible combination of the state of these values. This is explained in detail next.

- if $ds1 < ds2$ and $ds4 < ds5$, let us assume here that the corner is detected by $S1$ and $S2$ and corner A is detected. From Fig 4.15, $S1$ direction must belong to the interval [138°, 142.5°]. Consequently, the direction of $S4$ from Figure 4.8 must also belong to the interval [91°, 97.5°] because $S4$ and $S5$ are detecting wall 3 in Figure 5.2. Because the angle between $S1$ and $S4$ is 45°, $S4$ must belong to the interval [$138^o - 45^o = 93^o$, $142.5^o - 45^o = 97.5$]. This is correct because [93°, 97.5°] $\subset$ [91°, 97.5°].
- if $ds1 < ds2$ and $ds5 < ds4$, then $S1$ direction belongs to the interval [138, 142.5] and the direction $S5$ will be in the interval [82.5°, 91°]. Because the angle between $S1$ and $S5$ is 60° and from the direction of $S1$, the direction

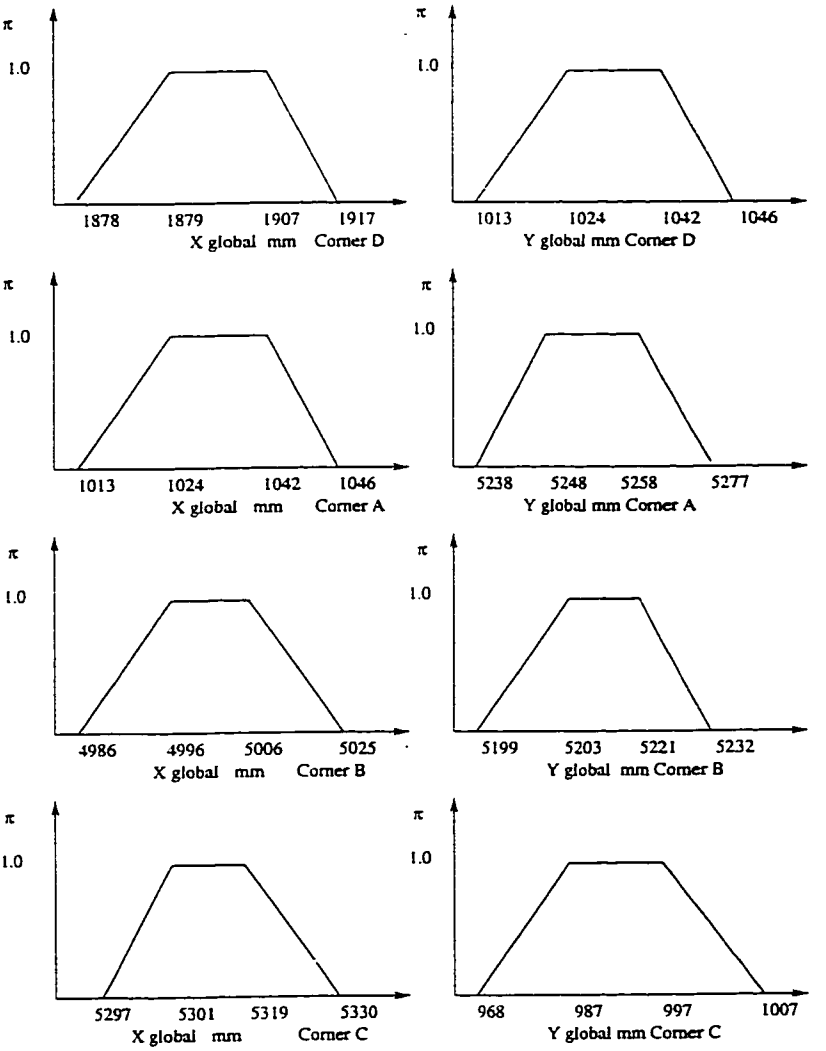

Figure 5.6: The four possible initial stationary location of the robot in our test environment.

of $S5$ must belong to the interval [78°, 82.5°]. This is consistent with the angle obtained from the angular uncertainty model for the wall. Note that we are considering only the possibility 1 from the reduced angular uncertainty for both the wall and the corner.

If we try all the possibilities we will always have the calculated angle of the $S4$ or $S5$ from the direction of $S1$ or $S4$ belongs to the interval obtained from the angular uncertainty model for the wall. Table 5.3 summarizes the remaining cases. It is shown in this table that whenever a corner is detected

State of $ds1$, $ds2$, $ds4$, and $ds5$	θ_{S1} or θ_{S2}	θ_{S4} or θ_{S5} Fig 4.8	Estim θ_{S4} or θ_{S5}
$ds2 < ds1$, $ds4 < ds5$	[127.5°, 130°]	[91°, 97.5°]	[97.5°, 100°]
$ds2 < ds1$, $ds5 < ds4$	[127.5°, 130°]	[82.5°, 91°]	[82.5°, 85°]
$ds1 = ds2$, $ds4 < ds5$	142.5°	97.5°	[91°, 97.5°]
$ds1 = ds2$, $ds5 < ds4$	142.5°	[82.5°, 91°]	82.5°
$ds1 = ds2$, $ds4 = ds5$	142.5°	97.5°	97.5°
$ds1 < ds2$, $ds4 = ds5$	[138°, 142.5°]	97.5°	[93°, 97.5°]
$ds2 < ds1$, $ds4 = ds5$	[127.5°, 130°]	97.5°	[97, 5°, 100°]

Table 5.3: Summary of all possible cases for $ds1$, $ds2$, $ds3$, and $ds4$.

with possibility one the wall also will be detected with possibility one.

6. Since the robot has these possible locations, more pieces of information are necessary to reduce these possibilities. This reduction occurs if new environmental features are recognized. As mentioned earlier, the robot rotates θ_{rotate} to follow the wall detected by $S4$ and $S5$ (in this special example). Then it moves parallel to this wall until new feature is recognized. There are three types of features that can be recognized by the robot while in motion; an edge, a front wall, and a new corner. The first feature is recognized by monitoring the state of the side sensor, i.e., the sensor that is facing a wall while the robot is moving parallel to this wall, $S0$ in our example. There are two cases for

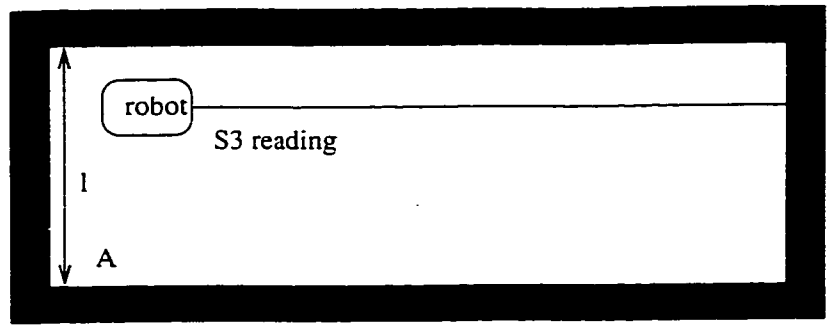

Figure 5.7: The detection of a front wall may reduce the initial possible locations.

this feature; either an edge that causes a decrease or an edge that causes an increase in the reading of $S0$. If there is such a feature in the given map to the robot, they are identified by different flags. The second feature is a front wall that is recognized by monitoring the state of sensors $S3$ and $S4$ or $S3$ and $S2$. Finally, a new corner is recognized if the readings obtained from $S3$ is approximately equal to the safety distance, and the corner detection routine is passed. The recognition of a front wall doesn't have a significant effect on the reduction of the initial location possibilities. The information obtained from this case is used to eliminate the possibilities of the initial location. This is illustrated in Figure 5.7. From this figure it is evident that the robot could not have started in corner A because l is smaller than the reading obtained from $S3$, given that the corner is detected by $S1$ and $S2$. This situation doesn't exist in our test environment, however, it may be available in any other environments. This test is implemented in our algorithm as follows:

- search the environment in a counter clockwise direction if the corner is detected by $S1$ and $S2$ and counter clockwise direction if the corner is detected by $S4$ and $S5$, to find the walls that identified a by corner flag;

a wall is identified by a corner flag if its beginning point is a corner. Then search all the next walls which the difference between its surface normal and the surface normal of the starting wall is 90^o.

- A wall is a candidate to be the front wall detected by $S3$ and $S2$ or $S3$ and $S4$ if the following condition is reached:
  $(x(k) \geq x(j)\ and\ x(k) < x(j+1))\ OR\ (x(k) \leq x(j)\ and\ x(k) > x(j+1))$.
  where, $x(k)$ is the x coordinate of the starting wall and $x(j)$ is the x coordinate of the candidate wall. This condition is valid while the robot is moving parallel to the $+y$ or $-y$. On the other hand, if the robot is moving parallel to $+x$ or $-x$ the following test is applied:
  $(y(k) \geq y(j)\ and\ y(k) < y(j+1))\ OR\ (y(k) \leq y(j)\ and\ y(k) > y(j+1))$.
  These two conditions are checked simultaneously because the robot is unable to realize in which direction it is moving.

- Every wall identified by a corner flag has an initial confidence value equal to one. After the following condition is checked, the confidence value is updated. For example, if the condition is not reached, the confidence value for that wall (has a corner flag) is set to zero which means that this initial location is impossible. On the other hand, if this condition is reached, the confidence value is kept as it is. $abs(y(k) - y(j)) > ds3\ OR$ $abs(x(k) - x(j)) > ds3$.

The above mentioned steps have more significance if the traveled distance is considered. However, because of the large accumulated error in the encoders' readings, it is difficult to make use of the traveled distance information. As mentioned earlier, this accumulated error is a general problem in all mobile robots and it needs further research. This issue needs to be studied extensively

to come up with a model for the uncertainty in the encoders' readings.

7. To make use of the information obtained from the side sensor, the following test is applied if there is an increase or decrease in the readings obtained from this sensor while the robot in motion. This test is applied if the amount of increase or decrease is greaterthan the length of the shortest wall in the environment.

   - search the map in clockwise direction to find the walls which have flags for the corner.
   - for each selected wall, search all the walls in the environment, starting from the next wall, to find the ones that have the same normal surface of the starting wall. Any of these walls are candidate to be the detected edge if the following test is passed:
     ($y(k+1) \geq y(j+1)$ and $y(k+1) < y(j+1)$) OR
     ($y(k+1) \leq y(j)$ and $y(k+1) > y(j+1)$) OR
     ($x(k+1) \leq x(j+1)$ and $x(k+1) > x(j+1)$) OR
     ($x(k+1) \geq x(j+1)$ and $x(k+1) < x(j+1)$) OR

   If this test is passed, then the distance of the robot from all the walls are estimated based on the radial imprecision possibility distributions, then it is matched with the initial stationary location of the robot. An example is illustrated in Figure 5.8. The degree of match is obtained from [23]:

$$M(A,B) = \frac{A_A + A_B}{2A_A A_B} * A_{AB} \tag{5.3}$$

   where A and B denote, respectively, the possibility distribution for the initial location and the current location (after the increase in the sensor readings)

of the robot, A_A denotes the area inclosed by the possibility distribution A, A_B denotes the area inclosed by the possibility distribution B, and A_{AB} is the area of the intersection between these two possibility distributions, i.e., the black area in Figure 5.8. The new possibility distribution results from the intersection of the other two possibility distributions that represent the current location of the robot as a result of having new piece of information about the robot initial location. Therefore, the confidence about the initial location is updated as:

Conf[k]=min(Conf[k], $M(A, B)$) Note that if the wall (that has a flag of a corner) doesn't pass the previous test and pass the matching test, its confidence value is zero.

8. The robot keeps moving trying to extract more information from its environment until the reading obtained from $S3$ is close to the safety distance. Then, the robot's initial location is the one with maximum confidence value. Note that the current location of the robot is always obtained from the readings of the side sensor. This location represents one coordinate, the other coordinate is obtained from the dead-reckoning which has a large error.

By these steps, the robot is able to detect a corner and a wall in the same scan and by different sensors. Then the initial location of the robot is estimated from the sonar readings obtained from these sensors. The alternatives of the initial location are reduced by navigating in the environment and extracting features that have relevant in the global map. Features with maximum matching degree with their relevant are used for estimating the dynamic location of the robot. Our localization method is not only valid for Pioneer 1, but it can be generalized for different robots' configurations such as ring configuration. In the next chapter the discussion and

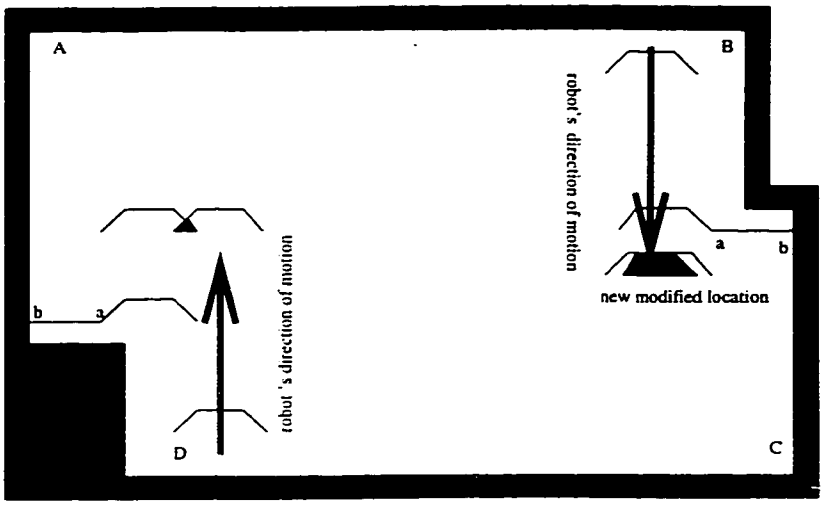

Figure 5.8: Matching between the initial location and the new one after an increase in the readings obtained from $S0$ occurs.

conclusions are introduced.

Chapter 6

Discussion and Conclusions

6.1 Discussion

There are different approaches in the literature for corner detection. One of them depends on vision sensors to detect corners [26]. However, this approach is not practical because it needs time for processing the obtained images, and then detect a corner. Another approach [27] uses sonar sensors for corner detection. This approach depends on processing the echo signals reflected from different objects in the environment. It was found that the amplitude of the echo reflected from walls and corners is a function of the incidence angle θ. This relation is usually approximated as a Gaussian curve. The maximum amplitude obtained if the incidence angle is zero. From this assumption the field of view of the sonar sensor for readings obtained from walls and corners is assumed to be the same. Therefore, it was difficult to differentiate corners from walls if only one sensor is used. Then two sonar sensors were placed at a certain distance from each other and mounted on a stepper motor to study the behavior of the reflected echo from walls and corners. It is assumed that when the sonar sensor acts as a receiver and a transmitter in the same time, the sensor can

be modeled as shown in Figure 6.1, especially when the surfaces are smooth (mirror like reflectors). From this model, the echo amplitudes $Aaa1$, $Aab1$, $Ab1a$, and Abb as shown in Fig 6.2 are considered as the bases to differentiate corners from walls. A corner is detected if $Aaa1(\theta) - Aab1(\theta) > 6\sigma$ or $Aab1(\theta) - Abb1(\theta) > 6\sigma$. A wall is detected if $Aaa1(\theta) - Aab1(\theta) > 6\sigma$ and $Abb1(\theta) - Aab1(\theta) > 6\sigma$, where σ is the standard deviation in the noise that affects the echo amplitude values. The value of σ is obtained from taking 100 readings of the echo amplitudes at each step in the scan. σ is 2 percent of $Ameas(\theta) = A(\theta)$+noise, where $Ameas(\theta)$ is the average of the 100 readings of the echo amplitude at angle θ.

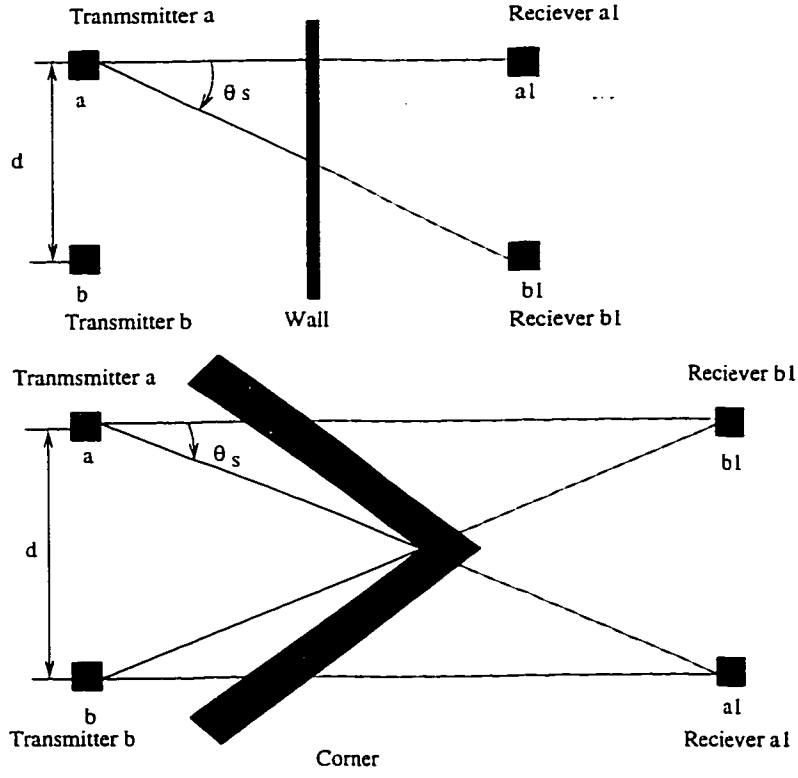

Figure 6.1: Two-transducer system at zero incidence angle from wall and corner. θ_s is the angle for echo amplitude for the corner.

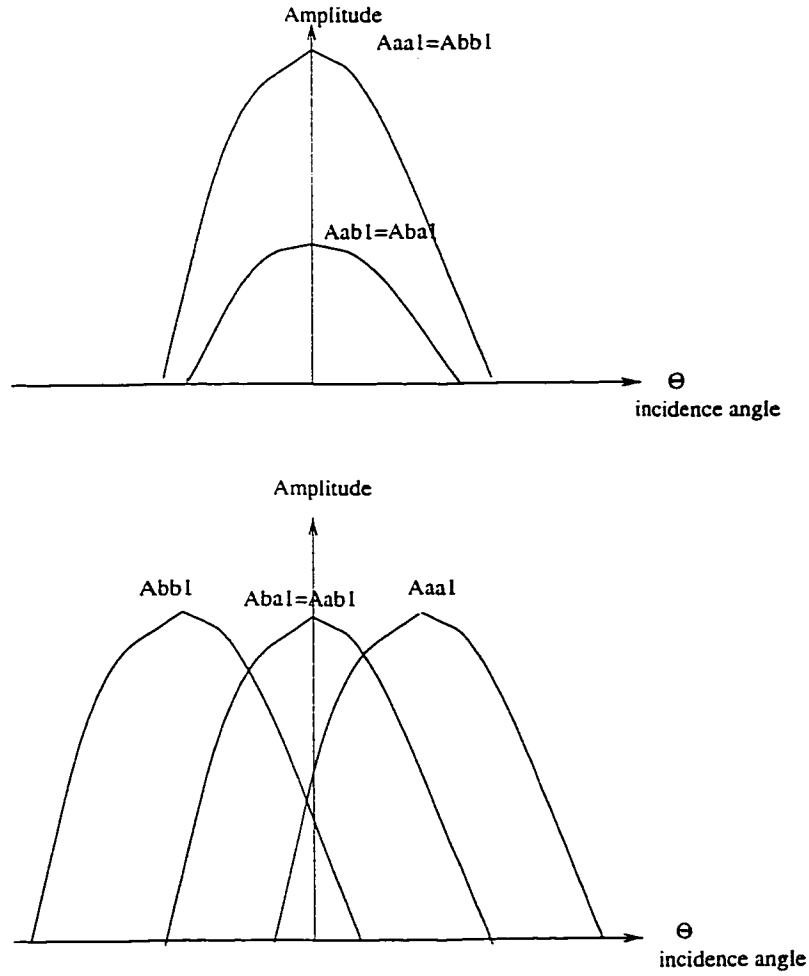

Figure 6.2: Amplitude versus incidence angle for wall reflector (top). Amplitude versus incidence angle for corner reflector (bottom).

This method has some limitations. Firstly the distance between the two transducers constrains the range at which a scan can be made, and this range is smaller than the sensor range. Secondly the time required to detect a corner or a wall by this method is large because at each step in the scan 100 readings must be obtained. Thirdly, this method depends on processing the echo signals to study the echo amplitude which needs more time. Moreover, it is verified experimentally (See Tables A.19 to A.30) that the radial imprecision calculated by considering the behavior of the corner as the wall's (method 1) is greater than when it is calculated by our method (method 2) when the sonar sensor is at distances larger than 75cm. Finally this method is not practical in map building. If this approach is compared with our approach, our approach is more efficient as it is based on TOF information which requires less processing. As it also uses more sensors, this increases the possibility of detecting a corner. Due to that, our method is especially effective on robots with 24 sensors arranged in a ring configuration.

Our approach also considers the angular uncertainty in sonar readings - a feature that is often neglected by other studies. The above mentioned method considers that the reduced echo is reflected from the wavefront of the beam and not from the closest part of the detected object. Then the radial imprecision is modeled as a noise that has Gausian distribution. This is again an irrealistic assumption as the sonar data are imprecise where Probability Theory cannot be used, but Possibility Theory can handle imprecision which we use in our study.

The angular uncertainty for readings coming from a corner is less than the angular uncertainty for readings coming from a wall Figure 4.3 and Figure 4.14. In other words, the field of view of the sonar sensor when it is scanning a corner is smaller than its field of view if it is scanning a wall. This is shown clearly in

Tables 4.3 and 4.13. Therefor, this characteristic of the sonar sensor can be used to recognize objects in the environment by using only one sensor.

From Figures A.1 to A.15 and Figures A.16 to A.27 the radial imprecision of the readings coming from a corner increases with the incidence angle θ. However, the readings coming from the wall do not always have this trend. The increase of the radial imprecision with the incidence angle is clear from equations (4.3) and (4.1).

6.2 Summary and Conclusions

In our study, models for radial imprecision and angular uncertainty are proposed by using possibility distribution. The *Possibility Theory* is valid when the available knowledge is imprecise and coherent as in sonar readings. This case cannot be handled by *Probability Theory*.

It is verified experimentally (See Tables A.19 to A.30) that the radial imprecision calculated by considering the behavior of the corner as the wall's (method 1) is greater than when it is calculated by our method (method 2) when the sonar sensor is at distances larger than 75cm. On the other hand, the radial imprecision calculated by method 1 is less than when it is calculated by our method (method 2) when the sensor is at distances less than 75cm (See Tables A.16, A.17, and A.18). Therefore, it is concluded that the behavior of the corner is the same as the wall's only when the sonar sensor is at distances less than 75cm. This is contrary to the generalization made by [27] that the behavior of the corner is the same as the wall's even though the experiments were done at distances less than 75cm.

A new simple corner detection method is applied on Pioneer 1. This method depends on direct interpretation (TOF) of the sonar readings obtained from different sensors in the same time. This method is not specific to Pioneer 1, and it can

be generalized for different configurations especially the ring configuration. Moreover, our approach for corner detection is more practical than any signal or image processing approaches because they are time consuming.

It is experimentally shown that the field of view of sonar sensor scanning a corner is less than the field of view of the sensor when it is scanning a wall.

The initial stationary global location of the robot is estimated after corner and wall detection. Since any environment contains more than one corner, the initial location has different alternatives. To reduce these alternatives, the robot navigates in its environment to collect more pieces of information about its initial location. While the robot is navigating in its environment, it extracts and accumulates additional features from the environment and matches them with relevant features in the global map. The dynamic location of the robot is estimated from the location of the features with maximum matching degree and the readings obtained from the sonar sensors.

The matching process between the extracted features and their relevant features in the global map given to the robot, is efficient, especially when the global map contains edges that have close widths, i.e., their widths are greater than 5cm.. The extracted features are used to correct the encoders readings. This is achieved from the knowledge of the linear length of the wall that is followed by the robot when an edge is detected.

The dynamic localization method used in our study is environment dependent. It is efficient in environments with unique detectable features. For example, if the test environment is a square room, the robot cannot eliminate the four alternatives for its initial location, a limitation that even more intelligent beings cannot overcome.

6.3 Future Work

- A model of uncertainty in encoders readings has to be well established to make dynamic localization more efficient. This can be achieved by studying the dynamic model of the robot including all the factors affecting their motion such as the friction of the floor and the accuracy of the encoders.

- One of the limitations of our localization approach is that the robot should move on a linear path. However, this limitation can be removed if a robot with 24 sonar sensors is used so that environmental features can be recognized easily and then matched with the given map. Another limitation of this method is that the robot's environment is considered empty without furniture. We need a method that will ignore small furniture and concentrate on significant features.

- We need a better way of matching between extracted features and their relevant in the global map. This can be done by subset hood measures which is more established than the matching method used in our study.

Bibliography

[1] A. Abidi and C. Gonzalez, *Data Fusion in Robotics and Machine Intelligence.* Academic Press, Inc., 1992.

[2] H. R. Everett, *Sensors for Mobile Robots Theory and Applications.* A K Peters, Ltd. Wellesley, Massachustts, 1995.

[3] R. Brooks, "Visual map making for a mobile robot," *IEEE International Conference on Robotics and Automation*, pp. 824–829, St. Louis,Missouri, March.25-28 1985.

[4] A.Elfes, "Sonar-based real-word mapping and navigation," *IEEE Journal of Robotics and Automation*, vol. RA-3, pp. 249–265, June 1987.

[5] H. Durrant-Whyte, "Where am i? a tutorial on mobile vehicle localization," *Industrial Robot*, vol. 21, no. 2, pp. 11–16, 1994.

[6] G. H. W. Jongkind and V. Alast, "Sensor and navigation system for mobile robots," in *Proc. Intelligent Autonomous Sys. Conf.*, pp. 258–264, 1986.

[7] D. Cho and J. Lim, "A new certainty grid based mapping and navigation system for an autonomous mobile robot," *The International Journal of Advanced Manufacturing Technology*, vol. 10, pp. 139–148, Spring 1995.

[8] B. Beaufrere and S. Zeghloul, "A mobile robot navigation method using a fuzzy logic approach," *Robotica*, vol. 13, pp. 437–448, 1995.

[9] K. Demirli, *Fuzzy Inference and its Application to Self-Navigation Systems.* University of Toronto, Ph.D Thesis, 1995.

[10] K. Demirli and I. Turksen, "Mobile robot navigation with generalized modus ponens type fuzzy reasoning," in *1995 IEEE International Conference on Systems, Man and Cybernetics*, pp. 3724–3729, Vancouver, British Columbia Canada, October 22–25, 1995.

[11] P. Freedman and J. Liu, "Using uncertain measurements to make plausible perceptual hypotheses: Application to autonomous navigating using sonar," in *Proceedings of the International Conference on Intelligent Autonomous Systems: IAS-3, Pittsburgeh, Pa, Feb 15-19*, 1993.

[12] A. Zelinsky, "Mobile robot map making using sonar," *Journal of Robotic Systems*, vol. 8, no. 5, pp. 557–577, 1991.

[13] A. Flynn, "Combining sonar and infrared sensors for mobile robot navigation," *The International Journal of Robotics research*, vol. 7, pp. 5–14, December 1988.

[14] O. Bozma and R. Kuc, "Single sensor map-building based on physical principles of reflection," in *Proc. IEEE/RSJ International Workshop on Intelligent Robots and Systems IROS'91. Nov 3-5*, pp. 1038–1043, 1991.

[15] O. Bozma and R. Kuc, "Building a sonar map in a specular environment using a single mobile sensor," *IEEE Transaction on Pattern Analysis and Machine Intelligence*, vol. 13, pp. 1260–1269, December 1991.

[16] Y. Nagashima and S. Yuta, "Ultrasonic sensing for mobile robot to recognize an environment-measuring the normal direction of walls-," in *Proceedings of the IEEE/RSJ International Conference on Intelligent Robots and Systems*, pp. 805–812, 1992.

[17] G. U. M. Poloni and M. Vendittelli, "Fuzzy logic and autonomous vehicles: Experiments in ultrasonic vision," *Fuzzy Sets and Systems*, vol. 69, pp. 15–27, 1995.

[18] J. Crowley, "World modeling and position estimation for a mobile robot using ultrasonic ranging," in *Proceedings of the IEEE International Conference on Robotics and Automation*, pp. 674–680, 1989.

[19] M. Drnmheller, "Mobile robot localization using sonar," *IEEE Transaction on Pattern Analysis and Machine Intelligence*, vol. PAMI-9, pp. 325–332, March 1987.

[20] K. Demirli and I. Türksen, "Fuzzy logic based mobile robot localization with sonar data," in *Canada-Japan bilateral workshop on Intelligent Manufacturing and Process, Design, Toronto, Canada, April 28-30*, 1996.

[21] K. Demirli and I. Türksen, "Sonar based mobile robot localization by using fuzzy triangulation," *submitted to IEEE Transaction on Robotics and Automation*, 1999.

[22] A. Saffiotti and L. Wesley, "Perception-based self localization using fuzzy locations," in *M. van Lambalgen (Ed.) Reasoning with Uncertainty in Robotics.Springer LNCS to appear*, pp. 368–386, 1996.

[23] J. Gasós and A. Martín, "Mobile robot localization using fuzzy maps," in *A. Ralescu and T. Martin, editors, Lecture Notes in Artificial Intelligence. Springer Verlag*, 1996 (to appear).

[24] A. Curran and K. Kyriakopoulos, "Sensor-based self-localization for wheeled mobile robots," *Journal of Robotic Systems*, vol. 12, no. 3, pp. 163–176, 1995.

[25] H. Beom and H. Cho, "Mobile robot localization using a single rotating sonar and two passive cylinders beacons," *Fuzzy Sets and Systems*, vol. 13, pp. 243–252, 1995.

[26] R. Malik and E. Polkowski, "Robot self-localization based on corner detection," *Mobile robots*, vol. 5, pp. 306–316, 1990.

[27] B. Barshan and R. Kuc, "Differentiating sonar reflection from corners and planes by employing an intelligent sensor," *IEEE Transaction on Pattern Analysis and Machine Intelligence*, vol. 12, pp. 560–569, June 1990.

[28] R. Kuc and V. Viard, "A physical based navigation strategy for sonar-giuded vehicles," *The International Journal of robotic Research*, vol. 10, pp. 75–87, April 1991.

[29] R. Kuc, "A spatial sampling criterion for sonar obstacle detection," *IEEE Transaction on Pattern Analysis and Machine Intelligence*, vol. 12, pp. 686–690, July 1990.

[30] R. Kuc and M. Siegel, "Physically based simulation model for acoustic sensor robot navigation," *IEEE Transaction on Pattern Analysis and Machine Intelligence*, vol. PAMI-9, pp. 766–778, November 1987.

[31] H. Zimmerman, "Uncertainty modelling and fuzzy sets," in *Tp appear in proceedings of workshop on modeling uncertainty.*

[32] G. Klir, "Where do we stand on measure of uncertainty, ambiguity, fuzziness, and the like," *Fuzzy Sets and Systems*, vol. 24, pp. 141–160, 1987.

[33] D. Dubois and H. Prade, *Possibility Theory.* Plenum Press, New York, 1988.

[34] G. Klir and B. Yuan, *Fuzzy sets and Fuzzy Logic.* Prentice Hall, New York, 1995.

[35] L. Zadeh, "Fuzzy sets on the basis for the theory of possibility," *Fuzzy Sets and Systems*, vol. 1, pp. 3–28, 1987.

[36] J. Cliff, *Possibilistic Process for Complex Systems Modeling, Ph.D dissertation, Suny Binghamton.* UMI Dissertation Services, Ann Arbor MI, 1994a.

[37] J. Cliff, "Possibilistic measurement and set statistics," in *Proceedings of NAFIPS, 1992, v.2,*, pp. 458–467, 1992.

[38] J. Cliff, "Empirical possibility and minimal information distortion," in *Fuzzy Logic : State of the art, editor R. Lowen, Kluwer*, 1993a.

[39] J. Cliff, "Some new results on possibilistic measurement," in *Proc of NAFIPS, Allentown, Pennsylvania*, pp. 227–231, 1993b.

[40] J. Cliff, "Possibilistic semantic and measurements methods in complex systems," in *Proc. 2nd International Symposioum on Uncertainty Modeling and Analysis, edited by Bilal Ayyub, IEEE computer Society Press*, pp. 208–215, 1993c.

[41] J. Cliff, "Possibilistic approach to qualitative model-based diagnosis," *Telematic and Informatics*, vol. 11, no. 4, pp. 365–384, 1994b.

[42] D. Duois and H. Prade, "The principle of minimum specificity as a basis for evidential reasoning," *Lecture notes in CS*, pp. 75–84, 1986.

[43] D. Dubois and H. Prade, "Combination of fuzzy information in the framework of possibility theory," in *Data Fusion In Robotics and Machine Intelligence* (A. Abidi and C. Gonzalez, eds.), pp. 481–505. Academic Press, Inc., 1992.

Appendix A

Sensor direction θ deg	Sonar reading (mm)	Error in sonar reading (mm)
-20	315	-49.0
-18	320	-57.1
-16	5201	*
-14	302	-44.3
-12	297	-41.4
-10	289	-35.0
-8	284	-31.5
-6	283	-31.6
-4	283	-32.4
-2	283	-32.8
0	285	-35.0
2	285	-34.8
4	286	-35.5
6	286	-34.6
8	286	-33.5
10	287	-33.0
12	291	-35.4
14	298	-40.4
16	309	-49.0
18	314	-51.1
20	321	0.6
22	316	-46.5
24	325	-51.3

Table A.1: Sonar readings from a wall 25cm away from the sensor.

Sensor direction θ deg	Sonar reading (mm)	Error in sonar reading(mm)
-14	578	-62.7
-12	559	-48.0
-10	541	-33.0
-8	535	-30.0
-6	535	-32.0
-4	534	-33.0
-2	535	-35.0
0	535	-35.0
2	535	-35.0
4	535	-33.8
6	536	-33.2
8	536	-31.0
10	537	-29.3
12	542	-31.0
14	557	-41.7

Table A.2: Sonar readings from a wall 50cm away from the sensor.

Sensor direction θ deg	Sonar reading (mm)	Error in sonar reading(mm)
-10	796	-34.4
-8	791	-34.0
-6	787	-33.0
-4	787	-35.0
-2	787	-36.5
0	787	-37.0
2	787	-36.5
4	787	-35.0
6	788	-34.0
8	788	-31.0
10	797	-30.2
12	797	-31.0

Table A.3: Sonar readings from a wall 75cm away from the sensor.

Sensor direction θ deg	Sonar reading (mm)	Error in sonar reading(mm)
-12	1073	-50.7
-10	1046	-30.5
-8	1039	-29.1
-6	1038	-32.5
-4	1038	-35.5
-2	1037	-36.4
0	1038	-38.0
2	1038	-37.4
4	1039	-36.6
6	1039	-33.5
8	1040	-30.0
10	1041	-25.6
12	1046	-23.7
14	1056	-25.4

Table A.4: Sonar readings from a wall 100cm away from the sensor.

Sensor direction θ deg	Sonar reading (mm)	Error in sonar reading(mm)
-10	1298	-28.7
-8	1294	-31.7
-6	1290	-33.1
-4	1290	-36.9
-2	1290	-39.2
0	1291	-41.0
2	1291	-40.2
4	1291	-38.0
6	1292	-35.0
8	1293	-30.7
10	1296	-26.7
12	1301	-23.0

Table A.5: Sonar readings from a wall 125cm away from the sensor.

Sensor direction θ deg	Sonar reading (mm)	Error in sonar reading(mm)
-12	1562	-28.5
-10	1548	-24.8
-8	1574	-32.2
-6	1543	-34.7
-4	1543	-39.0
-2	1543	-42.0
0	1544	-44
2	1544	-43.0
4	1544	-41.0
6	1542	-34.0
8	1546	-31.0
10	1550	-27.0
12	1557	-24.0

Table A.6: Sonar readings from a wall 150cm away from the sensor.

Sensor direction θ deg	Sonar reading (mm)	Error in sonar reading(mm)
-10	1832	-55.0
-8	1807	-40.0
-6	1806	-46.3
-4	1803	-49.0
-2	1802	-51.0
0	1802	-52.0
2	1802	-51.0
4	1803	-49.0
6	1804	-44.0
8	1804	-34.0
10	1808	-31.0
12	1809	-20.0
14	1872	-11.0
16	1872	-52.0

Table A.7: Sonar readings from a wall 175cm away from the sensor.

Sensor direction θ deg	Sonar reading (mm)	Error in sonar reading(mm)
-10	2070	-39.0
-8	2060	-40.0
-6	2057	-46.0
-4	2053	-48.0
-2	2053	-51.8
0	2054	-54.0
2	2054	-53.0
4	2054	-49.0
6	2055	-44.0
8	2055	-34.0
10	2057	-26.0
12	2061	-16.3
14	2069	-7.7

Table A.8: Sonar readings from a wall 200cm away from the sensor.

Sensor direction θ deg	Sonar reading (mm)	Error in sonar reading(mm)
-10	2325	-40.0
-8	2317	-44.9
-6	2316	-61.0
-4	2313	-57.5
-2	2312	-60.0
0	2314	-65.0
2	2314	-62.6
4	2314	-58.5
6	2315	-52.6
8	2319	-46.88
10	2321	-36.3
12	2329	-28.7

Table A.9: Sonar readings from a wall 225cm away from the sensor.

Sensor direction θ deg	Sonar reading (mm)	Error in sonar reading(mm)
-10	2580	-41.4
-8	2572	-47.4
-6	2571	-57.2
-4	2567	-60.9
-2	2567	-65.5
0	2567	-67.0
2	2567	-65.5
4	2568	-61.9
6	2568	-54.2
8	2569	-45.0
10	2572	-33.43
12	2577	-21.14
14	2590	-13.46

Table A.10: Sonar readings from a wall 250cm away from the sensor.

Sensor direction θ deg	Sonar reading (mm)	Error in sonar reading (mm)
-10	2844	-51.6
-8	2829	-52.0
-6	2825	-60.0
-4	2822	-65.3
-2	2821	-69.3
0	2821	-71.0
2	2821	-69.3
4	2822	-65.3
6	2822	-56.9
8	2825	-48.0
10	2826	-33.5
12	2828	-16.5
14	2855	-20.8

Table A.11: Sonar readings from a wall 275cm away from the sensor.

Sensor direction θ deg	Sonar reading (mm)	Error in sonar reading (mm)
-10	3090	-43.7
-8	3082	-52.5
-6	3081	-64.5
-4	3078	-70.7
-2	3077	-75.2
0	3077	-77.0
2	3077	-75.2
4	3077	-69.7
6	3078	-61.5
8	3082	-52.5
10	3083	-36.7
12	3084	-17.0
14	3095	-3.15

Table A.12: Sonar readings from a wall 300cm away from the sensor.

Sensor direction θ deg	Sonar reading (mm)	Error in sonar reading (mm)
-10	3372	-71.9
-8	3338	-56.0
-6	3335	-67.0
-4	3334	-76.0
-2	3332	-80.0
0	3331	-81.0
2	3331	-79.0
4	3331	-73.1
6	3332	-64.0
8	3335	-53.0
10	3336	-36.0
12	3338	-15.4
14	3348	1.5

Table A.13: Sonar readings from a wall 325cm away from the sensor.

Sensor direction θ deg	Sonar reading (mm)	Error in sonar reading(mm)
-10	3615	-61.0
-8	3593	-58.6
-6	3586	-66.7
-4	3585	-76.5
-2	3585	-82.9
0	3584	-84.0
2	3582	-79.9
4	3582	-73.5
6	3585	-65.72
8	3586	-51.6
10	3586	-32.0
12	3588	-9.8

Table A.14: Sonar readings from a wall 350cm away from the sensor.

Sensor direction θ deg	Sonar reading (mm)	Error in sonar reading(mm)
-10	3796	-38.9
-8	3792	-55.6
-6	3788	-67.6
-4	3786	-78.9
-2	3786	-83.7
0	3786	-86.0
2	3784	-82.0
4	3783	-74.0
6	3785	-64.6
8	3785	-48.6
10	3793	-36.0
12	3798	-15.3

Table A.15: Sonar readings from a wall 370cm away from the sensor.

Sensor direction	Sonar reading (mm)	Error method 1(mm)	Error method 2(mm)
-6	305	-83.0	-106.0
-4	300	-65.0	-98.0
-2	291	-49.0	-81.0
0	288	-33.0	-33.0
2	288	-45.0	-75.0
4	288	-53.0	-74.0
6	288	-60.0	-72.0
8	289	-67.0	-73.0
10	299	-82.0	-90.0

Table A.16: Sonar readings from a 90 corner at 25cm from the sensor and x=y=17.67cm from the near walls.

Sensor direction	Sonar reading (mm)	Error method 1(mm)	Error method 2(mm)
-10	573	-140.0	-133.0
-8	555	-110.0	-101.0
-6	543	-88.0	-81.0
-4	539	-70.0	-75.0
-2	535	-52.0	-69.0
0	538	-38.0	-38.0
2	539	-56.0	-77.0
4	539	-70.0	-75.0
6	543	-88.0	-81.0
8	551	-110.0	-93.0

Table A.17: Sonar readings from a 90 corner at 50cm from the sensor and x=y=35.35cm from the near walls.

Sensor direction	Sonar reading (mm)	Error method 1(mm)	Error method 2(mm)
-6	799	-117.0	-91.0
-4	795	-93.0	-87.0
-2	792	-67.0	-84.0
0	791	-41.0	-41.0
2	792	-67.0	-84.0
4	795	-93.0	-87.0
6	796	-114.0	-85.0
8	801	-137.0	-90.0
10	862	-180.0	-133.0

Table A.18: Sonar readings from a 90 corner at 75cm from the sensor and x=y=53.0cm from the near walls.

Sensor direction	Sonar reading (mm)	Error method 1(mm)	Error method 2(mm)
-8	1071	-185.0	-125.0
-6	1051	-140.0	-92.0
-4	1048	-110.0	-91.0
-2	1047	-80.0	-93.0
0	1047	-47.0	-47.0
2	1047	-80.0	-93.0
4	1048	-110.0	-91.0
6	1049	-140.0	-88.0
8	1054	-170.0	-91.0
10	1076	-210.0	-126.0

Table A.19: Sonar readings from a 90 corner at 100cm from the sensor and x=y=70.7cm from the near two walls.

Sensor direction	Sonar reading (mm)	Error method 1(mm)	Error method 2(mm)
-6	1298	-160.0	-83.0
-4	1293	-120.0	-80.0
-2	1293	-84.0	-84.0
0	1294	-42.0	-42.0
2	1293	-84.0	-84.0
4	1293	-120.0	-80.0
6	1295	-160.0	-77.0
8	1302	-195.0	-82.0
10	1327	-247.0	-120.0

Table A.20: Sonar readings from a 90 corner at 125cm from the sensor and x=y=88.4 from the near two walls.

Sensor direction	Sonar reading (mm)	Error method 1(mm)	Error method 2(mm)
-10	1603	-300.0	-144.0
-8	1548	-220.0	-70.0
-6	1542	-178.0	-73.0
-4	1539	-134.0	-78.0
-2	1539	-90.0	-40.0
0	1540	-40.0	-40.0
2	1540	-90.0	-80.0
4	1540	-135.0	-75.0
6	1545	-180.0	-77.0
8	1563	-236.0	-102.0

Table A.21: Sonar readings from a 90 corner 150cm from the sensor and x=y=106.0cm from the near two walls.

Sensor direction	Sonar reading (mm)	Error method 1(mm)	Error method 2(mm)
-8	1807	-250.0	-77.0
-6	1792	-200.0	-60.0
-4	1788	-150.0	-61.0
-2	1788	-92.0	-67.0
0	1788	-38.0	-38.0
2	1788	-92.0	-66.0
4	1790	-150.0	-65.0
6	1796	-200.0	-67.0
8	1812	-260.0	-86.0

Table A.22: Sonar readings from a 90 corner 175cm from the sensor and x=y=123.7cm from the near two walls.

Sensor direction	Sonar reading (mm)	Error method 1(mm)	Error method 2(mm)
-12	2038	-350.0	-3
-10	2031	-300.0	-10.0
-8	2034	-260.0	-34.0
-6	2032	-210.0	-45.0
-4	2039	-165.0	-69.0
-2	2039	-110.0	-76.0
0	2036	-36.0	-36.0
2	2040	-107.0	-78.0
4	2041	-167.0	-73.0
6	2052	-230.0	-84.0

Table A.23: Sonar readings from a 90 corner 200cm from the sensor and x=y=141.4cm from the near two walls.

Sensor direction	Sonar reading (mm)	Error method 1(mm)	Error method 2(mm)
-10	2301	-360.0	-45.0
-8	2297	-310.0	-58.0
-6	2291	-250.0	-62.0
-4	2290	-180.0	-72.0
-2	2285	-110.0	-70.0
0	2293	-43.0	-43.0
2	2295	-120.0	-90.0
4	2299	-190.0	-90.0
6	2314	-270.0	-108.0

Table A.24: Sonar readings from a 90 corner 225cm from the sensor and x=y=152.0cm from the near two walls.

Sensor direction	Sonar reading (mm)	Error method 1(mm)	Error method 2(mm)
-12	2577	-450.0	-27.0
-10	2555	-380.0	-9.0
-8	2550	-320.0	-22.0
-6	2547	-260.0	-34.0
-4	2546	-190.0	-46.0
-2	2547	-110.0	-56.0
0	2547	-47.0	-47.0
2	2549	-115.0	-60.0
4	2552	-190.0	-56.0
6	2568	-280.0	-76.0

Table A.25: Sonar readings from a 90 corner 250cm from the sensor and x=y=176.8 from the near two walls.

Sensor direction	Sonar reading (mm)	Error method 1(mm)	Error method 2(mm)
-12	2807	-487.0	-110.0
-10	2802	-430.0	-30.0
-8	2799	-363.0	-50.0
-6	2798	-300.0	-67.0
-4	2795	-220.0	-76.0
-2	2796	-135.0	-87.0
0	2796	-46.0	-46.0
2	2799	-140.0	-93.0
4	2804	-230.0	-94.0
6	2815	-312	-101.0

Table A.26: Sonar readings from a 90 corner 275cm from the sensor and x=y=194.5cm from the near two walls.

Sensor direction	Sonar reading (mm)	Error method 1(mm)	Error method 2(mm)
-12	3050	-520.0	10.0
-10	3048	-460.0	-17.0
-8	3042	-313.0	-60.0
-6	3043	-230.0	-70.0
-4	3042	-140.0	-80.0
-2	3042	-140.0	-80.0
0	3043	-43.0	-43.0
2	3047	-146.0	-90.0
4	3053	-240.0	-92.0
6	3062	-330.0	-94.0

Table A.27: Sonar readings from a 90 corner 300cm from the sensor and x=y=212.13cm from the near two walls.

Sensor direction	Sonar reading (mm)	Error method 1(mm)	Error method 2(mm)
-10	3351	-545.0	-117.0
-8	3335	-457.0	-114.0
-6	3320	-363.0	-107.0
-4	3300	-255.0	-85.0
-2	3291	-148.0	-78.0
0	3285	-35.0	-35.0
2	3289	-146.0	-74.0
4	3295	-250.0	-75.0
6	3323	-366.0	-113.0

Table A.28: Sonar readings from a 90 corner 325cm from the sensor and x=y=229.8cm from the near two walls.

Sensor direction	Sonar reading (mm)	Error method 1(mm)	Error method 2(mm)
-6	3556	-371.0	-76.0
-4	3543	-263.0	-69.0
-2	3536	-152.0	-67.0
0	3532	-32.0	-32.0
2	3535	-150.0	-65.0
4	3543	-263.0	-69.0
6	3555	-370.0	-74.0
8	3569	-470.0	-77.0

Table A.29: Sonar readings from a 90 corner 350cm from the sensor and x=y=247.5cm from the near two walls.

Sensor direction	Sonar reading (mm)	Error method 1(mm)	Error method 2(mm)
-8	3774	-498.0	-85.0
-6	3760	-393.0	-83.0
-4	3746	-280.0	-76.0
-2	3739	-162.0	-74.0
0	3730	-30.0	-30.0
2	3740	-163.0	-63.0
4	3746	-279.0	-76.0
6	3763	-396.0	-90.0

Table A.30: Sonar readings from a 90 corner 370cm from the sensor and x=y=261.6cm from the near two walls.

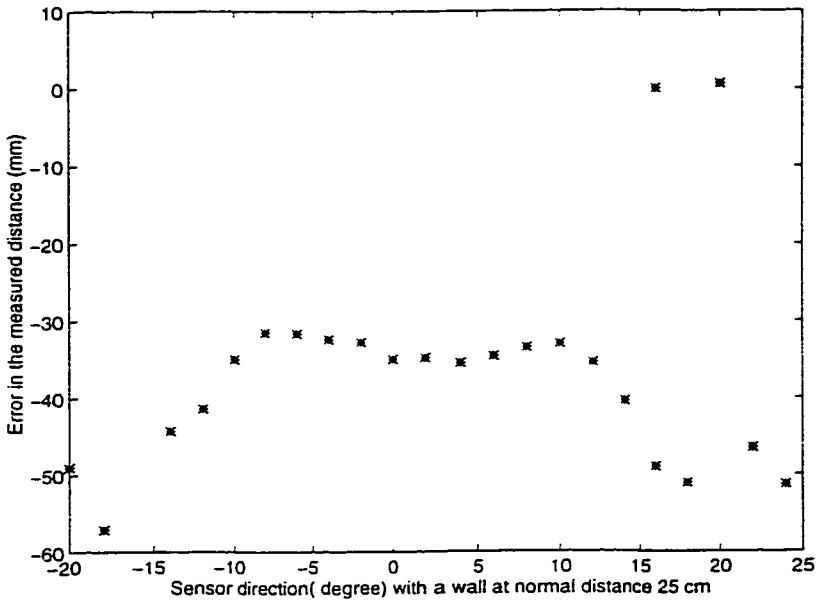

Figure A.1: Incidence angle versus radial imprecision for readings obtained from a wall at distance 25cm.

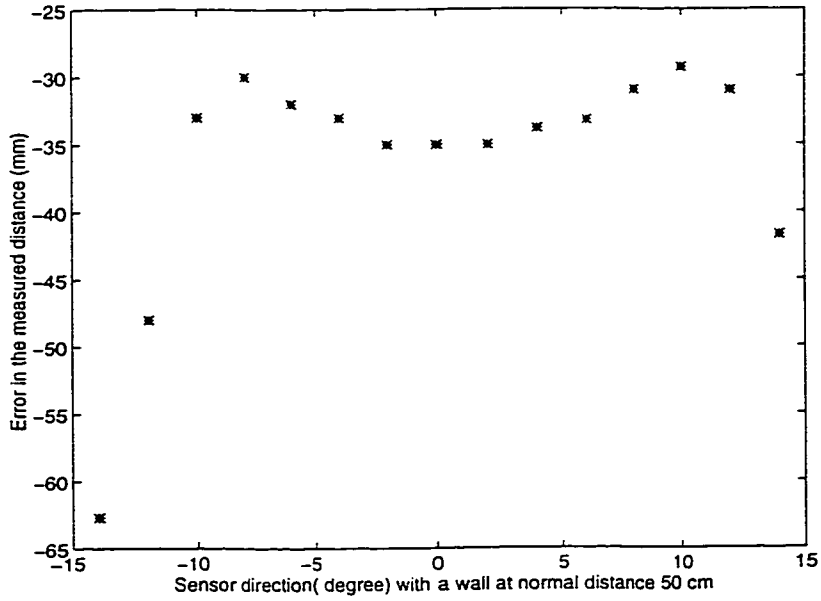

Figure A.2: Incidence angle versus radial imprecision for readings obtained from a wall at distance 50cm.

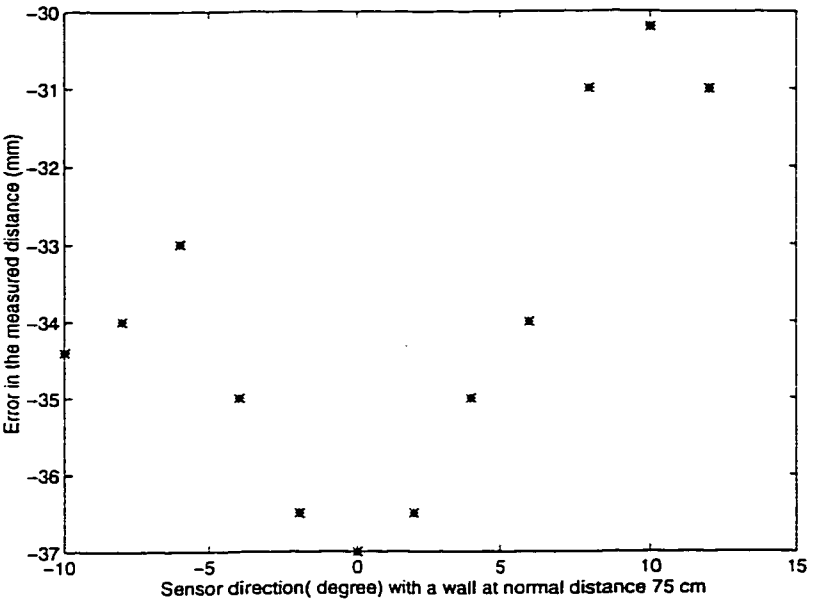

Figure A.3: Incidence angle versus radial imprecision for readings obtained from a wall at distance 75cm.

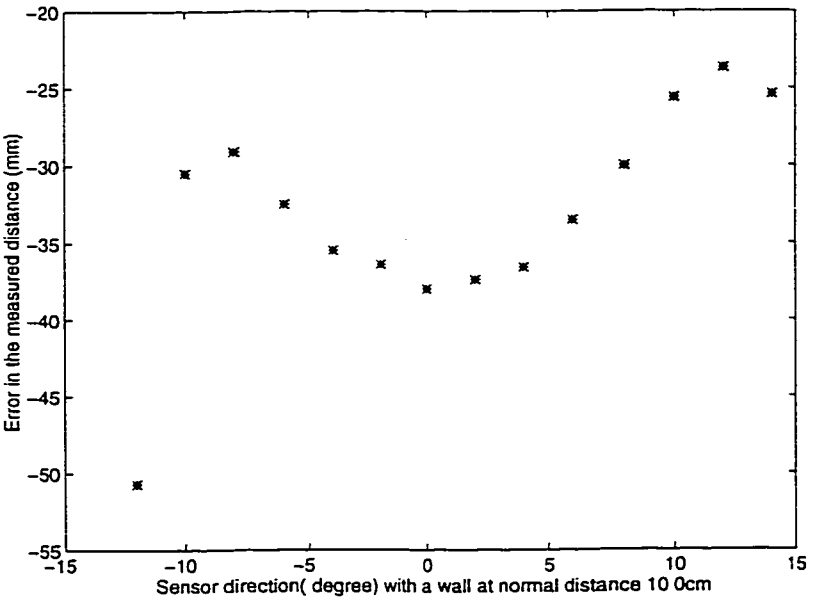

Figure A.4: Incidence angle versus radial imprecision for readings obtained from a wall at distance 100cm.

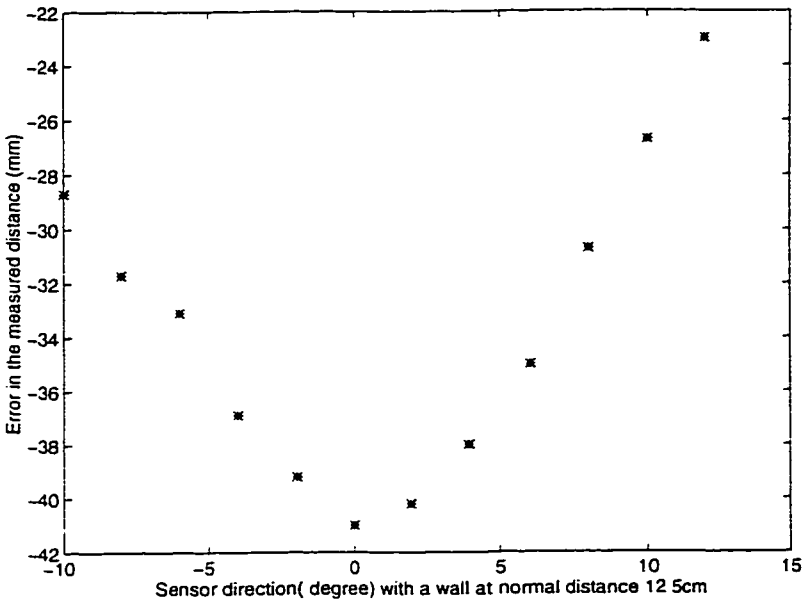

Figure A.5: Incidence angle versus radial imprecision for readings obtained from a wall at distance 125cm.

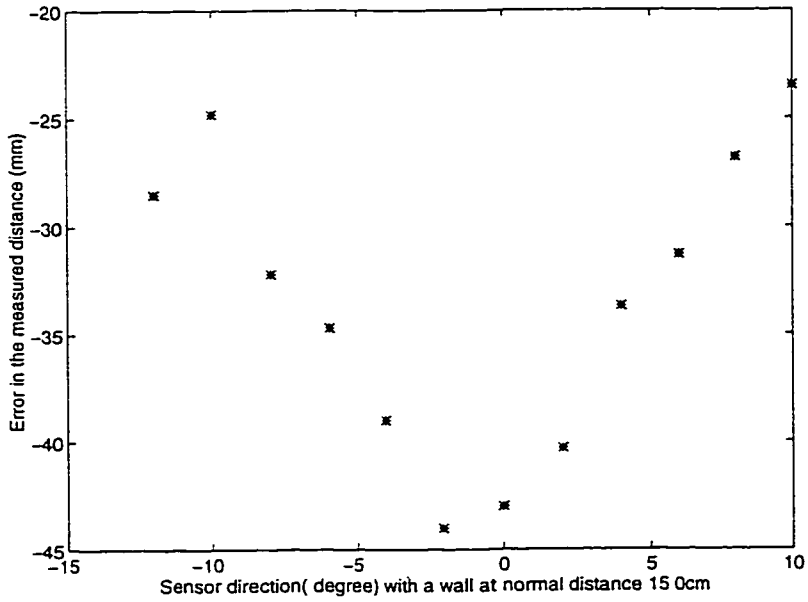

Figure A.6: Incidence angle versus radial imprecision for readings obtained from a wall at distance 150cm.

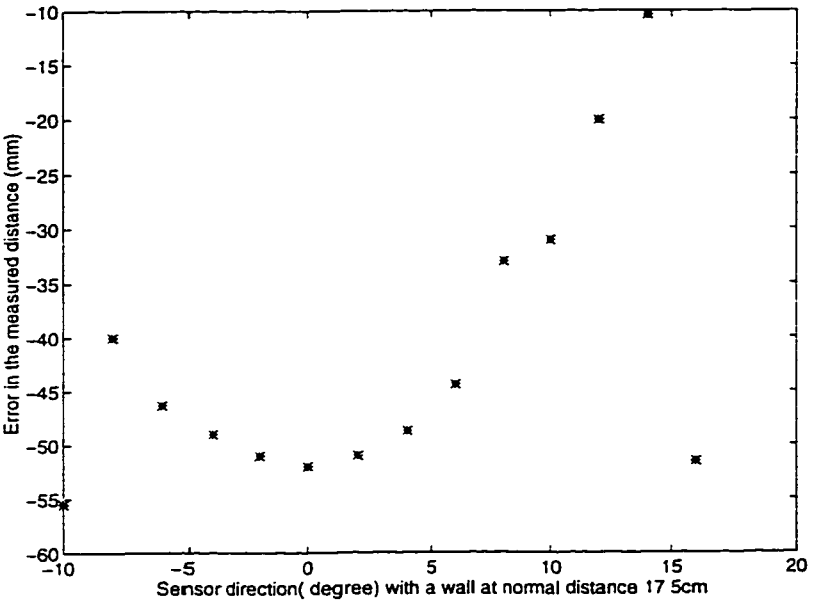

Figure A.7: Incidence angle versus radial imprecision for readings obtained from a wall at distance 175cm.

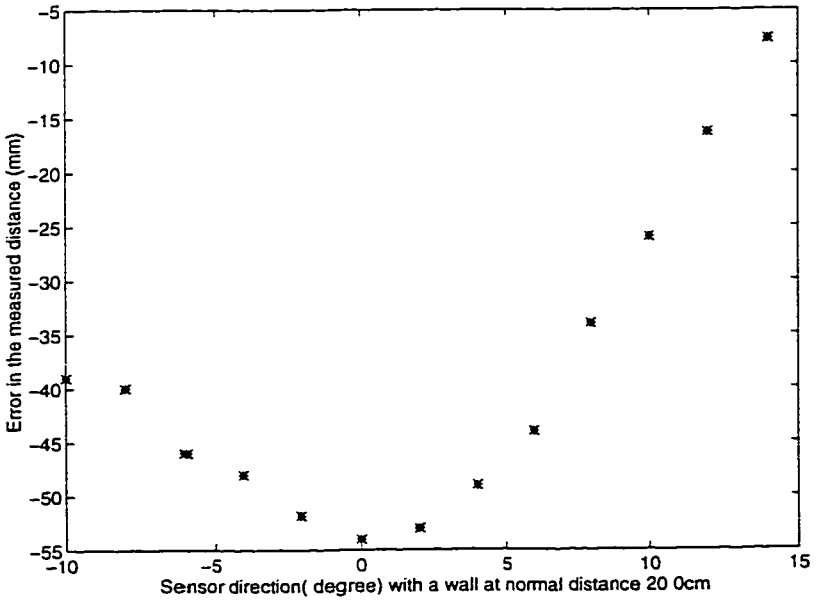

Figure A.8: Incidence angle versus radial imprecision for readings obtained from a wall at distance 200cm.

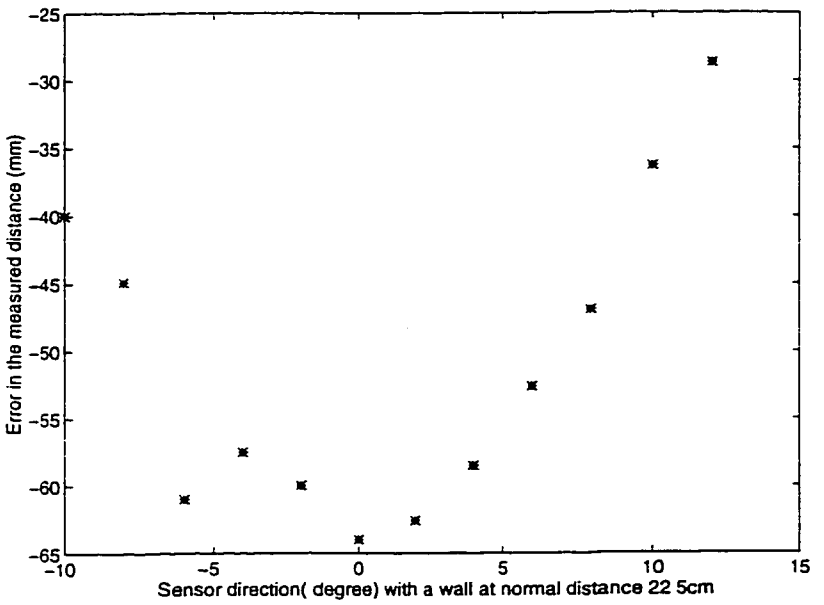

Figure A.9: Incidence angle versus radial imprecision for readings obtained from a wall at distance 225cm.

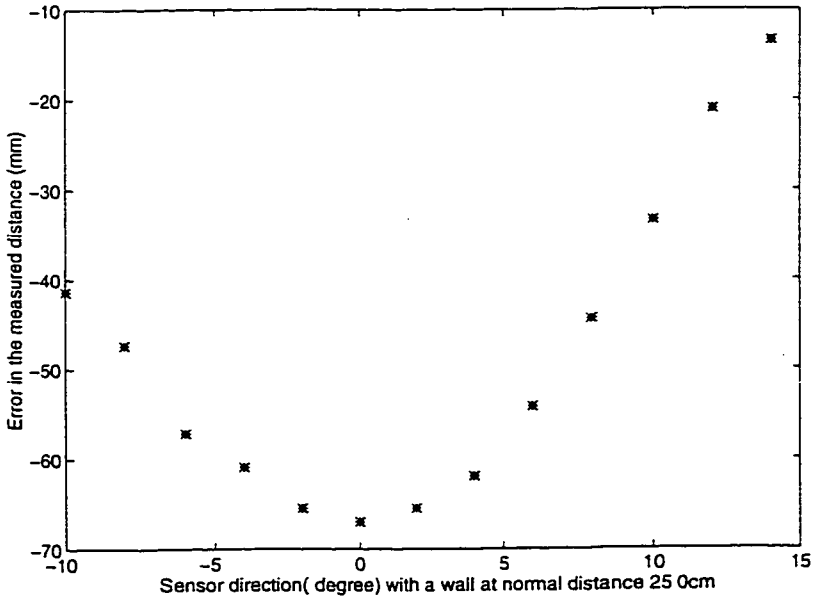

Figure A.10: Incidence angle versus radial imprecision for readings obtained from a wall at distance 250cm.

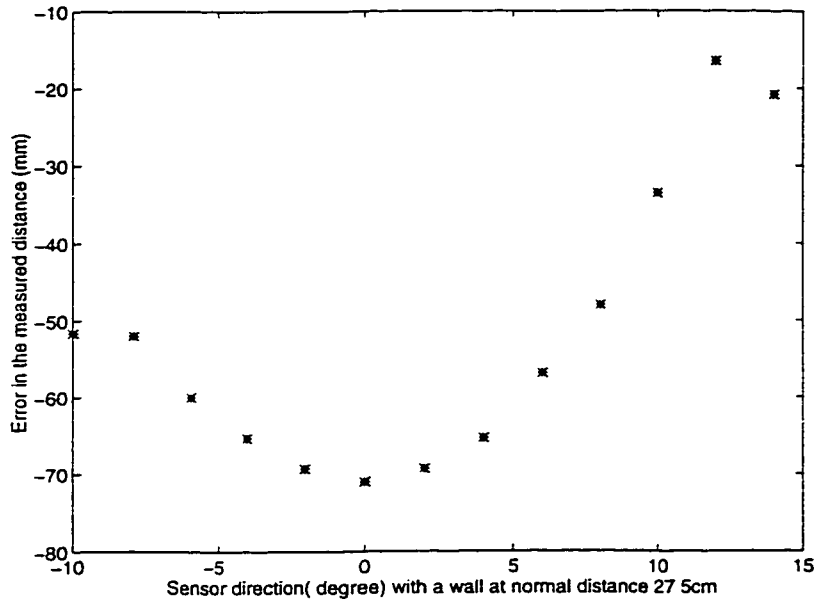

Figure A.11: Incidence angle versus radial imprecision for readings obtained from a wall at distance 275cm.

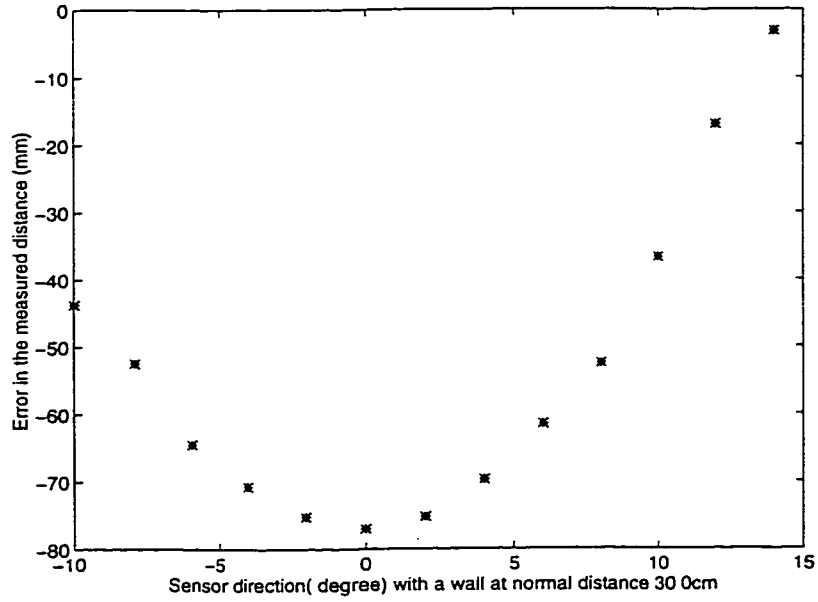

Figure A.12: Incidence angle versus radial imprecision for readings obtained from a wall at distance 300cm.

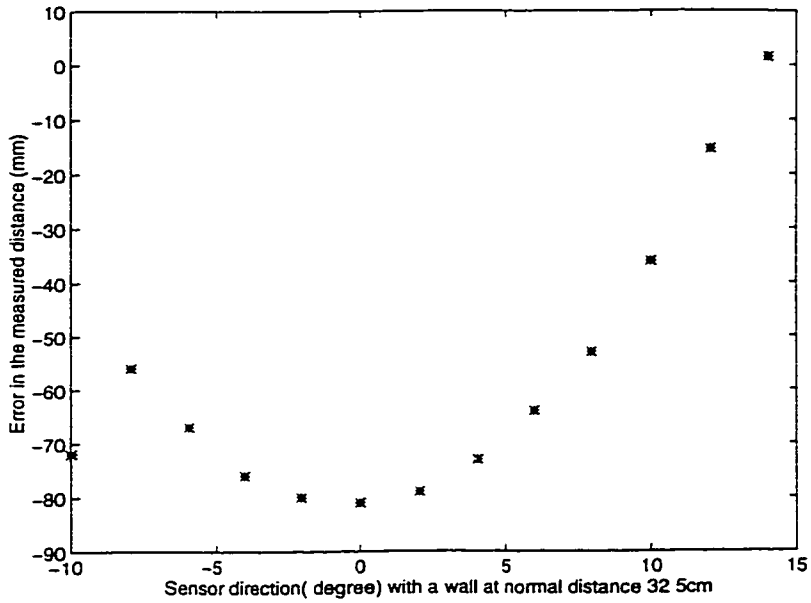

Figure A.13: Incidence angle versus radial imprecision for readings obtained from a wall at distance 325cm.

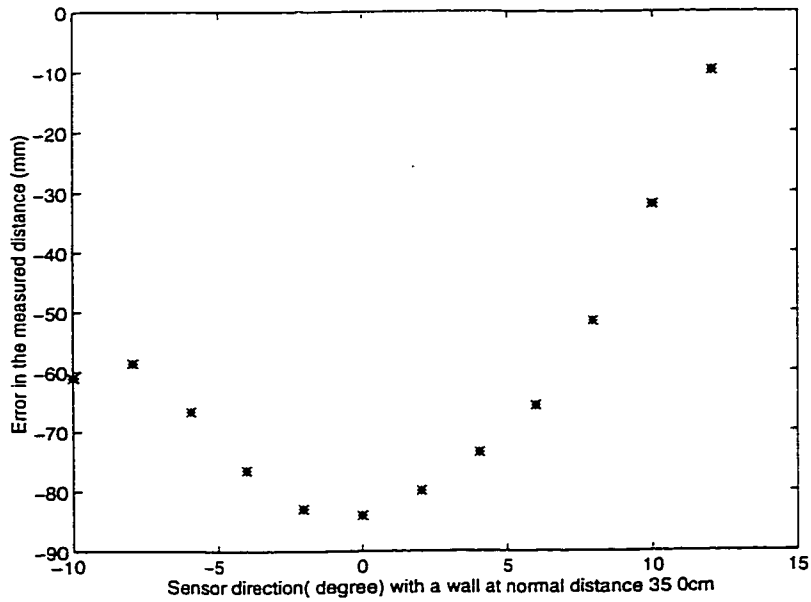

Figure A.14: Incidence angle versus radial imprecision for readings obtained from a wall at distance 350cm.

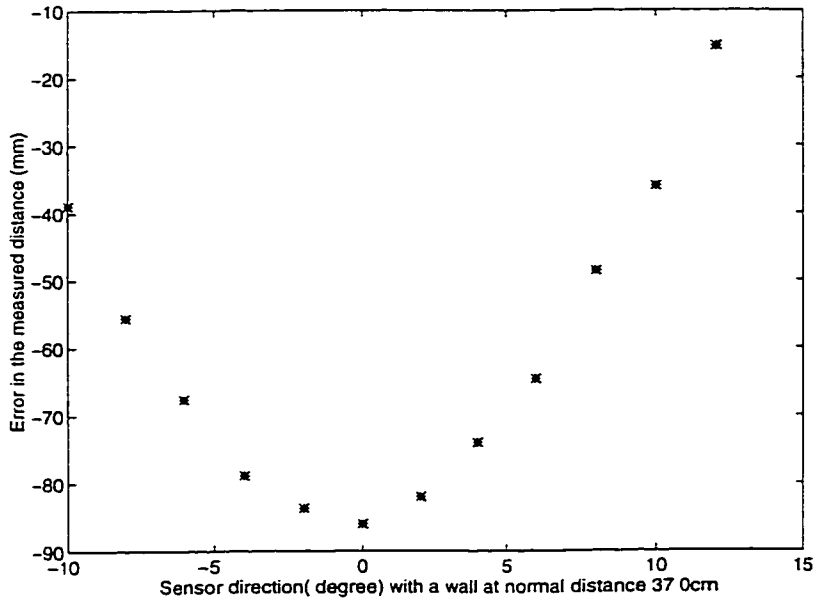

Figure A.15: Incidence angle versus radial imprecision for readings obtained from a wall at distance 370cm.

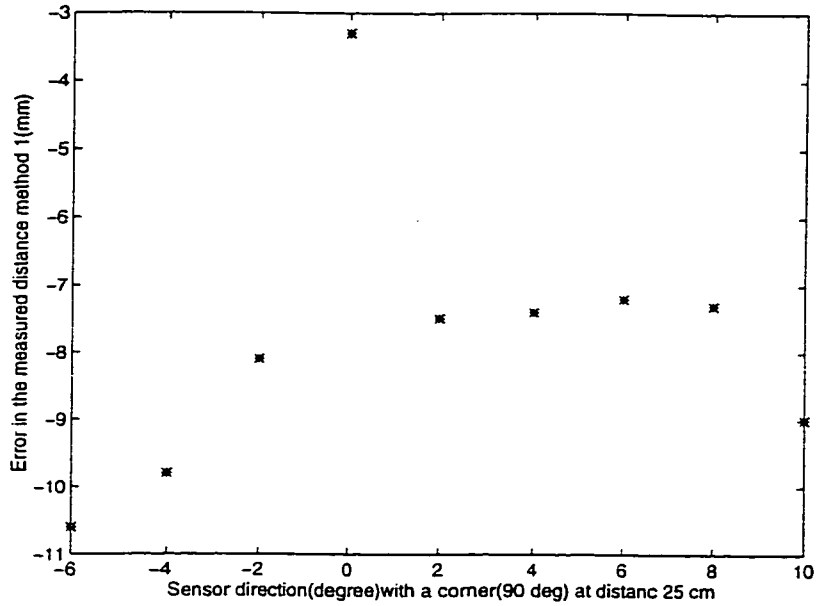

Figure A.16: Incidence angle versus radial imprecision for readings obtained from a corner at 25cm.

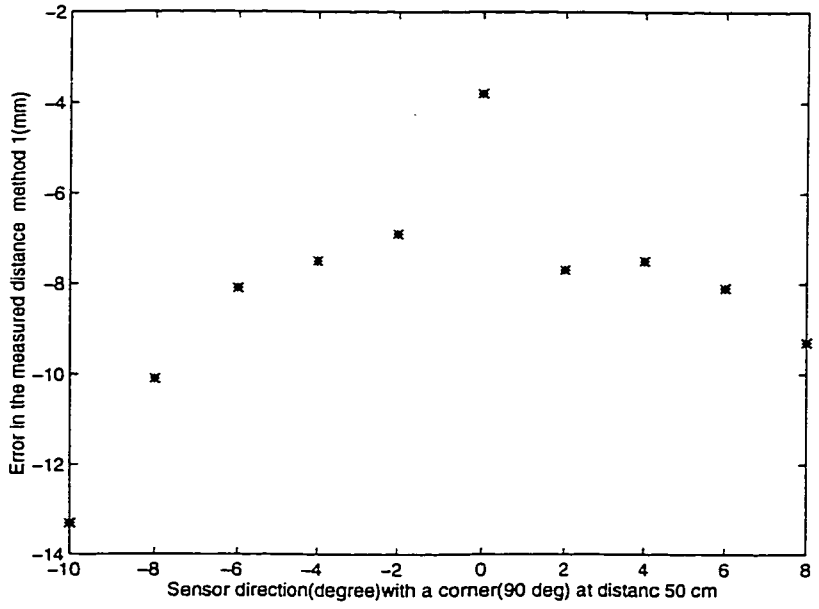

Figure A.17: Incidence angle versus radial imprecision for readings obtained from a corner at 50cm.

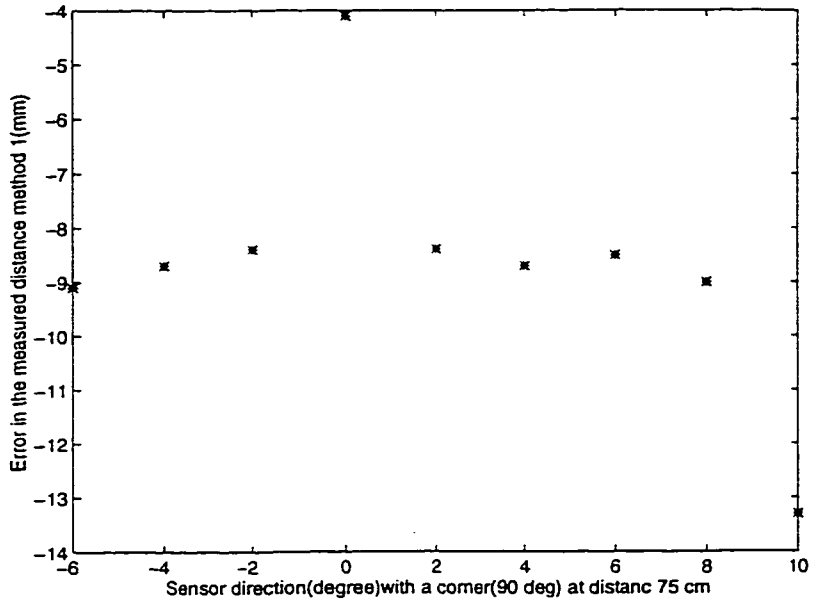

Figure A.18: Incidence angle versus radial imprecision for readings obtained from a corner at 75cm.

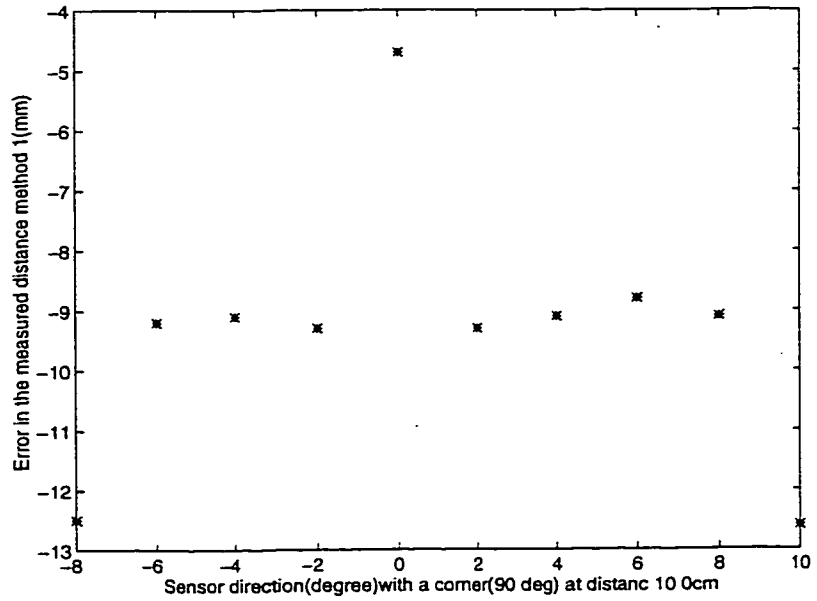

Figure A.19: Incidence angle versus radial imprecision for readings obtained from a corner at 100cm.

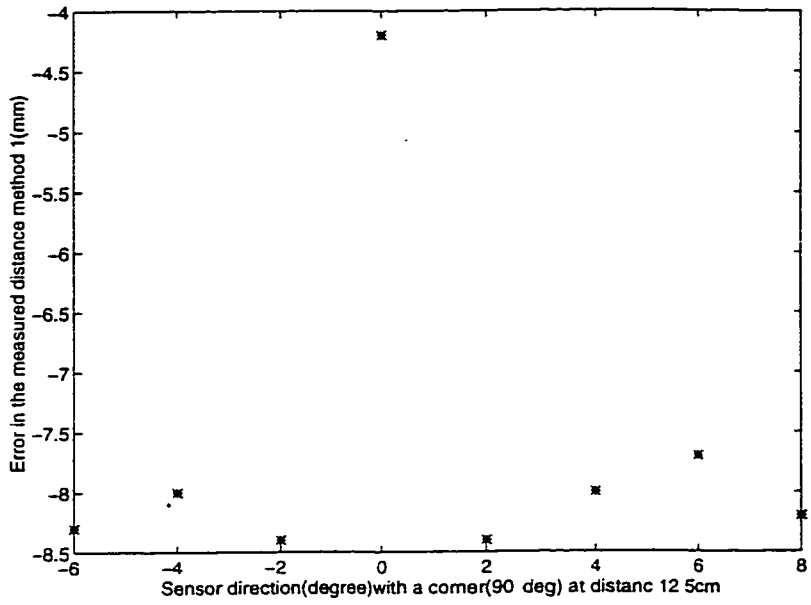

Figure A.20: Incidence angle versus radial imprecision for readings obtained from a corner at 125cm.

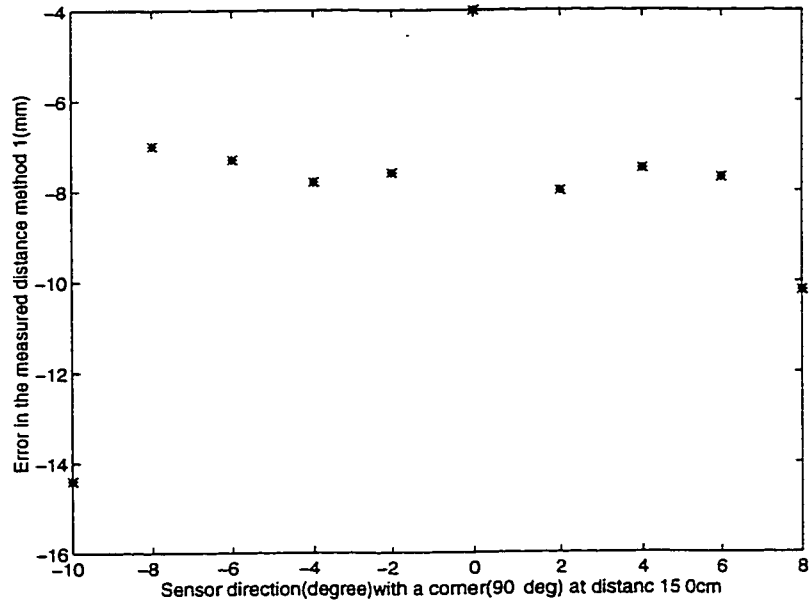

Figure A.21: Incidence angle versus radial imprecision for readings obtained from a corner at 150cm.

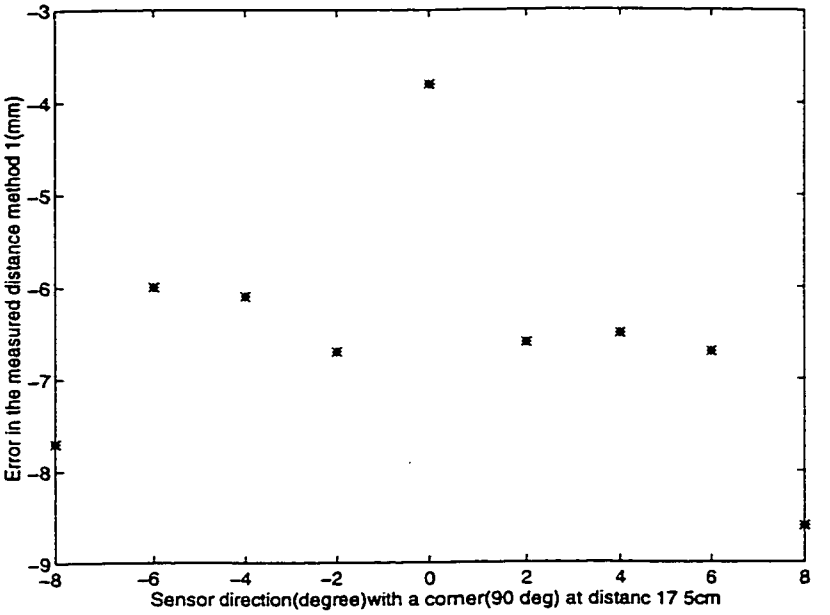

Figure A.22: Incidence angle versus radial imprecision for readings obtained from a corner at 175cm.

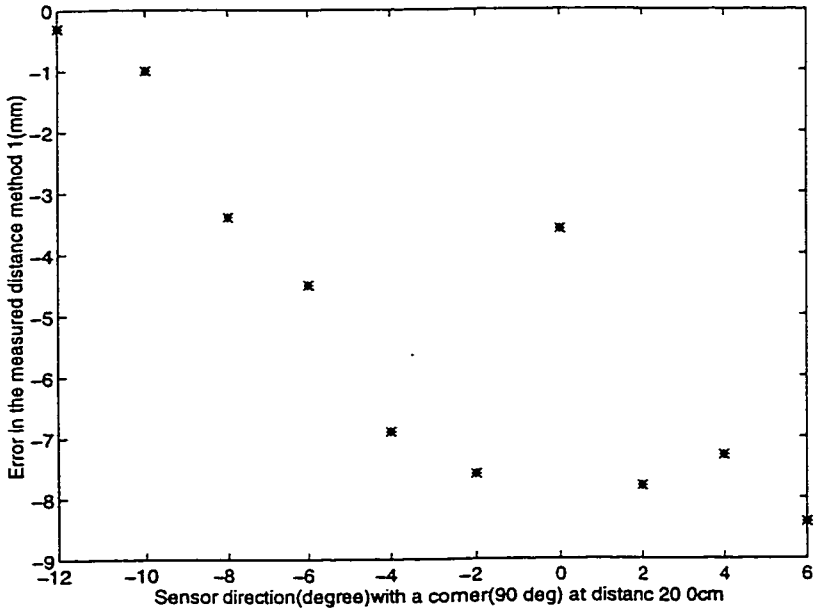

Figure A.23: Incidence angle versus radial imprecision for readings obtained from a corner at 200cm.

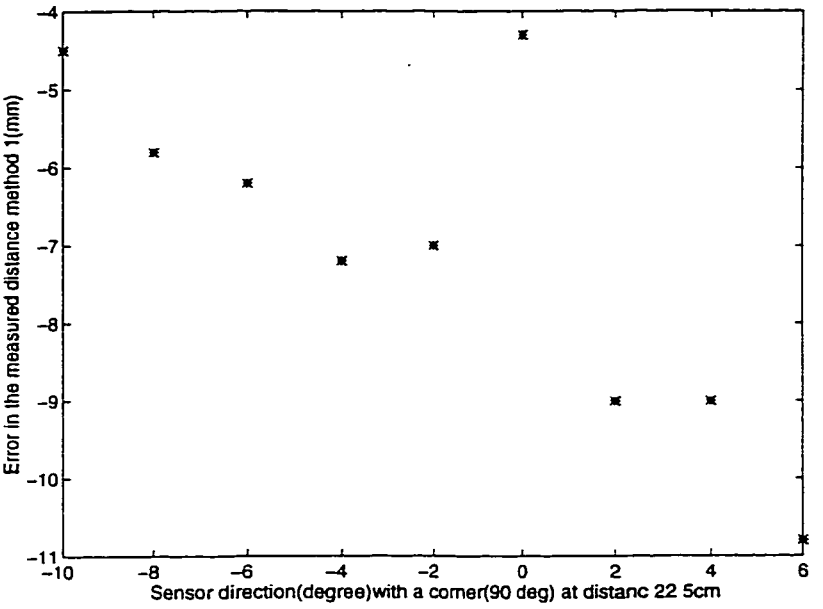

Figure A.24: Incidence angle versus radial imprecision for readings obtained from a corner at 225cm.

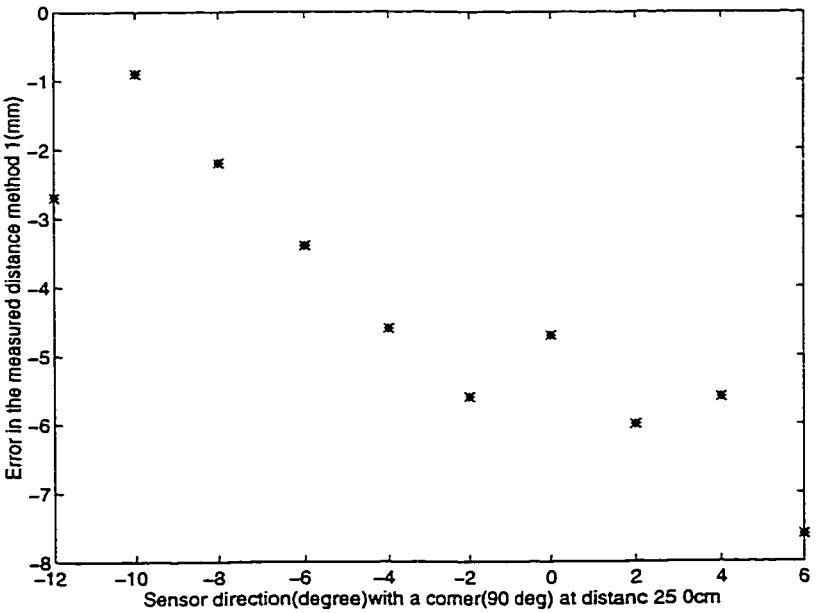

Figure A.25: Incidence angle versus radial imprecision for readings obtained from a corner at 250cm.

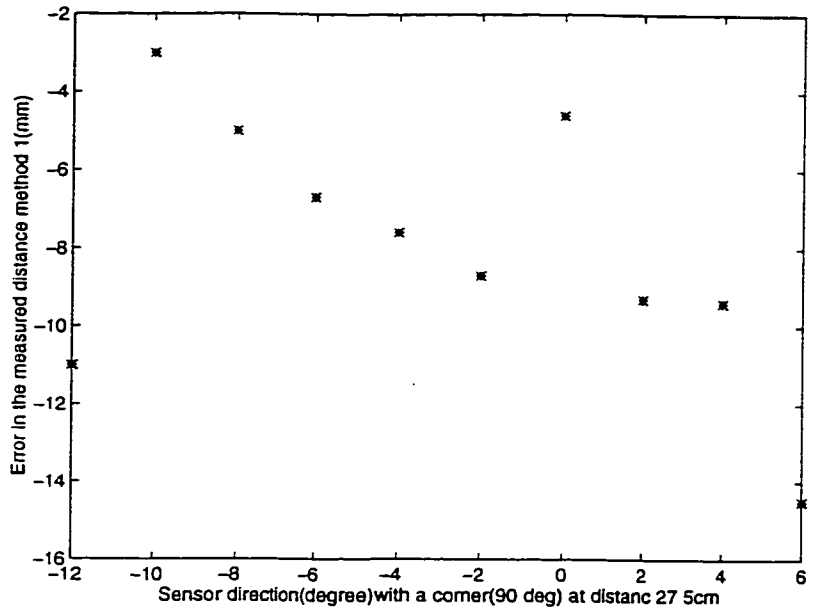

Figure A.26: Incidence angle versus radial imprecision for readings obtained from a corner at 275cm.

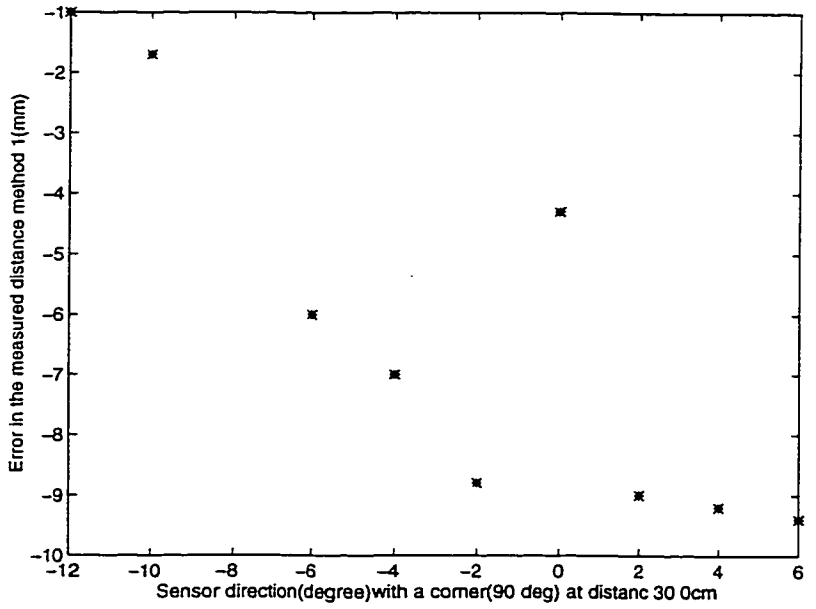

Figure A.27: Incidence angle versus radial imprecision for readings obtained from a corner at 300cm.